
NEW TYPE CURVES FOR THE ANALYSIS OF PRESSURE TRANSIENT DATA OF HORIZONTAL WELLS IN NON-NEWTONIAN FLUID RESERVOIRS

A Thesis

PRESENTED TO THE DEPARTMENT OF PETROLEUM ENGINEERING
AFRICAN UNIVERSITY OF SCIENCE AND TECHNOLOGY

In Partial Fulfillment of Requirements for the Award of Degree of

MASTER OF SCIENCE

By

ADENUGA, KAZEEM ADEBOWALE, B.Sc.

ABUJA, FCT.

DECEMBER, 2011

NEW TYPE CURVES FOR THE ANALYSIS OF PRESSURE TRANSIENT DATA OF HORIZONTAL WELLS IN NON-NEWTONIAN FLUID RESERVOIRS

By

ADENUGA Kazeem Adebawale

RECOMMENDED:

Dr. Alpheus Igbokoyi
Committee Chair

Professor Djebbar Tiab
Committee Member

Professor Godwin Chukwu
Committee Member

APPROVED:

Chief Academic Officer

Date:

ABSTRACT

This novel work is based on the study of Vongvuthipornchai and Raghavan, 1987. In this work a new 3-Dimensional non-linear partial differential equation describing the transient flow of non-Newtonian fluid in porous media is developed for a hypothetical no-flow boundary cuboid reservoir. The basic assumptions in the mathematical modeling of the differential equations are; permeability anisotropy with directional permeabilities k_x, k_y and k_z , an isothermal, single phase, slightly compressible fluid with steady state viscosity was assumed, the horizontal well was placed in the y-direction perpendicular to the direction of maximum permeability k_x . The effects of gravity were neglected and the reservoir fluid was considered to be a non-Newtonian pseudo plastic fluid that obeys the power law model.

The derived equation was discretized using finite difference approach; the system of linear equations obtained from the discretization was solved with the aid of a MATLAB 7.5.0^R code to obtain pressure data. Type curves involving the log-log plot of P_{wD} Vs t_D and $t_D * P_{wD}'$ Vs t_D were made for cases when there is permeability isotropy and anisotropy of different power law flow index n ranging from 0.1 to 1 for horizontal well length of 600ft, 1000ft and 1200ft.

The developed type curves were validated by considering a Newtonian case and using Tiab Direct synthesis (TDS) technique to analyze the radial flow regime for the determination of average permeability as well as the procedure presented in Vongvuthipornchai and Raghavan, 1987 to analyze the early linear flow for determining k_x and the Pseudo steady state flow regime was used to determine the drainage area. Subsequently, examples were given to determine mobility and k_x for a non-Newtonian fluid of $n = 0.1$ with methods presented in the work of works of Igbokeoyi and Tiab, 2007 and Vongvuthipornchai and Raghavan, 1987

The Validation of this work shows that the result obtained from the case when a Newtonian fluid was assumed were very close to the actual property been determined. Similarly, the results obtained from the example when $n = 0.1$ gave close values of k_x and reasonable value of mobility. This novel work will thus lay a back ground for further works in the analysis of pressure transient data of horizontal well in non-Newtonian or heavy oil reservoirs.

ACKNOWLEDGEMENT

I give Almighty God all the Praise and Adoration for His Mercies over me throughout my study at the AUST and most especially towards the last quarter of the programme. Thanks to the Petroleum Development Technology Fund (PTDF) for providing the Scholarship from which I benefitted from.

Special Appreciation goes to the following individual and friends:

- My main Supervisor, Dr Alpheus Igbokoyi for his excellent supervision, passion for innovative research, his patience, his availability and eagerness to render assistance, his understanding, encouragement when I feel like giving up. He has been a wonderful man to me. May God reward him abundantly
- My committee members; Prof. Djebbar Tiab whose TDS technique was a great help in this work and Prof. Godwin Chukwu whose Non-Newtonian Class was of great help.
- My closest friend in AUST, Awotiku Oluwabiyi for been a brother from another mother and father. May God bless your future endeavors
- Azeb, Titus, Anthony, Obinna, Shuaibu for keeping their doors open when I needed help, I really appreciate your help guys.
- To my family for their support and prayers throughout my stay in AUST
- To all my classmates for being interesting people, wishing you guys the best in future endeavors
- To everyone in AUST, staff, faculties, fellow students for their contribution to the success of my study at AUST.
- And to Shell Petroleum Development Cooperation (SPDC) for providing an opportunity to learn outside the class and apply what was learnt in class.

TABLE OF CONTENTS

ABSTRACT	iii
ACKNOWLEDGEMENT	iv
TABLE OF CONTENTS.....	v
LIST OF FIGURES.....	viii
LIST OF TABLES.....	x
CHAPTER ONE	x
1.0 INTRODUCTION	1
1.1 OVERVIEW AND PROBLEM DEFINITION	1
1.2 OBJECTIVE OF STUDY	2
1.3 MOTIVATION FOR STUDY	3
1.4 WORK OUTLINE	3
CHAPTER TWO	4
2.0 LITERATURE REVIEW	4
2.1 NON-NEWTONIAN FLUIDS	4
2.1.1 PRESSURE TRANSIENT ANALYSIS OF NON-NEWTONIAN FLUIDS	6
2.2 HORIZONTAL WELLS.....	20
2.2.1 HORIZONTAL WELL PRESSURE TRANSIENT ANALYSIS	20
2.3 MATHEMATICAL MODELING AND SOLUTIONS	21
2.3.1 ANALYTICAL SOLUTION	22
2.3.2 NUMERICAL SOLUTION TO DIFFUSIVITY EQUATION	24
2.3.3 FINITE DIFFERENCE APPROXIMATION	25
2.3.4 FINITE DIFFERENCE FORMULATION.....	26
2.4 CONVENTIONAL METHODS AND TYPE CURVES ANALYSIS OF PRESSURE TRANSIENT DATA	28
2.4.1 WELLBORE STORAGE	31
2.4.2 SKIN FACTOR	32
CHAPTER THREE	34
3.0 METHODOLOGY.....	34

3.1 BASIC ASSUMPTIONS	35
3.2 MATHEMATICAL FORMULATION OR MODELING	36
3.2.1 BOUNDARY CONDITION	46
3.2.2 FINITE DIFFERENCE APPROXIMATION OF MODELLED DIFFERENTIAL EQUATION.....	47
3.2.3 MATLAB R2007b IMPLEMENTATION.....	49
3.2.4 LOCATION OF HORIZONTAL WELL	50
3.3 ORDERING OF GRIDS AND COEFFICIENT MATRIX DEVELOPMENT	50
3.4 TYPE CURVE DEVELOPMENT	53
CHAPTER FOUR	54
4.0 VALIDATION, RESULTS AND DISCUSSION.....	54
4.1 VALIDATION OF RESULTS	54
4.1.1 VALIDATION OF kx FROM EARLY-LINEAR FLOW REGIME ANALYSIS.....	55
4.1.2 VALIDATION OF AVERAGE RESERVOIR PERMEABILITY FROM RADIAL FLOW REGIME ANALYSIS	58
4.1.3 VALIDATION OF DRAINAGE AREA FROM PSEUDO STEADY STATE FLOW REGIME ANALYSIS.	59
4.2 APPLICATIONS TO NON-NEWTONIAN RESERVOIR FLUIDS.....	60
4.2.1 ANALYSIS OF EARLY LINEAR FLOW REGIME FOR THE DETERMINATION OF kx	60
4.2.2 DETERMINATION OF AVERAGE RESERVOIR MOBILITY OR PERMEABILITY USING TIAB DIRECT SYNTHESIS TECHNIQUE	65
4.3 DEVELOPMENT OF TYPE CURVES	68
4.3.1 Horizontal Well length of 600ft $kx = 100md, ky = 50md ky = 25md h = 300ft$	68
4.3.2 Horizontal Well length of 1000ft $kx = 100md, ky = 50md ky = 25md h = 300ft$	68
4.3.3 Horizontal Well length of 1200ft $kx = 100md, ky = 50md ky = 25md h = 300ft$	73
4.3.4 Horizontal Well length of 600ft $kx = 75md, ky = 75md ky = 75md h = 300ft$	73
4.3.5 Horizontal Well length of 1000ft $kx = 75md, ky = 75md ky = 75md h = 300ft$	73
4.3.6 Horizontal Well length of 1200ft $kx = 75md, ky = 75md ky = 75md h = 300ft$	73
CHAPTER FIVE.....	83
5.0 CONCLUSIONS AND RECOMMENDATIONS.....	83
5.1 CONCLUSIONS	83
5.2 RECOMMENDATIONS.....	84
REFERENCES	85
NOMENCLATURE.....	88

APPENDIX A.....	91
A.1 Pressure data used for the validation of flow index $n = 0.1$	91
A.2 Pressure data for the validation of k_x , k and Drainage area.....	93
A.3 Pressure data for the determination of k_x for non-Newtonian fluid where $n=0.2$	96
APPENDIX B.....	99
DERIVATION OF DARCY EQUATION FOR NON-NEWTONIAN POWER-LAW FLUIDS.....	99

LIST OF FIGURES

Figure 2.1: Plots of Shear Stress Vs Shear rate for time-Dependent non-Newtonian Fluids	6
Figure 2.2: Dimensionless bottomhole pressure Vs dimensionless time for no –flow boundary for different flow index	12
Figure 2.3:Flowing well response for constant rate injection	19
Figure 2.4: A typical dimensionless pressure and semi-log pressure derivative for a horizontal well in a closed box-shaped reservoir.....	29
Figure 3.1: Diagram showing the flow through a porous cuboid reservoir model.....	36
Figure 3.2: Ordering of grid blocks to give a diagonal symmetrical Matrix.....	50
Figure 4.1: Log-Log Plot of $t_D * P_{wD}'$ Vs t_D for determining radial flow region.....	56
Figure 4.2: Log-Log Plot of P_{wD} Vs t_D for the validation of early linear flow analysis	57
Figure 4.3: Log-Log Plot of $t * \Delta P_{wf}'$ Vs t for $n=1$ for the validation of average reservoir permeability.....	61
Figure 4.4: Log-Log Plot of $t_D * P_{wD}'$ Vs t_D for $n=1$ for determination of drainage area	62
Figure 4.5: Log-Log plot of P_{wD} Vs t_D for the determination of K_x when $n=0.2$	64
Figure 4.6: Log-log Plot of dimensionless pressure drop against dimensionless time for $n=0.1$ to 1 $l_{yf}=600ft$; $k_x=100md$, $k_y=50md$, $k_z=25md$	68
Figure 4.7: Log-log Dimensionless derivative plot for $n=0.1$ to 1.0 $l_{yf}=600ft$; $k_x=100md$, $k_y=50md$, $k_z=25md$	69
Figure 4.8: Log-log Plot of dimensionless pressure drop against dimensionless time for $n=0.1$ - 1.0 $l_{yf}=1000ft$; $k_x=100md$, $k_y=50md$, $k_z=25md$	70
Figure 4.9: Log-log Dimensionless derivative plot for $n=0.1$ to 1.0 $l_{yf}=1000ft$ $k_x=100$, $k_y=50$, $k_z=25$	71
Figure 4.10: Log-log Plot of dimensionless pressure drop against dimensionless time for $n=0.1$ - 1 $l_{yf}=1200ft$; $k_x=100$, $k_y=50$, $k_x=25$	74
Figure 4.11: Log-log Dimensionless derivative plot for $n=0.1$ to 1.0 $l_{yf}=1200ft$; $k_x=100$, $k_y=50$, $k_x=25$	75
Figure 4.12: Log-log Plot of dimensionless pressure drop against dimensionless time for $n=0.1$ - 1 length of $600ft$ $k_x = 75md$, $k_y = 75md$ $k_y = 75md$ $h = 300ft$	76
Figure 4.13:Log-log Dimensionless derivative plot for $n=0.1$ to 1.0 $l_{yf}=600ft$; $k_x=k_y=k_z=75md$	77

Figure 4.14: Log-log Plot of dimensionless pressure drop against dimensionless time for $n=0.1 - 1$ $1000ft$ $k_x = 75md$, $k_y = 75md$ $k_z = 75md$ $h = 300ft$ 28

Figure 4.15: Log-log Dimensionless derivative plot for $n=0.1$ to 1.0 $l_{yf}=1000$; $k_y=k_x=k_z=75md$ 79

Figure 4.16: Log-log Plot of dimensionless pressure drop against dimensionless time for $n=0.1 - 1$ $l_{yf}=1200$; $k_x=k_y=k_z=75md$ 80

Figure 4.17: Log-log Dimensionless derivative plot for $n=0.1$ to 1.0 $l_{yf}=1200$; $k_y=k_x=k_z=75md$ 81

LIST OF TABLES

Table 4.1: Correction factors for falloff analysis for Pressure behaviors at fractured wells. (Adapted from Vongvuthiopornchai and Raghavan, 1987).....	54
Table 4.2: Reservoir Properties for generating pressure data to validate k_x	58
Table 4.3: Calculated values of k_x from equation 3 for $n = 0.1$ to 1.....	66

CHAPTER ONE

1.0 INTRODUCTION

1.1 OVERVIEW AND PROBLEM DEFINITION

Although recent studies on the steady and unsteady state flow of non-Newtonian fluid in porous media have brought about new well test analysis for non-Newtonian injection and falloff testing. These methods of analysis have been generally applied to vertical wells for the design and operation of enhanced oil recovery projects. Despite these wide applications, current trends in the industry indicate increasing application of horizontal wells in enhanced oil recovery operations with the use of non-Newtonian fluids such as polymer and micellar solutions. However, the proper understanding and analysis of horizontal well pressure data in non-Newtonian fluid reservoirs such as heavy oil reservoirs will aid in the characterization of heavy oil reservoirs in the nearest future.

The motivation for this work which is the first of its kind is to adequately model new 3-Dimensional equations that would explicitly describe the flow of Non-Newtonian reservoir fluids into horizontal wells; the new diffusivity equation will thus help in adequately evaluating heavy oil reservoirs in terms of, permeability, power-law flow index and mobility using obtained type curves. Furthermore a 3-dimensional study of linear flow of non-Newtonian fluid through porous media will aid further polymer injection processes for enhanced oil recovery.

From Economic and Productivity standpoint, the advantages of horizontal wells over conventional wells or sometimes over hydraulically fractured wells cannot be overemphasized; its application has been vastly employed for a variety of operations involving both Newtonian and Non-Newtonian fluids. The idea behind the use of horizontal well is to increase reservoir area contact .For example, in 1978 Esso Resources Canada drilled a horizontal well at the Cold Lake Leming pilot to field test thermally aided gravity drainage. In 1980, Texaco Canada completed a drilling program to tap unconsolidated bituminous sand at the shallow depths in the Athabasca lease. (Goode and Thambnayagam, SPE 14250).

In this work a new 3-Dimensional single phase Cartesian diffusivity equation is derived for the flow of non-Newtonian fluids in porous media. The diffusivity equation is solved numerically in

dimensionless terms with the aid of finite difference approach for a no-flow boundary condition. A simulation involving different horizontal well length in an a reservoir with permeability anisotropy was carried out with the aid of MATLAB R2007b to obtain pressure transient plots. Series of type curves were obtained from varying situations based on the length of the horizontal well; reservoir permeability, the flow index 'n' and mobility. The numerical solution to the diffusivity equation is validated by comparing with the solution obtained when reservoir fluid is assumed Newtonian.

This work will be valuable in the pressure transient analysis of Horizontal wells in heavy oil reservoir s. This will aid the determination of fluid and rock properties of heavy oil reservoirs, flow index of the reservoir fluid as well as near well bore effect such as Skin and wellbore storage. The work can also be applied to enhanced oil recovery mechanism such as polymer and surfactant injection.

1.2 OBJECTIVE OF STUDY

The objects of this work include the following;

- Developing and solving diffusivity equation of Non-Newtonian fluid flow in porous media for a 3-D linear system as applied to horizontal wells.
- The use of finite difference numerical approach to evaluate the solution of Non-Newtonian pressure transient for a horizontal well located in a closed box-shaped anisotropic reservoir.
- Developing type curves in terms of P_D , t_D and C_D for flow index $n=0.1-1.0$
- The development of type curves; Dimensionless Pressure and Pressure derivative plots for the analysis of pressure transient data of Newtonian and Non-Newtonian fluids.
- Application of the type curves to non-Newtonian fluid flow in horizontal wells to obtain reservoir data such as permeability, Skin and Porosity.
- Identification of a suitable fulcrum point from the developed type curve; this fulcrum point will form a reference point in application to type curve matching of both Newtonian and Non-Newtonian pressure transient analysis for Horizontal wells.

1.3 MOTIVATION FOR STUDY

- Worldwide deposits of heavy hydrocarbons are estimated to total almost 5½ trillion barrels, and four-fifths of these deposits are in the Western Hemisphere (<http://www.petroleumequities.com/HeavyOilReport.htm>). This work will alleviate the difficult production of Large Heavy oil reserves in Canada, Venezuela and other parts of the world in a way to alleviating dwindling global oil supplies.
- To adequately model new 3 Dimensional equations that would explicitly describe the flow of Non-Newtonian reservoir fluid into horizontal wells.
- The New diffusivity equation will thus help in evaluating heavy oil reservoirs as well as polymer injection processes for enhanced oil recovery in the future.
- To enable the adequate evaluation of Non-Newtonian reservoirs properties.
- To form a background on which the proper understanding of Enhanced Oil Recovery (EOR) Processes involving the injection of Polymers, Surfactant and other Non-Newtonian fluids would be based.

1.4 WORK OUTLINE

The first chapter of this work starts with a general overview from which the problem statement was derived. The second chapter details the literature reviews on the Rheology of non-Newtonian fluids, Pressure transient analysis of non-Newtonian fluids as well as literature review on well test analysis of horizontal wells. Chapter three contains the methodology used in this study which includes the mathematical and finite difference formulation; the chapter ends with a description on the development of type curves. Chapter four is made up of validation of results, results and discussion of results, in this chapter the validity of the methodology used in this work is been established. Chapter five is the concluding part of this study comprising the Conclusions and recommendations

CHAPTER TWO

2.0 LITERATURE REVIEW

As mentioned in chapter one, the main objective of this work is to develop type curves for horizontal wells in non-Newtonian reservoirs. This study is the first of its kind with regards to the development of type curves for the analysis of horizontal wells in Non-Newtonian reservoirs. The type curves are developed through simulation which involves the numerical solution through finite difference to the modeled non-linear Partial differential equation describing the flow of non-Newtonian fluid in porous media. In order to achieve this, a detailed literature review is made to aid the success of the study.

2.1 NON-NEWTONIAN FLUIDS

Fluids are generally classified as Newtonian and Non-Newtonian fluids based on the relationship that exist between shear stress and shear rate. For Newtonian fluids the shear stress is proportional to shear rate, while in Non-Newtonian fluid shear stress is not directly proportional to shear rate. There exist several models for the description of Non-Newtonian fluids. The most common of them all is the Bingham plastic fluid and the power law fluids model. According to Ikoku, 1979; it is generally believed that most of the non-Newtonian fluids used in enhanced oil recovery processes are pseudoplastic in nature and their Rheology can be approximated by a power law model.

For Newtonian fluids the shear stress is directly proportional to the shear rate. A Cartesian plot of shear stress against shear rate gives a straight line that passes through the origin. Mathematically;

$$\tau = \mu\gamma \dots\dots\dots 2.1$$

For Non-Newtonian power law model, fluids that are shear-rate dependent are pseudo plastic if the apparent viscosity decreases with increasing shear rate (Bourgoyne et al, 1986) , in this type of fluid the flow behavior index n in equation 2 is less than one ($n < 1$). Non-Newtonian fluids are regarded as dilatant fluids if the

apparent viscosity of the fluid increases with shear rate, in this type of fluids the flow behavior index is greater than one ($n > 1$). The mathematical expression for the power law model is as shown below;

$$\tau = K\gamma^n \dots\dots\dots 2.2$$

K is the consistency index of the fluid with unit $lbf \cdot s^n / ft^2$

n is the power law exponent or the flow – behavior index

According to Bourgoyne et al, the Bingham plastic model is defined by the expression;

$$\tau = \mu_p \gamma + \tau_y; \tau > \tau_y \dots\dots\dots 2.3$$

A Bingham plastic fluid will not flow until the applied shear stress τ exceeds a certain minimum value τ_y known as the yield point. After the yield point has been exceeded, changes in shear stress are proportional to the changes in the shear rate and the constant of proportionality is called the plastic viscosity μ_p . Figure 2.1 from Chukwu, 2011 (Drilling and Well completion lecture notes) shows the difference in the relationship that exists between shear stress and strain for the different non-Newtonian fluids as discussed above.

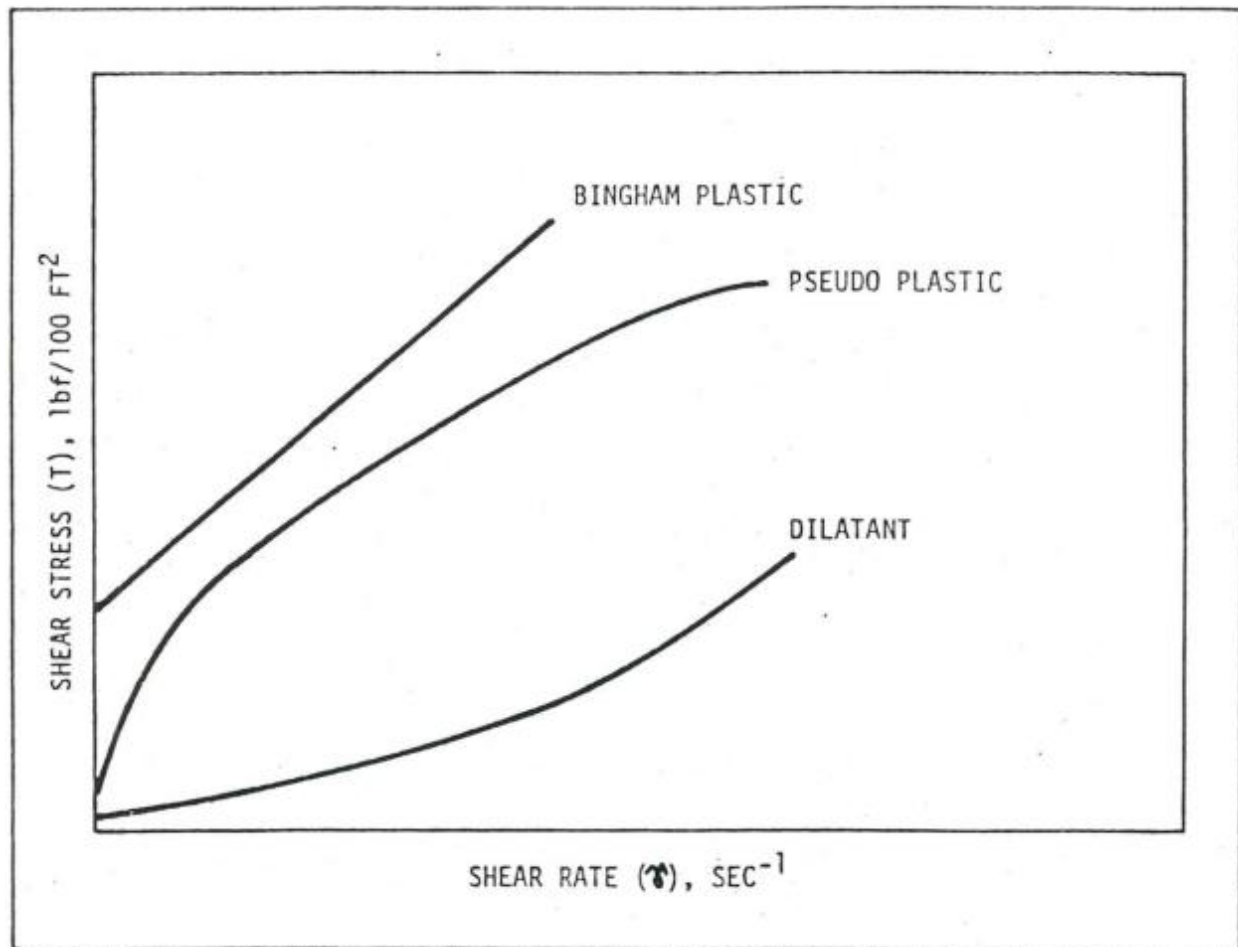


Figure 2.1: Plots of Shear stress Vs Shear rate for time-dependent non-Newtonian fluid (Adapted from Chukwu, Drilling and Well Completion lecture notes)

2.1.1 PRESSURE TRANSIENT ANALYSIS OF NON-NEWTONIAN FLUIDS

Several authors have worked on the pressure transient analysis of non-Newtonian fluids, ranging from the derivation of a new partial differential diffusivity equation that describes the flow of power law fluids in porous media and the analytical solution of the new equation as presented by Ikoku and Ramey, 1979 to present-day study on the subject.

Van Poolen and Jargon, 1969 were the first to study the steady and unsteady state flow of non-Newtonian fluid in porous media from Darcy's equation and the power law model. They presented in their work non-linear differential equations that describe the steady state linear and radial flow of non-Newtonian fluids. The

equations were solved numerically using the finite difference approach. The finite difference solution was presented as plots of dimensionless wellbore pressure against dimensionless time. In considering unsteady state flow for non-Newtonian fluids through porous media, Van Poolen and Jargon, 1969 described the flow of a slightly compressible fluid through porous media by the equation below;

$$\frac{1}{r} \frac{\partial y}{\partial x} \left(\frac{r}{\mu} \frac{\partial P}{\partial r} \right) = \frac{\phi c}{k} \frac{\partial P}{\partial t} \dots\dots\dots 2.4$$

Equation 2.4 was solved using finite difference approach; dividing the model into *i* number of grid cells and solve *i* number of simultaneous equation as obtained for each grid cell from equation 2.4 using initial and boundary conditions as stated below;

Initial condition;

$$P(r, 0) = 0 \dots\dots\dots 2.5$$

Boundary Condition at the wellbore;

$$\frac{q}{A} = \frac{-k}{\mu} \frac{dP}{dr} \dots\dots\dots 2.6$$

Boundary condition at radius of drainage;

$$P(r_e, t) = 0 \dots\dots\dots 2.7$$

Van Poolen and Jargon considered drawdown and falloff response of non-Newtonian fluid in porous media. They established a relationship between pressure differential and flow rate for a steady state flow. Their study lacked analytical methodology and was only for vertical wells; the study considered one dimensional flow and did not use the dimensionless log-log plot to analyze pressure data.

Consequently, the analysis of non-Newtonian injection Pressure data was studied by Ikoku and Ramey, 1979. From the Blake-Kozeny equation as shown in equation 2.8, the power law non-Newtonian model and Darcy

equation they derived a new non-linear partial differential equation that described the flow of non-Newtonian fluid in porous media.

$$u = \frac{D_p^2 \phi^3 \Delta P}{150 \mu (1-\phi)^2 L} \dots\dots\dots 2.8$$

In deriving their model for flow of non-Newtonian fluids through porous media, Ikoku and Ramey, 1979 assumed; radial flow, an isotropic reservoir of constant thickness, negligible compressibility, effects of gravity where ignored, the reservoir fluid was a pseudo plastic fluid described by the power law model. In their work, the law of conservation of mass, Darcy law and equation of state where used to derive the new equation. The dimensionless diffusivity equation that describes the radial flow of non-Newtonian fluid in porous media as obtained by Ikoku and Ramey is as shown in equation 9 below;

$$\frac{\partial^2 P_{DNN}}{\partial r_D^2} + \frac{n}{r_D} \frac{\partial P_{DNN}}{\partial r_D} = r_D^{1-n} \frac{\partial P_{DNN}}{\partial r_D} \dots\dots\dots 2.9$$

Equation 2.9 was solved analytically in the works of Ikoku and Ramey, 1979 in the Laplace domain. The inversion of the resulting Laplacian solution was obtained numerically. In their work a more interpretative method was applied because the slope of the straight-line section of the log-log plot of dimensionless pressure against dimensionless time for different n values is very close. This might make type curve matching erroneous when skin effect is considered. In the works of Ikoku and Ramey, a log-log plot of ΔP_{wf} against Δt gives a straight line from which the flow index n was obtained, the intercept at $t = 1$ was also used to determine the effective mobility provided ϕc_t is known. Furthermore, Ikoku and Ramey, 1979 proffered a method of calculating skin from the log-log plot of ΔP_{wf} against Δt as well as the determination of the radius of investigation from the steady state solution of equation 2.9. The study of Ikoku and Ramey, 1979 focused only on the analysis of pressure transient data to obtain mobility, radius of investigation and skin. The study considered one dimensional radial flow pressure transient in vertical wells and did not consider wellbore storage.

Furthermore, Ikoku, 1980 extended well test analysis of non-Newtonian fluids to non-Newtonian injection falloff testing. In his work the principle of superposition was used alongside the analytical solution of equation 2.9 to obtain the effective mobility ratio, reservoir permeability and skin factor. The validity of Ikoku, 1980 work was based on the assumption that the reservoir is liquid filled and the mobility of the injected fluid is essential equal to the mobility of the in-situ fluid. Like previous works Ikoku, 1980 only focused on one dimensional radial flow of non-Newtonian fluid as it applies to vertical wells.

Odeh and Yang, 1979 in their work derived a partial differential equation that describes the flow of non-Newtonian , power law slightly compressible fluids in porous media, the equation was solved and the unsteady state analytical solution was use to formulate a method for analyzing injection test data. The steady state solution was used to analyze isochronal test data which was used to calculate the transient drainage radius. The equation derived by Odeh and yang, 1979 is as shown below;

$$\frac{\partial^2 P}{\partial r^2} + \left(1 - \frac{1}{n}\right) \frac{1}{r} \frac{\partial P}{\partial r} = r^{1/n} B \frac{\partial P}{\partial t} \dots\dots\dots 2.10$$

Their results was applied to four fields where injection operations is been carried out, in their work, the error associated with the calculation of reservoir permeability from pressure transient analysis based on a Newtonian fluid assumption was considered as compared to when the non-Newtonian pressure transient analysis was made. Odeh and Yang, 1979 used a trial and error method to obtain the flow index n ., they also calculated permeability by a steady-state-type equation using the concept of equivalent transient drainage radius. Odeh and Yang, 1979 found out that the methods of analysis accepted for Newtonian fluids are not satisfactory for non-Newtonian fluids. Odeh and Yang's work like that of Ikoku and Ramey, 1978 focused on one dimensional radial pressure transient of non-Newtonian fluid in vertical wells

Ikoku and Ramey, 1980 considered the effect of skin and wellbore storage on the transient flow of non-Newtonian fluids in petroleum reservoirs, a numerical wellbore storage simulator was used in their study of

skin and wellbore storage during the transient flow of power-law fluids in infinitely large and finite circular reservoirs. Type- curve matching was used to analyze short-time well test data. They obtained a new expression valid for wellbore storage effect when skin exist for infinitely large reservoirs and not for finite circular reservoirs with no-flow or constant-pressure outer boundary. They derived a new expression for skin factor and effective well radius for power-law flow. Equation 9 was solved using the no-flow outer boundary and initial boundary conditions as stated below;

$$P_{DNN}(r, 0) = 0 \dots\dots\dots 2.11$$

$$\left(\frac{\partial P_{DNN}}{\partial r_D}\right)_{r_D=1} = -1 \text{ for } t_{DNN} > 0 \dots\dots\dots 2.12$$

$$\left(\frac{\partial P_{DNN}}{\partial r_D}\right)_{r_{eD}=1} = 0 \text{ for all } t_{DNN} \dots\dots\dots 2.13$$

Where;

$$P_{DNN} = \frac{P - P_i}{\left(\frac{q}{2\pi h}\right)^{\frac{n\mu_{eff}r_w^{1-n}}{k_r}} \dots\dots\dots 2.14$$

$$r_D = \frac{r}{r_w} \dots\dots\dots 2.15$$

$$r_{eD} = \frac{r_e}{r_w} \dots\dots\dots 2.16$$

$$t_{DNN} = \frac{t}{Gr_w^{3-n}} \dots\dots\dots 2.17$$

$$G = \frac{n\phi c_t \mu_{eff}}{k_r} \left(\frac{2\pi h}{q}\right)^{1-n} \dots\dots\dots 2.18$$

Equation 2.9 was solved in Laplace domain the works of Ikoku and Ramey, 1980 using the boundary conditions as stated in equations 2.11 to 2.13. The plots of the dimensionless pressure versus the dimensionless time as

obtained in the works of Ikoku and Ramey, 1980 for a no flow outer boundary condition is as shown in the figure below;

From figure 2.2 in the works of Ikoku and Ramey, it was noticed that at very high values of t_{DNN} , curves of different values of n tend to merge into a straight line of unit slope. In addition, Ikoku and Ramey, 1980 considered the effect of skin on pressure drop in the pressure transient of power-law fluid as shown in the expression below;

$$\Delta P_s = s \left(\frac{q}{2\pi h} \right)^n \frac{\mu_{eff} r_w^{1-n}}{k_r} \dots\dots\dots 2.19$$

According to Ikoku and Ramey, 1979 the pressure drop due to skin can be also be calculated using the expression;

$$\Delta P_s = \left(\frac{q}{2\pi h} \right)^n \frac{\mu_{eff} r_w^{1-n}}{k_r} \left[\left(\frac{r_s}{r_w} \right)^{1-n} - 1 \right] \cdot \left[\frac{k_r - k_s}{(1-n)k_s} \right] \dots\dots\dots 2.20$$

Thus

$$s = \left(\frac{k_r}{k_s} - 1 \right) \left[\left(\frac{r_s}{r_w} \right)^{1-n} - 1 \right] \left(\frac{1}{1-n} \right) \dots\dots\dots 2.21$$

In considering the effect of wellbore storage, Ikoku and Ramey, 1980 used a material balance concept that the production rate must equal the rate of fluid withdrawal from the formation. For injection, the well injection rate must equal the rate of storage of fluid in the wellbore plus the rate of entry into the formation. In dimensionless terms, the wellbore storage is as defined in the works of Ikoku and Ramey below;

$$C_{DNN} \frac{\partial P_{DNN}}{\partial t_{DNN}} + \left(-r_D^n \frac{\partial P_{DNN}}{\partial r_D} \right)_{r_D=1}^{1/n} = 1 \dots\dots\dots 2.22$$

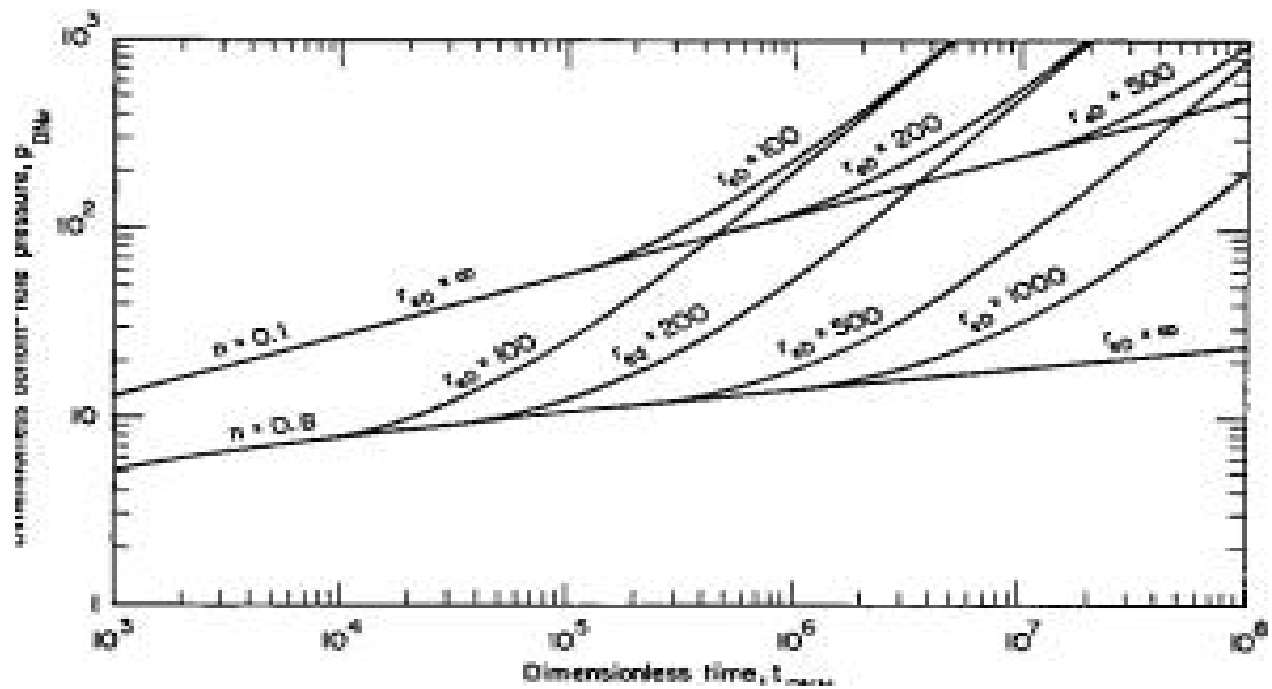


Figure 2.2: Dimensionless bottomhole pressure Vs dimensionless time for no flow at the outer boundary for different flow index (adapted from Ikoku and Ramey, 1980).

Where;

$$C_{DNN} = \frac{c}{2\pi h \phi c_t n r_w^2} \dots\dots\dots 2.23$$

Furthermore, Ikoku and Ramey, 1980 obtained log-log plots of P_{DNN} Vs t_{DNN} for infinitely large reservoirs as well as finite circular reservoirs considering the effects of wellbore storage and skin factors for different values of flow index. In their plots it was found that the effect of skin is more pronounced at low values of t_{DNN} and decreases as t_{DNN} increases. In the works of Ikoku and Ramey, 1980 negative skin was not considered and the study was directed towards vertical wells in one dimensional radial flow.

Olarewaju, 1992 demonstrated the difference in behavior between non-Newtonian and Newtonian fluid in homogeneous and double porosity reservoirs, he also presented practical pressure and derivative type -curve solutions for analyzing data from such reservoir system. He considered wellbore storage and also pointed out

that the rise in pressure decreases with increase in n , In obtaining the type curves for non-Newtonian fluids when wellbore storage is considered, Olarewaju, 1992 presented that derivative type curves for non-Newtonian fluids do not converge to a horizontal 0.5 line as generally noticed for Newtonian flow type curves when wellbore storage is considered. It was also noted in his work that the semi-log straight line that exist beyond the radial flow in the characteristic semi-log $of \Delta P \text{ Vs } \Delta t$ existing for Newtonian fluids is not present for non-Newtonian fluids, rather a semi-log curve exist. A practical example was made in his study to show how the type curves developed can be used to calculate mobility and reservoir permeability for a given effective viscosity and porosity. Olarewaju, 1992 concluded in his work that the conventional semi-log analysis cannot be used if the fluid flowing in the reservoir is non-Newtonian. Although he was able to develop type curves for the analysis pressure transient of non-Newtonian fluids as well as show the misinterpretation that could arise in using a Newtonian type curves to analyze pressure transient of non-Newtonian fluids, His study was only directed to vertical wells alone and in one dimensional radial flow.

In the study of Katime-Meindl and Tiab, 2001, they presented an interpretation technique for pressure behavior of non-Newtonian fluids flow in a homogeneous reservoir without the use of type-curve matching with the aid of the Tiab's direct synthesis technique considering no-flow and constant pressure boundary conditions. In their study a step by step approach for obtaining mobility, wellbore storage coefficient, skin factor and the distance to the nearest boundary without type-curve matching was introduced. Katime-Meindl and Tiab, 2001 study was based on the assumption made in Ikoku and Ramey, 1979 study. The Stehfest algorithm was used to invert the Laplace domain solution that incorporated skin and wellbore storage. Several derivative type-curve where developed for different wellbore storage and skin for various flow indexes in their work. In the study a new equation that is similar to the generally known wellbore storage equation which is in terms of $t * \Delta P'$ was obtained.

An equation was also obtained in their work to estimate the starting time of the infinite acting line of the pressure derivative dimensionless plot for different n values which was in agreement with the values obtained in the works of Ikoku and Ramey, 1979. Furthermore, they proffered techniques of obtaining the mobility ratio when the infinite acting radial line is not obvious or when there is noise in the pressure derivative data, Katime-Meindl and Tiab, 2001 also presented method of calculating the distance to the boundary as well. An example was made on a vertical well in Katime-Meindl and Tiab, 2001 to validate the study. The study did not consider the pressure transient analysis of non-Newtonian fluids in horizontal well.

More recently, Igbokoyi and Tiab, 2007 obtained new type curves for the analysis of pressure transient data dominated by skin and wellbore storage as applied to non-Newtonian fluids. In their comprehensive work, the Laplace domain solution of Ikoku and Ramey, 1979 formed the Mathematical basis of their model. Their type-curve did not use the dimensionless grouping of skin factor and wellbore storage as used in Bourdet and Gringarten, 1980. In their work, they grouped the dimensionless wellbore storage with dimensionless time. The log-log pressure derivative plots at the infinite acting radial flow for the non-Newtonian fluids of various indexes intersected the Newtonian infinite acting pressure derivative line at $\frac{t_D}{c_D} = 1$ which formed a fulcrum point for type-curve matching. In addition the Tiab direct synthesis technique was also applied in the evaluation of non-Newtonian well test data in non-Newtonian fluid flow which did not involve any type-curve matching. An infinite acting behavior was also assumed. The analytical solution in their work was similar to that of Ikoku and Ramey, 1979. Stehfest algorithm was used to invert the solution obtained in the Laplace domain. Igbokoyi and Tiab, 2007 obtained pressure derivative plots for different skin for various flow indexes. Skin factor, dimensionless wellbore storage and mobility were estimated by type curve matching in their study. The Tiab direct synthesis technique was applied based on the unique intersection of the characteristic line on the log-log plot of the type-curve developed. The step in the TDS technique was used to obtain expression to calculate permeability, skin, mobility ratio and wellbore storage. Igbokoyi and Tiab, 2007

validated their study by applying it to a case when $n=1$ found in Lee, 1982 using the type-curve matching approach, TDS and the conventional method. It was found out in their study that the results obtained from the TDS and that for the conventional method for the long time section was higher. Although the works of Igbokoyi and Tiab was quite comprehensive it fails to address horizontal well test analysis of non-Newtonian fluids.

Vongvuthipornchai and Raghavan, 1987 studied the pressure falloff behavior for non-Newtonian power law fluids in vertically fractured wells after injection. In their study they considered wells intercepting infinite-conductivity and uniform flux fractures, the procedures for identifying the flow regimes was also considered in the study. In addition, Vongvuthipornchai and Raghavan, 1987 considered the falloff pressure response of unfractured wells by also examining the validity of using the superposition principle to analyze pressure falloff data provided the pseudo radial flow does exist. They found out that there is the need for corrections in the pressure transient expression obtained by Odeh and Yang, 1979 for a power law index n less than 0.6. The methodology of this present study is similar to the methodology of the study of Vongvuthipornchai and Raghavan, 1987. The underlying assumptions and mathematical model used in Vongvuthipornchai and Raghavan, 1987 work is similar to those used in the works of Murtha and Ertekin, 1983 and that of Ikoku and Ramey, 1979. In their study skin region was incorporated by using the thick skin concept. In their analysis of injection pressure response, they used the same equation as used in Ikoku and Ramey, 1979 to validate the value on n by plotting P_{wD} Vs $t^{\frac{1-n}{3-n}}$. The numerical solution of dimensionless pressure and slopes of Cartesian plots was compared with the solution obtained by Odeh and yang, 1979 and the values were found to be comparatively close. Furthermore, the influence of producing time on falloff data was also considered in their study and this was used in the determination of n from the slope of the pressure response curve on log-log plot. In the study of the effect of superposition in the analysis of falloff data they concluded that the direct application of superposition principle in the analysis of falloff data can result in significant errors as the value

of n decreases, hence the need for a correction factor. It was also shown in the works of Vongvuthipornchai and Raghavan, 1987 that shut-in responses follow the same curve irrespective of the injection time t_D provided that $t_D \gg \Delta t_D$.

Vongvuthipornchai and Raghavan, 1987 validated their work with an example application to show the effect of the correction factor. Vongvuthipornchai and Raghavan, 1987 finally considered both injection and falloff pressure behavior of non-Newtonian fluids at fractured wells in analyzing fractured wells a methodology which is applied in this study a new definition of dimensionless time was formulated based on the fracture half-length, L_{xf} which was given by;

$$t_{Dxf} = \frac{kt}{\phi c_t \mu^* L_{xf}^2} \dots\dots\dots 2.24$$

Where μ^* is given by

$$\mu^* = H \left| \frac{qB}{2\pi h L_{xf}} \right|^{n-1} \dots\dots\dots 2.25$$

It should be noted that H used in the works of Vongvuthipornchai and Raghavan, 1987 is the same as μ_{eff} used in the works of Ikoku and Ramey, 1979, also the definition of the dimensionless pressure is as written below;

$$P_{wD} = \frac{2\pi kh [P_{wf}(t) - P_i]}{qB\mu^*} \dots\dots\dots 2.26$$

The Pressure response was studied for both infinite conductivity and uniform flux fracture. According to the study, Infinite conductivity solution is useful if the well is hydraulically fractured and if the fracture length is small, generally infinite conductivity is classified if the dimensionless fracture conductivity is greater and equal to 500. Uniform flux solution were proposed to be useful in situations where wells are stimulated by acid fracturing or where wells are inadvertently fractured by high injection pressures. Their computations indicated

that at early times a well-defined straight line with slope equal to 0.5 on the log-log coordinates will be evident, they concluded that P_{wD} is given by;

$$P_{wD} = \sqrt{\pi t_{Dxf}} \dots\dots\dots 2.27$$

Furthermore, Vongvuthipornchai and Raghavan, 1987 used pressure derivative technique to analyze the response of a well intercepting a planar fracture during the injection of a non-Newtonian power-law fluid. In order to achieve type-curve matching a correlation was formulated for convenient analysis of falloff data. The analysis of pressure behavior at wells intercepting uniform-flux was similar of those of infinite-conductivity in the study of Vongvuthipornchai and Raghavan, 1987. Similarly a simultaneous match of Pressure and Pressure derivative log-log plots were used to improve matching. Vongvuthipornchai and Raghavan, 1987, the partial linear coordinate differential equation that governs the transient flow of a non-Newtonian and slightly compressible liquid for vertically fractured well in a closed cube reservoir model is as shown in equation 2.28 below. The works of Vongvuthipornchai and Raghavan, 1987 did not consider the pressure transient of non-Newtonian fluids in Horizontal wells and only considered 2 dimensional flows.

$$\frac{\partial}{\partial x_D} \left(\frac{\mu^*}{\mu_a} \frac{\partial P_D}{\partial x_D} \right) + \frac{\partial}{\partial y_D} \left(\frac{\mu^*}{\mu_a} \frac{\partial P_D}{\partial y_D} \right) = \frac{\partial P_D}{\partial t_{Dxf}} \dots\dots\dots 2.28$$

Where P_D is the dimensionless pressure at any point in the reservoir and (x_D, y_D) , x_D, y_D are the dimensionless distance based on L_{xf} (the length of the fracture)

$$P_D(x_D, y_D, t_{Dxf}) = \frac{2\pi kh}{qB\mu^*} [P(x, y, t) - P_i] \dots\dots\dots 2.29$$

$$x_D = \frac{x}{L_{xf}} \dots\dots\dots 2.30$$

$$y_D = \frac{y}{L_{xf}} \dots\dots\dots 2.31$$

Both Infinite conductivity and uniform flux were assumed in the study, for infinite conductivity the wellbore boundary condition for injection at a constant rate was given by;

$$\int_0^1 \left(\frac{\mu^*}{\mu_a} \frac{\partial P_D}{\partial y_D} \right)_{y_D=0} dx_D = -\frac{\pi}{2} \dots\dots\dots 2.32$$

And

$$P_D(x_D \leq 1, y_D = 0, t_{Dxf}) = P_{wD}(t_{Dxf}) \dots\dots\dots 2.33$$

For the uniform flux idealization, Vongvuthipornchai and Raghavan, 1987 assumes that the flux is uniform on the fracture surface $P_D(x_D \leq 1, y_D = 0)$. In this case equation 46 was not valid; i.e., the pressure along the fracture surface is a variable and $P_{wD}(t_{Dxf}) = P_D(0,0, t_{Dxf})$ initial condition is given by;

$$P_D(x_D \leq 1, y_D = 0, t_{Dxf}) = P_{wD}(t_{Dxf}) \dots\dots\dots 2.34$$

A log-log plot of P_{wD} Vs t_D showing the flowing well response as obtained by Vongvuthipornchai and Raghavan, 1987 for constant rate injection is as shown in the figure below;

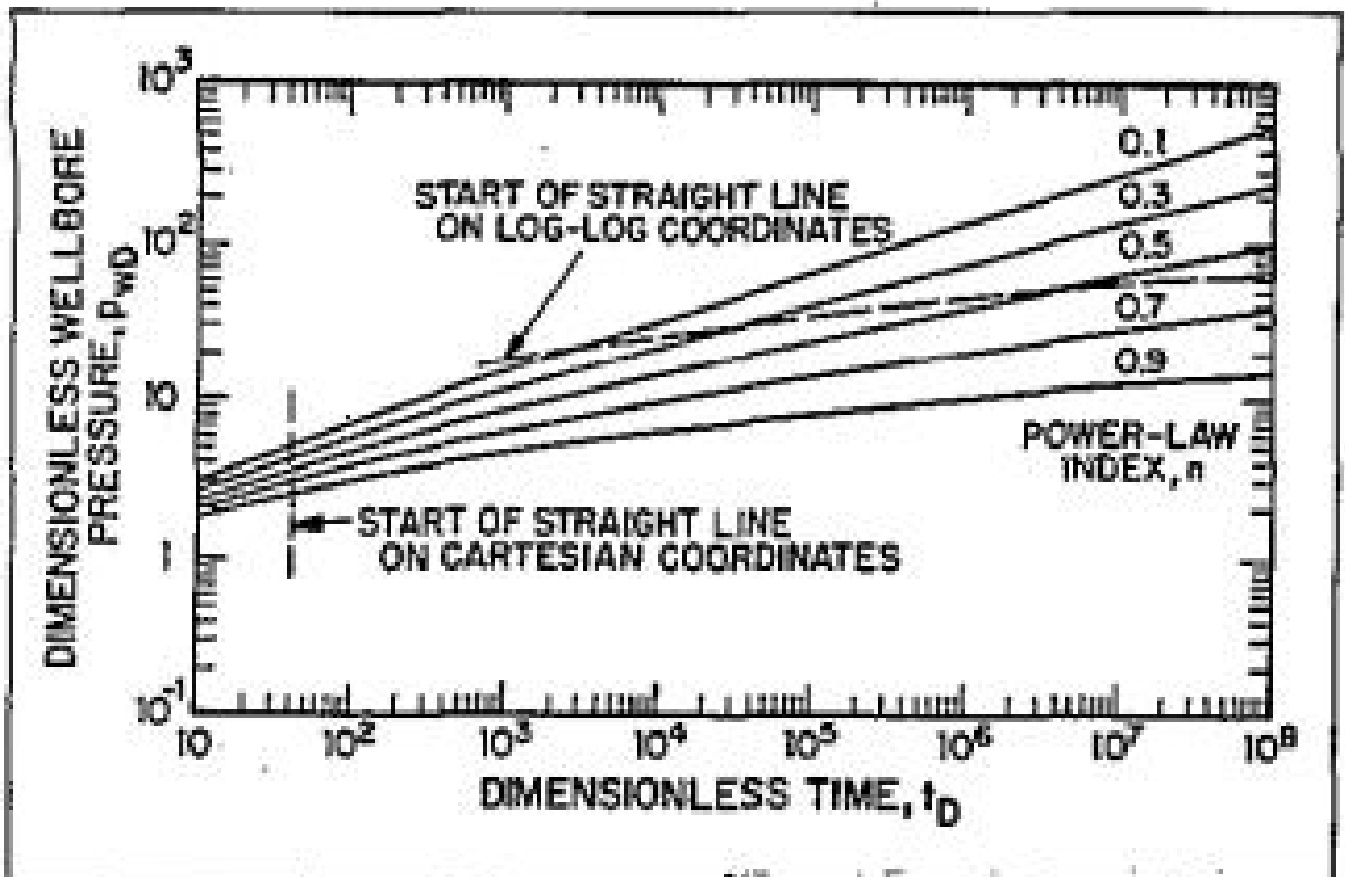


Figure 2.3: Flowing well response for constant rate injection (Adapted from Vongvuthipornchai and Raghavan, 1987)

It is generally believed that most of the non-Newtonian fluids used in enhanced oil recovery processes are pseudo plastic in nature and their Rheology can be approximated by the power-law model (Ikoku, 1979). Generally speaking most of the works on pressure transient analysis of non-Newtonian fluid were directed towards fall off and build up test and vertical wells, very little have been done on draw down tests and horizontal wells which is the focus of this present study, also most of the works have considered analytical solutions in the cylindrical coordinates with a few numerical solution of the differential equation describing the flow of non-Newtonian fluid in porous media.

2.2 HORIZONTAL WELLS

Horizontal wells accelerate recovery and hence improve economics in a broad range of reservoir characteristics (Medeiros et al, 2007 IPTC11781). Horizontal wells can greatly increase the contact area of the wellbore and the pay zone; so they are commonly applied in reservoirs to enhance the production and recovery, especially in low permeability formations (Al Rbeawi and Tiab, 2011, SPE 142316). They also have been used successfully: (a) to intersect fractures and effectively drain reservoirs; (b) in water and gas driven reservoirs to minimize water and gas coning ; (c) in both high and low producing reservoirs to reduce the number of producing wells; (d) in tertiary recovery application to enhance the contact between the well and the reservoir, and (e) finally in offshore reservoirs as well as in environmentally sensitive areas to cut down the cost of drilling and the number of production facilities (Al Rbeawi and Tiab, 2011, SPE 142316). These advantages of horizontal wells have made it widely applicable in the petroleum industry over the past few decades. Amongst other applications, Horizontal wells are used in Enhanced oil recovery processes such as steam injection; steam Assisted Gravity Drainage (SAGD), cyclic injection production techniques and production of tight formations.

2.2.1 HORIZONTAL WELL PRESSURE TRANSIENT ANALYSIS

According to Rbeawi and Tiab, 2011(SPE 142316), five flow regimes have been observed for regular length horizontal wells; early radial flow, early linear flow, pseudo radial flow, channel flow or late linear flow and pseudo-steady state flow. While only four flow regimes have been observed for the extra-long well; linear flow, pseudo-radial flow, channel flow, and pseudo-steady state flow or boundary affected flow. In most cases all these flow regimes are not seen, for example the early radial flow might not be seen if it is obscured by wellbore storage effects or near well-bore effects. Similarly, the pseudo steady state or boundary effect flow is noticed if the draw down test is run for a long time. There are two types of pressure transient behavior depending on effective dimensionless drain hole half-length, L_D . If $L_D < 10$, flow is characterized by an initial

radial flow perpendicular to the drain hole axis followed by a transition to a pseudo-radial flow period. If $L_D > 10$, the initial radial flow period ends instantaneously for all practical purposes. Flow is then characterized by early time linear flow followed by a transition to late time pseudo-radial flow (Molts and Ramey, 1966). It has also been established in the literature that the pressure response of drain hole or horizontal wells is similar to those of vertical fractures, hence sometimes horizontal well are model as fractures. For cases where $L_D > 10$, the uniform flux drain hole solution matches the uniform flux vertical fracture solution. From the definition of L_D , the similarity between drain holes and vertical fractures is directly proportional to the ratios and $\frac{x_f}{h}$ and $\sqrt{\frac{k_z}{k_y}}$. (Molts and Ramey, 1966). Pressure derivative plots i.e. plots of logarithm of dimensionless pressure derivative against logarithm of dimensionless time usually serve as a reliable means of analyzing pressure transient of horizontal wells.

Pressure transient response was obtained by using the initial and boundary conditions in the works of Babu and Odeh (1988). In the study, pressure drop ΔP were obtained at an arbitrary point (x,y,z) in the reservoir by integrations of appropriate Green's functions. In the work of Issaka and Ambastha (1992) the equation as obtained in Babu and Odeh 's study was solved numerically using the Simpson's rule for space integration and trapezoidal rule for the time integration.

Most studies have considered horizontal well pressure transient analysis for Newtonian fluids while there have been no study on the pressure transient analysis of non-Newtonian fluids in horizontal wells. This study seeks to address this problem.

2.3 MATHEMATICAL MODELING AND SOLUTIONS

The Mathematical modeling of the diffusivity equation is based on the law of conservation of mass, the Darcy equation and the equation state. The Importance of this non-linear differential equation has attracted different types of solution ranging from analytical, numerical and semi-analytical solutions.

2.3.1 ANALYTICAL SOLUTION

The equation governing flow is the diffusivity equation as derived from the continuity equation, an equation of state, and Darcy's Law (Matthews, C.S and Russell, D.G: pressure buildup and Flow Tests in wells, Monograph Series, SPE, Dallas (1967))

$$\eta_x \frac{\delta^2 p(M,t)}{\delta x^2} + \eta_y \frac{\delta^2 p(M,t)}{\delta y^2} + \eta_z \frac{\delta^2 p(M,t)}{\delta z^2} - \frac{\delta p(M,t)}{\delta t} = 0 \dots\dots\dots 2.35$$

Where;

$$\eta_x = \frac{k_j}{\phi \mu c}, j = x, y, z \text{ or } r \dots\dots\dots 2.36$$

Equation (1) was expressed in dimensionless terms in the work of Clonts and Ramey, 1966 (SPE 15116) to obtain pressure transient response for drain holes, the dimensionless version of equation was thus solved using Simpson Rule using instantaneous source functions together with the Newman product method. Clonts and Ramey in their study considered a drain hole represented as a constant-rate line source of length $2x_f$ in a reservoir of height h with impermeable upper and lower boundaries. The reservoir was assumed infinite in the x and y directions, with directional permeabilities k_x , k_y and k_z where the horizontal well was located at a height z_w above the bottom of the reservoir. Infinite conductivity and uniform flux conditions were also considered in their study. The reservoir pressure distribution as obtained by Clonts and Ramey is as given below;

$$P_D(x_D, y_D, z_D, z_{wD}, L_D, t_D) = \frac{\sqrt{\pi}}{4} \sqrt{\frac{k}{k_y}} \int_0^{t_D} \left[\operatorname{erf} \left(\frac{\sqrt{\frac{k}{k_x} + x_D}}{2\sqrt{\tau}} \right) + \operatorname{erf} \left(\frac{\sqrt{\frac{k}{k_y} - x_D}}{2\sqrt{\tau}} \right) \right] * \left[\exp \left(\frac{-y_D^2}{4\tau} \right) * \left[1 + 2 \sum_{n=1}^{\infty} \exp(-n^2 \pi^2 L_D^2 \tau) \cos n \pi z_D \cos n \pi z_{wD} \right] \right] \frac{d\tau}{\sqrt{\tau}} \dots\dots\dots 2.37$$

Where, $P_D = \text{dimensionless pressure at any point in the reservoir}$

$t_D = \text{dimensionless time based on } L/2$

P_D and t_D are expressed as;

$$P_D(x_D, y_D, z_D, z_{wD}, L_D, t_D) = \frac{kh}{141.2q\mu B} [p_i - p(x, y, z, L, t)] \dots\dots\dots 2.38$$

$$t_D = \frac{0.001055kt}{\phi c_t \mu L^2} \dots\dots\dots 2.39$$

In the works of Ozkan et al (SPE 16378) k was taken to be the permeability of an equivalent isotropic system;

$k = \sqrt[3]{k_x k_y k_z}$ or to be the equivalent horizontal permeability $k = \sqrt{k_x k_y}$. The dimensionless x_D and y_D

and z_D are represented as:

$$x_D = \frac{2x}{L} * \sqrt{\frac{k}{k_x}} \dots\dots\dots 2.40$$

$$y_D = \frac{2y}{L} * \sqrt{\frac{k}{k_y}} \dots\dots\dots 2.41$$

$$z_D = \frac{z}{h} \dots\dots\dots 2.42$$

Short time approximation was derived in the works of Clonts and Ramey, 1966 (SPE 15116) by approximating an instantaneous source function for each of the three component system i.e (x,t), (y,t) and (z,t) to give;

$$P = \frac{1}{4L_D} Ei \left[-\frac{z_D^2 + y_D^2}{4t_D} \right] \dots\dots\dots 2.43$$

Equation 2.43 above was found to be identical to a radial flow situation where $r_D^2 = z_D^2 + y_D^2$. The aforementioned thus indicate that the early flow towards the drain hole or horizontal well is radial. The end of the early radial flow period was obtained in the work as;

$$t_D \leq \min \left\{ \begin{array}{l} \frac{(1-x_D)^2}{20} \\ \left[z_D + \frac{2(z_{wD}-1)}{L_D} \right]^2 \\ \frac{20}{20} \\ \left[z_D + \frac{2z_{wD}}{L_D} \right]^2 \\ \frac{20}{20} \end{array} \right. \dots\dots\dots 2.45$$

The long time approximation as for pressure transient behavior for horizontal well was obtained by Clonts and Ramey, 1966 in a way similar to the determination of the short time approximation as;

$$P_D(x_D, y_D, z_D, z_{wD}, L_D, t_D) = \frac{\pi}{4} \int_0^{t_D} 1 + 2 \sum_{n=1}^{\infty} [\exp(-n^2 \pi^2 L_D^2 \tau_D) \cos n \pi z_{wD} - \cos n \pi (z_D L_D + z_{wD})] \left[\operatorname{erf} \frac{(1+x_D)}{\sqrt{2\tau_D}} + \operatorname{erf} \frac{(1-x_D)}{\sqrt{2\tau_D}} \right] \left[\exp\left(-\frac{y_D^2}{4\tau_D}\right) \right] d\tau_D + \int_{\tau_D}^{t_D} \frac{1}{\sqrt{2\tau_D}} d\tau_D \dots\dots\dots 2.46$$

The above equation applies when;

$$t_D = \max \left\{ \begin{array}{l} \frac{5}{\pi^2 L_D^2} \\ 25 y_D^2 \\ \left[\frac{25 \left(\frac{1}{2} + x_D \right)^2}{3} \right] \\ \left[\frac{25 \left(\frac{1}{2} - x_D \right)^2}{3} \right] \end{array} \right. \dots\dots\dots 2.47$$

Uniform flux assumption is usually made for mathematical convenience in the modeling of conventional horizontal well models because the pressure responses obtained by uniform flux models are similar to those obtained by infinite conductivity models (Ozkan, 2001).

2.3.2 NUMERICAL SOLUTION TO DIFFUSIVITY EQUATION

Analytical solutions to diffusivity equations have become more rigorous and ineffective when more complex reservoir systems are being modeled. The application of using numerical methods to solve the diffusivity equation in highly heterogeneous reservoirs is gaining prominence. This involves the division of the reservoir

into fine grids and the use of very small time steps. In most cases tools like finite difference, finite volume, Boundary element and finite element methods are used to convert the diffusivity Partial differential equations into linear systems of equations, this process is called Discretization. Of all these numerical methods the finite difference numerical solution to partial differential equation is widely used because of its simplicity. This work involves the application of finite difference approach to solve the modeled non-Newtonian diffusivity equation.

2.3.3 FINITE DIFFERENCE APPROXIMATION

Finite difference is a numerical tool used to solving Ordinary and Partial differential equations, especially non-linear differential equations. In petroleum engineering, finite difference is used to solve partial differential equation that describes the flow of fluid in porous media i.e. the diffusivity equation. The finite-difference method is implemented by superimposing a finite-difference grid over the reservoir to be modeled. The chosen grid system is then used to approximate the spatial derivatives in the continuous equations. These approximations are obtained by truncating the Taylor series expansion of the unknown variable Ertekin et al , 2001

The Block centered scheme which is defined by the centers of each grid block and the point distributed finite-difference schemes defined by the distribution of grid points over the reservoir before boundaries are specified are the widely used in reservoir simulation applicable to the spherical, cylindrical, elliptical and linear or rectangular coordinate system. The rectangular coordinate system is commonly used in reservoir simulation such as predicting well performance and to model pattern element in pattern flooding. The block centered system is commonly used because the volume associated with each grid point is clearly defined; it also adheres more closely to the material balance concept of reservoir engineering. Through discretization a system of equations can be obtained to compute the unknown properties such as pressure or saturation for every grid cell that the reservoir has been divided into. Furthermore, differential equations can be digitized

using the central difference, forward difference or the backward difference approximations. The central difference approximation is used for the second derivative in the diffusivity equation because of its higher order of approximation;

$$\frac{\partial^2 P}{\partial x^2} = \frac{P_{i+1} - 2P_i + P_{i-1}}{\Delta x^2} \dots\dots\dots 2.48$$

The first order derivative is usually approximated by the backward difference approximation as shown below;

$$\frac{\partial P}{\partial x} = \frac{P_i - P_{i-1}}{\Delta x} \dots\dots\dots 2.49$$

The choice of the finite difference approximation to used is dependent on the stability of the systems of equations obtained. Stability is a property that describes the capacity of a small error to propagate and grow with subsequent calculations Ertekin et al , 2001. The grid system is used to divide the reservoir into small partitions which will have the characteristic properties assigned. In most cases, finer grids are used for important features such as the producing zones while larger size grids may be used for aquifers and less important features. Boundary conditions are implemented in two ways; firstly, when there are no discrete points at the boundary which is in most cases used for no flow boundaries while the other method is applicable when points are specified on the boundary. The grids are distributed over the entire reservoir.

2.3.4 FINITE DIFFERENCE FORMULATION

If the flow of fluid through one dimensional system, say a 1D grid block is described by a second order differential equation as shown below in Ertekin et al, 2001;

$$\frac{\partial}{\partial x} \left(\beta_c \frac{A_x k_x}{\mu_l B_l} \frac{\partial P}{\partial x} \right)_l \approx \frac{1}{\Delta x_i} \left[\left(\beta_c \frac{A_x k_x}{\mu_l B_l} \frac{\partial P}{\partial x} \right)_{i+\frac{1}{2}} - \left(\beta_c \frac{A_x k_x}{\mu_l B_l} \frac{\partial P}{\partial x} \right)_{i-\frac{1}{2}} \right] \dots\dots\dots 2.50$$

This can be further re-written as;

$$\frac{1}{\Delta x_i} \left[\left(\beta_c \frac{A_x k_x}{\mu_l B_l} \right)_{i+\frac{1}{2}} \left(\frac{\partial P}{\partial x} \right)_{i+\frac{1}{2}} - \left(\beta_c \frac{A_x k_x}{\mu_l B_l} \right)_{i-\frac{1}{2}} \left(\frac{\partial P}{\partial x} \right)_{i-\frac{1}{2}} \right] * \Delta x_i + q_{isci} = \left(\frac{V_b \phi c_l}{\alpha_c B_l^o} \frac{\partial P}{\partial t} \right)_i \dots\dots\dots 2.51$$

The use of central difference to approximate $\left(\frac{\partial P}{\partial x} \right)_{i+\frac{1}{2}}$ and $\left(\frac{\partial P}{\partial x} \right)_{i-\frac{1}{2}}$ gives

$$\left(\frac{\partial P}{\partial x} \right)_{i+\frac{1}{2}} = \frac{P_{i+1} - P_i}{x_{i+1} - x_i} = \frac{P_{i+1} - P_i}{x_{i+\frac{1}{2}}} \dots\dots\dots 2.52$$

$$\left(\frac{\partial P}{\partial x} \right)_{i-\frac{1}{2}} = \frac{P_i - P_{i-1}}{x_i - x_{i-1}} = \frac{P_i - P_{i-1}}{x_{i-\frac{1}{2}}} \dots\dots\dots 2.53$$

Equation 2.51 thus becomes;

$$\left(\beta_c \frac{A_x k_x}{\mu_l B_l \Delta x} \right)_{i+\frac{1}{2}} (P_{i+1} - P_i) - \left(\beta_c \frac{A_x k_x}{\mu_l B_l \Delta x} \right)_{i-\frac{1}{2}} (P_i - P_{i-1}) + q_{isci} = \left(\frac{V_b \phi c_l}{\alpha_c B_l^o \Delta t} \right)_i (P_i^{n+1} - P_i^n) \dots\dots\dots 2.54$$

Although the central -difference approximation is a higher order approximation, it is generally not used because of stability problems and difficulties in applying the initial conditions Aziz and Settari, 1990. Like with when approximating finite difference for special derivative, the forward and backward finite difference is used for first order time derivative while the second central difference approximation is used for second order time derivative. For example, the backward - difference approximation for a first order derivative with respect to time.

$$\frac{\partial P}{\partial t} = \frac{P_i^{n+1} - P_i^n}{\Delta t} \dots\dots\dots 2.55$$

While the forward difference approximation is given as;

$$\frac{\partial P}{\partial t} = \frac{P_i^{n+1} - P_i^n}{\Delta t} \dots\dots\dots 2.56$$

Although equation 2.55 and 2.56 looks similar the difference between them is that in the forward difference approximation of the pressure derivative with respect to time, the right hand side derivative with respect to

space is approximated using a finite difference at time n , while the backward difference uses a derivative with respect to space at time $n+1$. The central difference approximation with respect to time considers a base time of n as shown in the equation below;

$$\frac{\partial P}{\partial t} = \frac{P_{i+1}^{n+1} - P_{i-1}^n}{2\Delta t} \dots\dots\dots 2.57$$

The two most common boundary conditions are the constant pressure boundary condition and the no-flow boundary condition. A constant pressure boundary condition implies that the pressure gradient at the reservoir boundary is constant as denoted by the equation below;

$$\frac{\partial P}{\partial x} = \frac{P_i - P_{i-1}}{\Delta x} = C \dots\dots\dots 2.58$$

Where C is a constant which may be time dependent or not, it should be noted that the boundary condition can be expressed as forward, backward or central difference as it was discussed for the time derivative discretization. For a no flow boundary condition; $C=0$ in equation 2.58.

The explicit and implicit finite difference formulations are usually used to determine the pressure for each time step. Because of the time levels assigned to the pressures on the left sides of the equations, forward – difference equation results in an explicit calculation for the new –time-level pressures in the $n+1$ time basis while the backward –difference equation results in an implicit calculation for the new-time-level pressures.

The next chapter will discuss more about the application of finite difference in this study.

2.4 CONVENTIONAL METHODS AND TYPE CURVES ANALYSIS OF PRESSURE TRANSIENT DATA

Over the years type curves have become an important tool in the analysis of well test data especially when dealing with horizontal wells, with the aid of type curve matching as presented by Ramey, 1976 (SPE 5878).

Type curve matching has thus help on the evaluation of reservoir properties such as the permeabilities k_x , k_y and k_z as well as near well bore effects such as skin and wellbore storage. The L_D match point yields the ratio $\frac{k_x}{k_y}$

and the P_D match point yield k_y , the x_D match point combined with other directional permeability data yields $\frac{k_y}{k_z}$ the $\phi\mu c_t$ may be determined by the time match (Clonts and Ramey, 1966). The skin factor is usually determined by subtracting the pseudo skin factor determined just before the long time approximation from the total skin factor. Skin factor is negative for a stimulated wellbore and positive for a damaged wellbore.

To use pressure derivatives in well test analysis, it is necessary to develop design equations and type curves based on pressure derivatives for the system in question (Issaka and Ambastha, 1992). The most widely used form of type curves employed in well test analysis is the log-log plot of dimensionless pressure derivative versus dimensionless time. A typical type curve as obtained in the study of Issaka and Ambastha for a horizontal well located in a closed reservoir is as shown below:

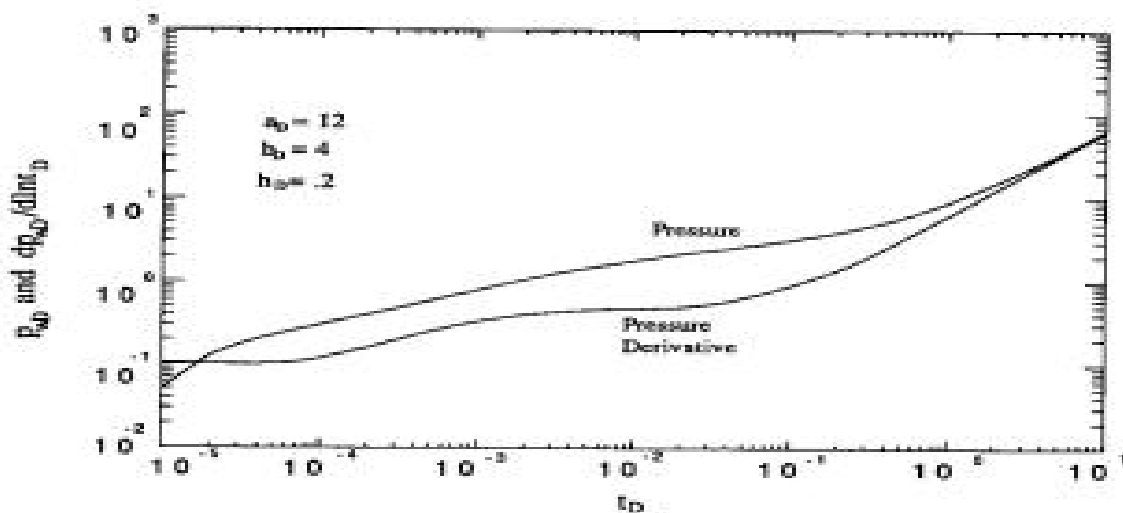


Figure 2.4: A typical dimensionless pressure and Semi-log pressure derivative response for a horizontal well in a closed box-shaped reservoir (Adapted from Issaka and Ambastha, 1992)

A typical horizontal well type curve as shown in figure 2.4 is characterized by: an early radial flow which a slope of zero, in this flow regime the convergence of flow is from the vertical plane perpendicular to the axis of the horizontal well; early linear flow of a line of 0.5 slope; late pseudo-radial flow of a slope of zero; late

linear flow represented by a straight line of slope of 0.5 and a pseudo-steady state flow characterized by a unit slope. A conventional plot of P_{wf} against t in the early radial flow gives a straight line whose slope is as given;

$$m_{er} = \frac{162.6qB\mu}{\sqrt{k_y k_z} L h} \dots\dots\dots 2.59$$

From equation 13 above the term $\sqrt{k_y k_z}$ can be easily obtained. In the works of Ozkan, 2001, for a long horizontal well satisfying the criteria;

$$L \geq 100 h \sqrt{\frac{k}{k_z}} \dots\dots\dots 2.60$$

The intermediate linear flow regime is obvious; a conventional Cartesian plot of P_{wf} against \sqrt{t} will give a straight line with a slope of;

$$m_{il} = \frac{8.13qB\sqrt{\mu}}{\sqrt{\phi c_t L h k_y} h} \dots\dots\dots 2.61$$

From equation 2.61 above the permeability $\sqrt{k_y}$ can be obtained

The pseudo-radial or late radial flow is thus characterized on a conventional P_{wf} against t plot as a straight line with the slope;

$$m_{lr} = \frac{162.6q\mu B}{\sqrt{k_x k_y} h} \dots\dots\dots 2.62$$

From equation 2.62 above the term $\sqrt{k_x k_y}$ which is regarded as the horizontal permeability can be obtained.

From the afore mentioned procedure it could be seen that the conventional methods can only be used to determine the horizontal permeability, k_y and $\sqrt{k_y k_z}$. However, It also be noted that type-curve matching can only provide the horizontal permeability $\sqrt{k_x k_y}$ and the vertical permeability, thus a combination of

conventional and type curve pressure transient analysis will enable the permeabilities description of a reservoir.

It should be noted that the analysis of horizontal well test data might be incomplete due to near wellbore conditions such as wellbore storage and skin, restrictions caused by extremely long wells causing a delay in the pseudo-radial flow and the non-existence of the intermediate linear or pseudo-radial flow.

2.4.1 WELLBORE STORAGE

As stated earlier, the presence of wellbore storage affects the pressure transient of horizontal wells. In the analysis of the drawbacks of conventional pressure transient method, Ozkan (2001) showed that a moderate – to-Small wellbore storage can destroy the early and intermediate –time flow periods. Unlike vertical wells, the analysis of horizontal well pressure data after the wellbore storage effect cannot provide information about the directional permeabilities obtainable without the influence of the wellbore storage. Techniques such as advance convolution are used to remove the effect of well bore storage on horizontal well pressure transient for the complete analysis of well test data.

According to Ikoku and Ramey, 1979 the physical effect of wellbore storage is to cause a sand-face injection or production that initially is zero and increases toward the surface wellhead flow rate as a function of time, even though the surface injection or production is held constant. From their work , they assumed fluid is stored in the wellbore by virtue of compression, the wellbore storage constant C (m^3/Pa) is defined by the material balance;

$$C = V_w c \dots\dots\dots 2.63$$

$$q = C \frac{\partial P_{wf}}{\partial t} + q_{sf} \dots\dots\dots 2.64$$

2.4.2 SKIN FACTOR

The definition of Skin by Ozkan, 2001 considers the steady-state skin factor putting into consideration the possible non-uniformity of the skin zone. The skin factor has been found to be a function of flux which is in turn a function of time and location along the horizontal well length as seen from equation 2.70. The skin factor obtained from equation 2.70 is thus time –dependent besides flow period when the flux remains constant. According to Ozkan,2001, analysis of well test data are subjected to some error due to the presence of non-uniform skin distribution, errors are minimal when skin distribution are regarded to be uniform. The differences in the skin at the heel and at the toe of a horizontal well due to non-uniform skin distribution can lead to erroneous determination of horizontal permeability. The presence of uniform or non-uniform skin also masks the analysis of horizontal well test data. Therefore, the effect of skin factor should be incorporated into the analytical solution of the pressure transient equation as presented by Ozkan and Raghavan, 1997 in the equation below;

$$P_{hD}(x_D, t_D) = P(x_D, r_{wD}, z_{wD}, t_D) + q_{hD}(x_D, t_D)S(x_D) \dots\dots\dots 2.65$$

$$q_{hD} = \frac{q_h(x,t)L_h}{q} \dots\dots\dots 2.66$$

$$S(x_D) = \frac{\frac{kh}{141.2qB\mu} \Delta P_s(x,t)}{q_{hD}(x,t)} \dots\dots\dots 2.67$$

ΔP_s =pressure drop across the skin zone.

Assuming that;

$$\tilde{S}(x_D) = q_{hD}(x_D, t_D)S(x_D) \dots\dots\dots 2.68$$

$$P_{wD}(x_{D,}) = P_D(r_{wD}, z_{wD}, t_D) + q_{hD}(x_D, t_D)\tilde{S}(0, t_D) \dots\dots\dots 2.69$$

$$\tilde{S} = 1.151 \left(\frac{\Delta P_{wf}}{m} - \frac{P_D}{1.151} \right) \dots\dots\dots 2.70$$

ΔP_{wf} is the drawdown measured at the heel of the well at a given time t , m is the logarithmic derivative of the drawdown with respect to time defined at the same time and P_D is the dimensionless pressure without skin effect.

CHAPTER THREE

3.0 METHODOLOGY

The approach used in carrying out this study is as listed below;

- Establishing basic assumptions
- Modeling of Partial differential diffusivity equation that describes the flow of non-Newtonian fluids based on the assumptions made. The modeling involved the use of the law of conservation of mass, the Darcy equation and the equation of state from which the viscosity ratio $\frac{\mu^*}{\mu_a}$ is obtained.
- Expressing the diffusivity equations in terms of dimensionless terms using the appropriate dimensionless variables.
- Formulating initial and boundary conditions that would aid solution of the diffusivity equation
- Discretizing the diffusivity equation with the aid of finite difference approximation
- Writing of a MATLAB code to solve the system of equations obtained from discretization. This will help in obtaining dimensionless pressured for each time step.
- Writing a MATLAB program for the convergence of the viscosity ratio $\frac{\mu^*}{\mu_a}$
- Making log-log plots of P_{wfD} (*dimensionless bottom hole flowing pressure*) vs t_D for different well and reservoir configurations when Newtonian fluids are considered for validation purpose.
- Making log-log plots of P_{wfD} (*dimensionless bottom hole flowing pressure*) vs t_D for different well and reservoir configurations and non-Newtonian reservoir fluids.
- Developing type curves $t_D * P'_{wD}$ vs t_D for non-Newtonian reservoir fluids with power law index $n = 0.1 - 1.0$.

3.1 BASIC ASSUMPTIONS

The Basic assumptions made in the modeling of the problem are;

- Isothermal, single-phase and slightly compressible fluid.
- Linear fluid flow into the wellbore,
- Steady state effective viscosity.
- Homogeneous reservoir with an average porosity with permeability anisotropy. Permeability differs with direction, k_x , k_y and k_z taking k_x to be the maximum permeability
- The Horizontal well was placed in the direction perpendicular to the maximum permeability, that is along the *y-coordinates*
- Power-law Model was used to describe the Non-Newtonian fluid.
- Negligible effects of gravity.
- Reservoir is of constant thickness
- Pseudo-plastic fluid is being considered ($0 < n < 1.0$)
- No flow reservoir boundary is assumed

The methodology used in this work is based on the one used in the works of Vongvuthipornchai and Raghavan, 1987

3.2 MATHEMATICAL FORMULATION OR MODELING

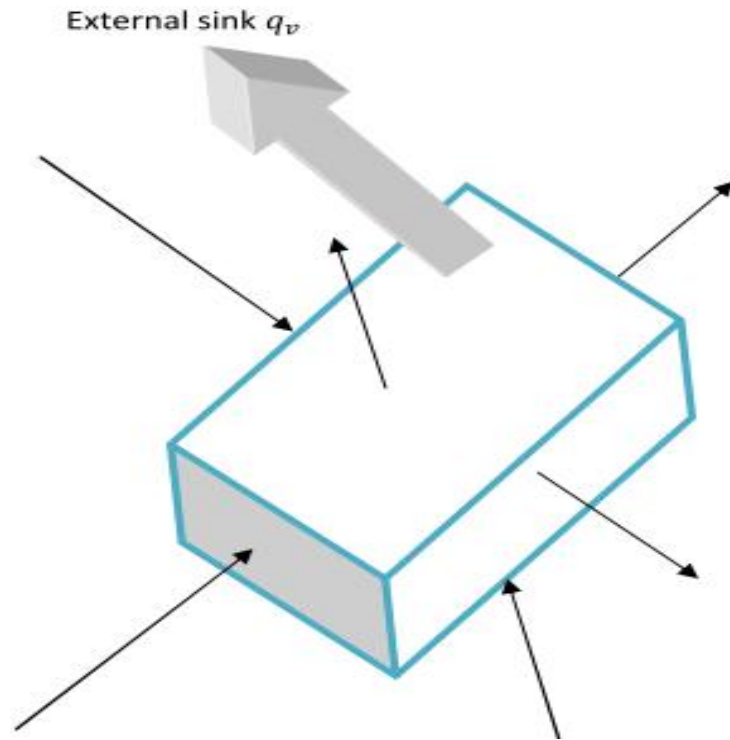


Figure 3.1: Diagram showing the flow through a porous cuboid reservoir model

From the law of conservation of mass;

mass flow rate into the cuboid – mass flow rate out of cuboid – sink = accumulation

$$\left(m_{x-\frac{\Delta x}{2}} - m_{x+\frac{\Delta x}{2}}\right)\Delta t + \left(m_{y-\frac{\Delta y}{2}} - m_{y+\frac{\Delta y}{2}}\right)\Delta t + \left(m_{z-\frac{\Delta z}{2}} - m_{z+\frac{\Delta z}{2}}\right)\Delta t - q_s\Delta t = (\phi\Delta x\Delta y\Delta z\rho)_{t+\Delta t} - (\phi\Delta x\Delta y\Delta z\rho)_t \dots\dots\dots 3.1$$

$m = \text{mass flow rate } \left(\frac{lb}{s}\right)$

$\rho = \text{density } \left(\frac{lb}{ft^3}\right)$

$\phi = \text{porosity } (\%)$

$$m = \rho u A \dots\dots\dots 3.2$$

A= cross-sectional Area

Substituting equation 3.2, Equation 3.1 thus becomes;

$$\left((\rho u_x A_x)_{x-\frac{\Delta x}{2}} - (\rho u_x A_x)_{x+\frac{\Delta x}{2}} \right) \Delta t + \left((\rho u_y A_y)_{y-\frac{\Delta y}{2}} - (\rho u_y A_y)_{y+\frac{\Delta y}{2}} \right) \Delta t + \left((\rho u_z A_z)_{z-\frac{\Delta z}{2}} - (\rho u_z A_z)_{z+\frac{\Delta z}{2}} \right) \Delta t - q_s \Delta t = (\phi \Delta x \Delta y \Delta z \rho)_{t+\Delta t} - (\phi \Delta x \Delta y \Delta z \rho)_t \dots\dots\dots 3.3$$

Dividing through by Δt yields;

$$\left((\rho u_x A_x)_{x-\frac{\Delta x}{2}} - (\rho u_x A_x)_{x+\frac{\Delta x}{2}} \right) + \left((\rho u_y A_y)_{y-\frac{\Delta y}{2}} - (\rho u_y A_y)_{y+\frac{\Delta y}{2}} \right) + \left((\rho u_z A_z)_{z-\frac{\Delta z}{2}} - (\rho u_z A_z)_{z+\frac{\Delta z}{2}} \right) - q_s = \frac{(\phi \Delta x \Delta y \Delta z \rho)_{(t+\Delta t)} - (\phi \Delta x \Delta y \Delta z \rho)_t}{\Delta t} \dots\dots\dots 3.4$$

Re-arranging equation 3.4 gives;

$$-\left((\rho u_x A_x)_{x+\frac{\Delta x}{2}} - (\rho u_x A_x)_{x-\frac{\Delta x}{2}} \right) + \left((\rho u_y A_y)_{y+\frac{\Delta y}{2}} - (\rho u_y A_y)_{y-\frac{\Delta y}{2}} \right) + \left((\rho u_z A_z)_{z+\frac{\Delta z}{2}} - (\rho u_z A_z)_{z-\frac{\Delta z}{2}} \right) - q_s = \frac{(\phi \Delta x \Delta y \Delta z \rho)_{(t+\Delta t)} - (\phi \Delta x \Delta y \Delta z \rho)_t}{\Delta t} \dots\dots\dots 3.5$$

Dividing through by $\Delta x \Delta y \Delta z$ gives

$$-\left[\left(\frac{(\rho u_x)_{x+\frac{\Delta x}{2}} - (\rho u_x)_{x-\frac{\Delta x}{2}}}{\Delta x} \right) + \left(\frac{(\rho u_y)_{y+\frac{\Delta y}{2}} - (\rho u_y)_{y-\frac{\Delta y}{2}}}{\Delta y} \right) + \left(\frac{(\rho u_z)_{z+\frac{\Delta z}{2}} - (\rho u_z)_{z-\frac{\Delta z}{2}}}{\Delta z} \right) \right] - \frac{q_s}{V_b} = \frac{(\phi \rho)_{t+\Delta t} - (\phi \rho)_t}{\Delta t} \dots\dots\dots 3.6$$

Taking limits as $\Delta x \rightarrow 0, \Delta y \rightarrow 0, \Delta z \rightarrow 0, \Delta t \rightarrow 0,$

$$\lim_{\substack{\Delta x \rightarrow 0, \\ \Delta y \rightarrow 0, \\ \Delta z \rightarrow 0, \\ \Delta t \rightarrow 0,}} \left[- \left[\left(\frac{(\rho u_x)_{x+\frac{\Delta x}{2}} - (\rho u_x)_{x-\frac{\Delta x}{2}}}{\Delta x} \right) + \left(\frac{(\rho u_y)_{y+\frac{\Delta y}{2}} - (\rho u_y)_{y-\frac{\Delta y}{2}}}{\Delta y} \right) + \left(\frac{(\rho u_z)_{z+\frac{\Delta z}{2}} - (\rho u_z)_{z-\frac{\Delta z}{2}}}{\Delta z} \right) \right] - \frac{q_s}{V_b} = \frac{(\phi \rho)_{t+\Delta t} - (\phi \rho)_t}{\Delta t} \dots\dots\dots 3.7 \right]$$

$$-\frac{\partial(\rho u_x)}{\partial x} - \frac{\partial(\rho u_y)}{\partial y} - \frac{\partial(\rho u_z)}{\partial z} - \frac{q_s}{V_b} = \frac{\partial(\phi\rho)}{\partial t} \dots\dots\dots 3.8$$

From the equation of state, the formation volume factor is incorporated into equation 3.8 above;

$$B = \frac{\rho_{sc}}{\rho} = \frac{V_{sc}}{V}$$

Where;

ρ_{sc} = density at standard conditions , ρ = density at reservoir conditions

V_{sc} = Volume at standard conditions , V =volume at reservoir conditions

$$u_0 = \frac{D_p^2 \Phi^3 \Delta P}{150 \mu (1-\Phi)^2 L} \dots\dots\dots 3.9$$

$$u_0 = -\frac{k \partial P}{\mu \partial L} \dots\dots\dots 3.10$$

For Non-Newtonian fluids the relationship between the Blake- Kozeny equation (equation 3.9) and the Darcy equation (equation 3.10) yields. From the modified Blake-Kozeny equation for one dimensional flow of power law fluids;

$$u_0 = \frac{n\Phi}{3n+1} \left(\frac{D_p \Phi}{3(1-\Phi)} \right)^{\frac{n+1}{n}} \left(\frac{6\Delta p}{25HL} \right)^{\frac{1}{n}} \dots\dots\dots 3.11$$

The combination of equations 3.9, 3.10 and 3.11 as derived in appendix B gives the relationship;

$$u_0 = - \left[\frac{k}{\mu_{eff}} \frac{\Delta P}{L} \right]^{\frac{1}{n}} \dots\dots\dots 3.12$$

Thus for the Cartesian coordinate system, equation 3.12 becomes;

$$u_x = - \left[\frac{k_x}{\mu_{eff}} \frac{\partial P}{\partial x} \right]^{\frac{1}{n}} \dots\dots\dots 3.13a$$

$$u_y = - \left[\frac{k_y}{\mu_{eff}} \frac{\partial P}{\partial y} \right]^{\frac{1}{n}} \dots\dots\dots 3.13b$$

$$u_z = - \left[\frac{k_z}{\mu_{eff}} \frac{\partial P}{\partial z} \right]^{\frac{1}{n}} \dots\dots\dots 3.13c$$

The effect of gravity is neglected in equations 3.13 (a),(b) and (c). Substituting equations 13(a),(b) and (c) into equation 9 yields;

$$\frac{\partial \left(\rho \left[\frac{k_x}{\mu_{eff}} \frac{\partial P}{\partial x} \right]^{1/n} \right)}{\partial x} + \frac{\partial \left(\rho \left[\frac{k_y}{\mu_{eff}} \frac{\partial P}{\partial y} \right]^{1/n} \right)}{\partial y} + \frac{\partial \left(\rho \left[\frac{k_z}{\mu_{eff}} \frac{\partial P}{\partial z} \right]^{1/n} \right)}{\partial z} - \frac{q_s}{V_b} = \frac{\partial(\phi\rho)}{\partial t} \dots\dots\dots 3.14$$

Multiplying through by V_b ;

$$\frac{\partial \left(\rho A_x \left[\frac{k_x}{\mu_{eff}} \frac{\partial P}{\partial x} \right]^{1/n} \right) \Delta x}{\partial x} + \frac{\partial \left(\rho A_y \left[\frac{k_y}{\mu_{eff}} \frac{\partial P}{\partial y} \right]^{1/n} \right) \Delta y}{\partial y} + \frac{\partial \left(\rho A_z \left[\frac{k_z}{\mu_{eff}} \frac{\partial P}{\partial z} \right]^{1/n} \right) \Delta z}{\partial z} - q_s = V_b \frac{\partial(\phi\rho)}{\partial t} \dots\dots\dots 3.15$$

Note that q_s can be obtained in terms of volumetric rate thus;

$$q_s = q_v * \rho_{sc} \dots\dots\dots 3.16$$

$$\frac{\partial \left(\rho A_x \left[\frac{k_x}{\mu_{eff}} \frac{\partial P}{\partial x} \right]^{1/n} \right) \Delta x}{\partial x} + \frac{\partial \left(\rho A_y \left[\frac{k_y}{\mu_{eff}} \frac{\partial P}{\partial y} \right]^{1/n} \right) \Delta y}{\partial y} + \frac{\partial \left(\rho A_z \left[\frac{k_z}{\mu_{eff}} \frac{\partial P}{\partial z} \right]^{1/n} \right) \Delta z}{\partial z} - q_v = V_b \frac{\partial(\phi\rho)}{\partial t} \dots\dots\dots 3.17$$

$$\frac{\partial \left(\rho A_x \left[\frac{k_x}{\mu_{eff}} \frac{\partial P}{\partial x} \right]^{1/n} \right) \Delta x}{\partial x} + \frac{\partial \left(\rho A_y \left[\frac{k_y}{\mu_{eff}} \frac{\partial P}{\partial y} \right]^{1/n} \right) \Delta y}{\partial y} + \frac{\partial \left(\rho A_z \left[\frac{k_z}{\mu_{eff}} \frac{\partial P}{\partial z} \right]^{1/n} \right) \Delta z}{\partial z} - q_s = V_b \left(\phi \frac{\delta\rho}{\delta t} + \rho \frac{\delta\phi}{\delta t} \right) \dots\dots\dots 3.18$$

Recall that

$$C = \frac{1}{\rho} \frac{\partial\rho}{\partial P} \Rightarrow \frac{\partial\rho}{\partial P} = C\rho$$

Therefore; $\frac{\partial\rho}{\partial t} = \frac{\partial\rho}{\partial P} * \frac{\partial P}{\partial t} = C\rho \frac{\partial P}{\partial t} \dots\dots\dots 3.19$

Substituting equation 3.19 into equation 3.18 gives:

$$\frac{\partial \left(\rho A_x \left[\frac{k_x}{\mu_{eff}} \frac{\partial P}{\partial x} \right]^{1/n} \right) \Delta x}{\partial x} + \frac{\partial \left(\rho A_y \left[\frac{k_y}{\mu_{eff}} \frac{\partial P}{\partial y} \right]^{1/n} \right) \Delta y}{\partial y} + \frac{\partial \left(\rho A_z \left[\frac{k_z}{\mu_{eff}} \frac{\partial P}{\partial z} \right]^{1/n} \right) \Delta z}{\partial z} = \left[V_b \left(C\phi\rho \frac{\partial P}{\partial t} + \rho \frac{\delta\phi}{\delta t} \right) + q_s \right] \dots\dots\dots 3.20$$

Converting q_s from mass flow rate to volumetric flow rate

$$q_s = q_v * B * \rho \dots\dots\dots 3.21$$

Substituting equation 3.21 into equation 3.20 gives;

$$\frac{\partial \left(\rho A_x \left[\frac{k_x}{\mu_{eff}} \frac{\partial P}{\partial x} \right]^{1/n} \right) \Delta x}{\partial x} + \frac{\partial \left(\rho A_y \left[\frac{k_y}{\mu_{eff}} \frac{\partial P}{\partial y} \right]^{1/n} \right) \Delta y}{\partial y} + \frac{\partial \left(\rho A_z \left[\frac{k_z}{\mu_{eff}} \frac{\partial P}{\partial z} \right]^{1/n} \right) \Delta z}{\partial z} = \left[V_b \left(C \phi \rho \frac{\partial P}{\partial t} + \rho \frac{\delta \phi}{\delta t} \right) + q_v B \rho \right] \dots\dots 3.22$$

Thus differentiating equation 3.23 gives the following;

$$\left[\left[\frac{k_x}{\mu_{eff}} \frac{\delta P}{\delta x} \right]^{1/n} A_x \frac{\partial \rho}{\partial x} + \rho A_x \left[\frac{k_x}{\mu_{eff}} \right]^{1/n} \frac{\partial}{\partial x} \left(\frac{\partial P}{\partial x} \right)^{1/n} \right] \delta x + \left[\left[\frac{k_y}{\mu_{eff}} \frac{\delta P}{\delta y} \right]^{1/n} A_y \frac{\partial \rho}{\partial y} + \rho A_y \left[\frac{k_y}{\mu_{eff}} \right]^{1/n} \frac{\partial}{\partial y} \left(\frac{\partial P}{\partial y} \right)^{1/n} \right] \delta y + \left[\left[\frac{k_z}{\mu_{eff}} \frac{\delta P}{\delta z} \right]^{1/n} A_z \frac{\partial \rho}{\partial z} + \rho A_z \left[\frac{k_z}{\mu_{eff}} \right]^{1/n} \frac{\partial}{\partial z} \left(\frac{\partial P}{\partial z} \right)^{1/n} \right] \delta z = \left[V_b \left(C \phi \rho \frac{\partial P}{\partial t} + \rho \frac{\delta \phi}{\delta t} \right) + q_v B \rho \right] \dots\dots\dots 3.23$$

Expanding further using the relationship;

$$\frac{\partial \rho}{\partial x} = \frac{\partial \rho}{\partial P} * \frac{\partial P}{\partial x} \Rightarrow \frac{\partial \rho}{\partial x} = \frac{\partial P}{\partial x} * \rho C \dots\dots\dots 3.24$$

$$\left[\left[\frac{k_x}{\mu_{eff}} \frac{\delta P}{\delta x} \right]^{1/n} A_x \frac{\partial P}{\partial x} \rho C + \rho A_x \left[\frac{k_x}{\mu_{eff}} \right]^{1/n} \frac{\partial}{\partial x} \left(\frac{\partial P}{\partial x} \right)^{1/n} \right] \delta x + \left[\left[\frac{k_y}{\mu_{eff}} \frac{\delta P}{\delta y} \right]^{1/n} A_y \frac{\partial P}{\partial y} \rho C + \rho A_y \left[\frac{k_y}{\mu_{eff}} \right]^{1/n} \frac{\partial}{\partial y} \left(\frac{\partial P}{\partial y} \right)^{1/n} \right] \delta y + \left[\left[\frac{k_z}{\mu_{eff}} \frac{\delta P}{\delta z} \right]^{1/n} A_z \frac{\partial P}{\partial z} \rho C + \rho A_z \left[\frac{k_z}{\mu_{eff}} \right]^{1/n} \frac{\partial}{\partial z} \left(\frac{\partial P}{\partial z} \right)^{1/n} \right] \delta z = \left[V_b \left(C \phi \rho \frac{\partial P}{\partial t} + \rho \frac{\delta \phi}{\delta t} \right) + q_v B \rho \right] \dots\dots\dots 3.25$$

Thus for a constant density fluid with negligible viscosity, where C=0 equation 3.25 thus becomes;

$$\left[A_x \left[\frac{k_x}{\mu_{eff}} \right]^{1/n} \frac{\partial}{\partial x} \left(\frac{\partial P}{\partial x} \right)^{1/n} \right] \delta x + \left[\rho A_y \left[\frac{k_y}{\mu_{eff}} \right]^{1/n} \frac{\partial}{\partial y} \left(\frac{\partial P}{\partial y} \right)^{1/n} \right] \delta y + \left[\rho A_z \left[\frac{k_z}{\mu_{eff}} \right]^{1/n} \frac{\partial}{\partial z} \left(\frac{\partial P}{\partial z} \right)^{1/n} \right] \delta z = \left[V_b \left(C \phi \frac{\partial P}{\partial t} + \frac{\delta \phi}{\delta t} \right) + q_v B \right] \dots\dots\dots 3.26$$

Dividing through by V_b and differentiating equation 3.36 yields;

$$\frac{1}{n} \left[\frac{k_x}{\mu_{eff}} \right]^{1/n} \frac{\partial^2 P}{\partial x^2} \left(\frac{\partial P}{\partial x} \right)^{1-n} + \frac{1}{n} \left[\frac{k_y}{\mu_{eff}} \right]^{1/n} \frac{\partial^2 P}{\partial y^2} \left(\frac{\partial P}{\partial y} \right)^{1-n} + \frac{1}{n} \left[\frac{k_z}{\mu_{eff}} \right]^{1/n} \frac{\partial^2 P}{\partial z^2} \left(\frac{\partial P}{\partial z} \right)^{1-n} = \left[\left(C \phi \frac{\partial P}{\partial t} + \frac{\delta \phi}{\delta t} \right) + \frac{q_v B}{V_b} \right] \dots\dots\dots 3.27$$

From the chain rule; $\frac{\partial \phi}{\partial t} = \frac{\partial P}{\partial t} * \frac{\partial \phi}{\partial P}$ equation 3.27 thus becomes

$$\frac{1}{n} \left[\left[\frac{k_x}{\mu_{eff}} \right]^{\frac{1}{n}} \frac{\partial^2 P}{\partial x^2} \left(\frac{\partial P}{\partial x} \right)^{\frac{1-n}{n}} + \left[\frac{k_y}{\mu_{eff}} \right]^{\frac{1}{n}} \frac{\partial^2 P}{\partial y^2} \left(\frac{\partial P}{\partial y} \right)^{\frac{1-n}{n}} + \left[\frac{k_z}{\mu_{eff}} \right]^{\frac{1}{n}} \frac{\partial^2 P}{\partial z^2} \left(\frac{\partial P}{\partial z} \right)^{\frac{1-n}{n}} \right] = \left[\left(C \phi \frac{\partial P}{\partial t} + \frac{\partial P}{\partial t} * \frac{\partial \phi}{\partial P} \right) + \frac{q_v B}{V_b} \right] \dots 3.28$$

$$\frac{1}{n} \left[\left[\frac{k_x}{\mu_{eff}} \right]^{\frac{1}{n}} \frac{\partial^2 P}{\partial x^2} \left(\frac{\partial P}{\partial x} \right)^{\frac{1-n}{n}} + \left[\frac{k_y}{\mu_{eff}} \right]^{\frac{1}{n}} \frac{\partial^2 P}{\partial y^2} \left(\frac{\partial P}{\partial y} \right)^{\frac{1-n}{n}} + \left[\frac{k_z}{\mu_{eff}} \right]^{\frac{1}{n}} \frac{\partial^2 P}{\partial z^2} \left(\frac{\partial P}{\partial z} \right)^{\frac{1-n}{n}} \right] = \left[\phi \frac{\partial P}{\partial t} \left(C + \frac{1}{\phi} \frac{\partial \phi}{\partial P} \right) + \frac{q_v B}{V_b} \right] \dots 3.29$$

Taking $\left(C + \frac{1}{\phi} \frac{\partial \phi}{\partial P} \right) = c_t$

$$\frac{1}{n} \left[\left[\frac{k_x}{\mu_{eff}} \right]^{\frac{1}{n}} \frac{\partial^2 P}{\partial x^2} \left(\frac{\partial P}{\partial x} \right)^{\frac{1-n}{n}} + \left[\frac{k_y}{\mu_{eff}} \right]^{\frac{1}{n}} \frac{\partial^2 P}{\partial y^2} \left(\frac{\partial P}{\partial y} \right)^{\frac{1-n}{n}} + \left[\frac{k_z}{\mu_{eff}} \right]^{\frac{1}{n}} \frac{\partial^2 P}{\partial z^2} \left(\frac{\partial P}{\partial z} \right)^{\frac{1-n}{n}} \right] = \left[c_t \phi \frac{\partial P}{\partial t} + \frac{q_v B}{V_b} \right] \dots 3.30$$

Recalling from equation 13a, 13b and 13c;

$$\left(\frac{\partial P}{\partial x} \right)^{\frac{1}{n}} = -u_{0x} \left[\frac{\mu_{eff_x}}{k_x} \right]^{\frac{1}{n}} \Rightarrow \left(\frac{\partial P}{\partial x} \right)^{\frac{1}{n}-1} = -u_{0x} \left[\frac{\mu_{eff_x}}{k_x} \right]^{\frac{1}{n}} * -u_{0x}^{-n} \left[\frac{\mu_{eff_x}}{k_x} \right]^{-1} = u_{0x}^{1-n} \left[\frac{\mu_{eff_x}}{k_x} \right]^{\frac{1-n}{n}} \dots 3.31a$$

Similarly,

$$\left(\frac{\partial P}{\partial y} \right)^{\frac{1}{n}-1} = u_{0y}^{1-n} \left[\frac{\mu_{eff_y}}{k_y} \right]^{\frac{1-n}{n}} \dots 3.31b$$

$$\left(\frac{\partial P}{\partial z} \right)^{\frac{1}{n}-1} = u_{0z}^{1-n} \left[\frac{\mu_{eff_z}}{k_z} \right]^{\frac{1-n}{n}} \dots 3.31c$$

Putting equation 31a, 31b and 31c into the expression in equation 3.30 gives;

$$\frac{1}{n} \left[\left[\frac{k_x}{\mu_{eff_x}} \right]^{\frac{1}{n}} \frac{\partial^2 P}{\partial x^2} u_{0x}^{1-n} \left[\frac{\mu_{eff_x}}{k_x} \right]^{\frac{1-n}{n}} + \left[\frac{k_y}{\mu_{eff_y}} \right]^{\frac{1}{n}} \frac{\partial^2 P}{\partial y^2} u_{0y}^{1-n} \left[\frac{\mu_{eff_y}}{k_y} \right]^{\frac{1-n}{n}} + \left[\frac{k_z}{\mu_{eff_z}} \right]^{\frac{1}{n}} \frac{\partial^2 P}{\partial z^2} u_{0z}^{1-n} \left[\frac{\mu_{eff_z}}{k_z} \right]^{\frac{1-n}{n}} \right] = \left[c_t \phi \frac{\partial P}{\partial t} + \frac{q_v B}{V_b} \right] \dots 3.32$$

Further simplification of equation 3.32 yields;

$$\frac{1}{n} \left[\left[\frac{k_x}{\mu_{eff_x}} \right] \frac{\partial^2 P}{\partial x^2} u_{0x}^{1-n} + \left[\frac{k_y}{\mu_{eff_y}} \right] \frac{\partial^2 P}{\partial y^2} u_{0y}^{1-n} + \left[\frac{k_z}{\mu_{eff_z}} \right] \frac{\partial^2 P}{\partial z^2} u_{0z}^{1-n} \right] = \left[c_t \phi \frac{\partial P}{\partial t} + \frac{q_v}{v_b} B \right] \dots\dots\dots 3.33$$

From equation A-10 in Ikoku and Ramey,(1979), and equations 6 and 10 in Vongvuthipornchai and Raghavan,(1987).

$$u = \frac{q_v}{2\pi h l_{yf}}; \frac{\mu_a}{\mu_{eff}} = \left(\frac{q_v}{2\pi h l_{yf}} \right)^{n-1} \Rightarrow u^{1-n} = \frac{\mu_{eff}}{\mu_a}$$

$$\frac{1}{n} \left[\left[\frac{k_x}{\mu_{eff_x}} \right] \frac{\partial^2 P}{\partial x^2} \frac{\mu_{eff}}{\mu_a} + \left[\frac{k_y}{\mu_{eff_y}} \right] \frac{\partial^2 P}{\partial y^2} \frac{\mu_{eff}}{\mu_a} + \left[\frac{k_z}{\mu_{eff_z}} \right] \frac{\partial^2 P}{\partial z^2} \frac{\mu_{eff}}{\mu_a} \right] = \left[c_t \phi \frac{\partial P}{\partial t} + \frac{q_v}{v_b} B \right] \dots\dots\dots 3.35$$

Dividing through by $\frac{k_x}{\mu_{eff_x}}$ where;

$$\mu_{eff} = \frac{H \left(9 + \frac{3}{n} \right)^n * (150k\phi)^{\left(\frac{1-n}{2} \right)}}{12} \dots\dots\dots 3.36$$

The derivation of equation 3.36 is as shown in appendix B

$$\frac{1}{n} \left[\frac{\partial^2 P}{\partial x^2} \frac{\mu_{eff}}{\mu_a} + \left[\frac{k_y}{k_x} \right] \left[\frac{k_x}{k_y} \right]^{\frac{1-n}{2}} \frac{\partial^2 P}{\partial y^2} \frac{\mu_{eff}}{\mu_a} + \left[\frac{k_z}{k_x} \right] \left[\frac{k_x}{k_z} \right]^{\frac{1-n}{2}} \frac{\partial^2 P}{\partial z^2} \frac{\mu_{eff}}{\mu_a} \right] = \frac{\mu_{eff_x}}{k_x} \left[c_t \phi \frac{\partial P}{\partial t} + \frac{q_v}{v_b} B \right] \dots\dots\dots 3.37$$

$$\frac{1}{n} \left[\frac{\partial^2 P}{\partial x^2} \frac{\mu_{eff}}{\mu_a} + \left[\frac{k_y}{k_x} \right] \left[\frac{k_x}{k_y} \right]^{\frac{1-n}{2}} \frac{\partial^2 P}{\partial y^2} \frac{\mu_{eff}}{\mu_a} + \left[\frac{k_z}{k_x} \right] \left[\frac{k_x}{k_z} \right]^{\frac{1-n}{2}} \frac{\partial^2 P}{\partial z^2} \frac{\mu_{eff}}{\mu_a} \right] = \frac{\mu_{eff_x}}{k_x} \left[c_t \phi \frac{\partial P}{\partial t} + \frac{q_v}{v_b} B \right] \dots\dots\dots 3.38$$

The Dimensionless parameters are as defined below;

$$x_D = \frac{2x \sqrt{\frac{k_x}{k_x}}}{l_{yf}}; \quad y_D = \frac{2y \sqrt{\frac{k_x}{k_y}}}{l_{yf}}; \quad z_D = \frac{z \sqrt{\frac{k_x}{k_z}}}{l_{yf}}; \quad \Delta x_D = \frac{x_D}{n_x}; \quad \Delta y_D = \frac{y_D}{n_y}; \quad \Delta z_D = \frac{z_D}{n_z}$$

$$t_D = \frac{4k_x t}{\mu^* \phi c_t l_{yf}^2}; \quad P_D = \frac{2\pi \sqrt{k_x k_y} h (P_i - P_{wf})}{q \mu^* B}; \quad \Delta x = \frac{x}{n_x}; \quad \Delta y = \frac{y}{n_y}; \quad \Delta z = \frac{z}{n_z}$$

It should be noted that in $t_D, l_{yf} = \frac{l_{yf}}{2}$

Where n_i is the number of grid cells in the i th dimension

$i = x, y \text{ or } z$

From the above stated dimensionless parameters;

$$x = x_D l_{yf}; \quad z = z_D l_{yf} \sqrt{\frac{k_z}{k_x}}; \quad y = y_D l_{yf} \sqrt{\frac{k_y}{k_x}}; \quad t = \frac{t_D \mu^* \phi c_t l_{yf}^2}{k_x}; \quad (P_i - P_{wf}) = \frac{q \mu^* B P_D}{2\pi \sqrt{k_x k_y h}}$$

Substituting the above into equation 3.38

$$\frac{1}{n} \left[\frac{\partial^2 \left(\frac{-q \mu^* B P_D}{2\pi \sqrt{k_x k_y h}} \right)}{\partial (x_D l_{yf})^2} \frac{\mu_{eff}}{\mu_a} + \left[\frac{k_y}{k_x} \right] \left[\frac{k_x}{k_y} \right]^{\frac{1-n}{2}} \frac{\partial^2 \left(\frac{-q \mu^* B P_D}{2\pi \sqrt{k_x k_y h}} \right)}{\partial \left(y_D l_{yf} \sqrt{\frac{k_y}{k_x}} \right)^2} \frac{\mu_{eff}}{\mu_a} + \left[\frac{k_z}{k_x} \right] \left[\frac{k_x}{k_z} \right]^{\frac{1-n}{2}} \frac{\partial^2 \left(\frac{-q \mu^* B P_D}{2\pi \sqrt{k_x k_y h}} \right)}{\partial \left(z_D l_{yf} \sqrt{\frac{k_z}{k_x}} \right)^2} \frac{\mu_{eff}}{\mu_a} \right] =$$

$$\frac{\mu_{eff_x}}{k_x} \left[c_t \phi \frac{\partial \left(\frac{-q \mu^* B P_D}{2\pi \sqrt{k_x k_y h}} \right)}{\partial \left(\frac{t_D \mu^* \phi c_t l_{yf}^2}{k_x} \right)} + \frac{q_v}{V_b} B \right] \dots \dots \dots 3.39$$

$$\frac{1}{n} \left[\frac{\partial^2 \left(\frac{-q \mu^* B P_D}{2\pi \sqrt{k_x k_y h}} \right)}{\partial (x_D l_{yf})^2} \frac{\mu_{eff_x}}{\mu_a} + \left[\frac{k_x}{k_y} \right]^{\frac{1-n}{2}} \frac{\partial^2 \left(\frac{-q \mu^* B P_D}{2\pi \sqrt{k_x k_y h}} \right)}{\partial (y_D l_{yf})^2} \frac{\mu_{eff_x}}{\mu_a} + \left[\frac{k_x}{k_z} \right]^{\frac{1-n}{2}} \frac{\partial^2 \left(\frac{-q \mu^* B P_D}{2\pi \sqrt{k_x k_y h}} \right)}{\partial (z_D l_{yf})^2} \frac{\mu_{eff_x}}{\mu_a} \right] =$$

$$\frac{\mu_{eff_x}}{k_x} \left[c_t \phi \frac{\partial \left(\frac{-q B P_D}{2\pi \sqrt{k_x k_y h}} \right)}{\partial \left(\frac{t_D \phi c_t l_{yf}^2}{k_x} \right)} + \frac{q_v 5.615}{V_b} B \right] \dots \dots \dots 3.40$$

$$\left(-\frac{q B \mu_{eff_x}}{2\pi n \sqrt{k_x k_y h} l_{yf}^2} \right) \left[\frac{\partial^2 P_D \mu^*}{\partial x_D^2 \mu_a} + \left[\frac{k_x}{k_y} \right]^{\frac{1-n}{2}} \frac{\partial^2 P_D \mu^*}{\partial y_D^2 \mu_a} + \left[\frac{k_x}{k_z} \right]^{\frac{1-n}{2}} \frac{\partial^2 P_D \mu^*}{\partial z_D^2 \mu_a} \right] = \frac{\mu_{eff_x}}{k_x} \left[c_t \phi \frac{\partial \left(\frac{-q B P_D}{2\pi \sqrt{k_x k_y h}} \right)}{\partial \left(\frac{t_D \phi c_t l_{yf}^2}{k_x} \right)} + \right.$$

$$\left. \frac{q_v}{V_b} B \right] \dots \dots \dots 3.41$$

$$-\frac{1}{n} \left[\frac{\partial^2 P_D \mu^*}{\partial x_D^2 \mu_a} + \left[\frac{k_x}{k_y} \right]^{\frac{1-n}{2}} \frac{\partial^2 P_D \mu^*}{\partial y_D^2 \mu_a} + \left[\frac{k_x}{k_z} \right]^{\frac{1-n}{2}} \frac{\partial^2 P_D \mu^*}{\partial z_D^2 \mu_a} \right] = \left[\frac{\partial P_D}{\partial t_D} - \frac{2\pi \sqrt{\frac{k_y}{k_x}} h l y_f^2}{V_b} \right] \dots\dots\dots 3.42$$

$$\left(-\frac{qB \mu_{eff_x}}{2\pi n \sqrt{k_x k_y} h l y_f^2} \right) \left[\frac{\partial^2 P_D \mu^*}{\partial x_D^2 \mu_a} + \left[\frac{k_x}{k_y} \right]^{\frac{1-n}{2}} \frac{\partial^2 P_D \mu^*}{\partial y_D^2 \mu_a} + \left[\frac{k_x}{k_z} \right]^{\frac{1-n}{2}} \frac{\partial^2 P_D \mu^*}{\partial z_D^2 \mu_a} \right] = \frac{\mu_{eff_x}}{k_x} \left(-\frac{qB}{2\pi n \sqrt{k_x k_y} h l y_f^2} \right) \left[\frac{\partial P_D}{\partial t_D} - \frac{2\pi n \sqrt{k_x k_y} h l y_f^2}{V_b} \right] \dots\dots\dots 3.43$$

Note that $V_b = \Delta x \Delta y \Delta z$

$$\frac{1}{n} \left[\frac{\partial^2 P_D \mu^*}{\partial x_D^2 \mu_a} + \left[\frac{k_x}{k_y} \right]^{\frac{1-n}{2}} \frac{\partial^2 P_D \mu^*}{\partial y_D^2 \mu_a} + \left[\frac{k_x}{k_z} \right]^{\frac{1-n}{2}} \frac{\partial^2 P_D \mu^*}{\partial z_D^2 \mu_a} \right] = \left[\frac{\partial P_D}{\partial t_D} - \frac{2\pi \sqrt{\frac{k_y}{k_x}} h l y_f^2}{\Delta x \Delta y \Delta z} \right] \dots\dots\dots 3.44$$

In a case where there is no source or sink equation 3.44 becomes

$$\frac{1}{n} \left[\frac{\partial^2 P_D \mu^*}{\partial x_D^2 \mu_a} + \left[\frac{k_x}{k_y} \right]^{\frac{1-n}{2}} \frac{\partial^2 P_D \mu^*}{\partial y_D^2 \mu_a} + \left[\frac{k_x}{k_z} \right]^{\frac{1-n}{2}} \frac{\partial^2 P_D \mu^*}{\partial z_D^2 \mu_a} \right] = \frac{\partial P_D}{\partial t_D} \dots\dots\dots 3.45$$

The viscosity ratio $\frac{\mu^*}{\mu_a}$ varies spatially, thus equation 3.45 can be written as;

$$\frac{1}{n} \left[\frac{\partial}{\partial x_D} \left(\frac{\mu^* \partial P_D}{\mu_a \partial x_D} \right) + \left[\frac{k_x}{k_y} \right]^{\frac{1-n}{2}} \frac{\partial}{\partial y_D} \left(\frac{\mu^* \partial P_D}{\mu_a \partial x_D} \right) + \left[\frac{k_x}{k_z} \right]^{\frac{1-n}{2}} \frac{\partial}{\partial z_D} \left(\frac{\mu^* \partial P_D}{\mu_a \partial x_D} \right) \right] = \frac{\partial P_D}{\partial t_D} \dots\dots\dots 3.46$$

This becomes;

$$\left[\frac{\partial}{\partial x_D} \left(\frac{\mu^* \partial P_D}{\mu_a \partial x_D} \right) + \left[\frac{k_x}{k_y} \right]^{\frac{1-n}{2}} \frac{\partial}{\partial y_D} \left(\frac{\mu^* \partial P_D}{\mu_a \partial x_D} \right) + \left[\frac{k_x}{k_z} \right]^{\frac{1-n}{2}} \frac{\partial}{\partial z_D} \left(\frac{\mu^* \partial P_D}{\mu_a \partial x_D} \right) \right] = n \frac{\partial P_D}{\partial t_D} \dots\dots\dots 3.47$$

When a sink is considered equation 3.47 can be written as;

$$\frac{1}{n} \left[\frac{\partial}{\partial x_D} \left(\frac{\mu^* \partial P_D}{\mu_a \partial x_D} \right) + \left[\frac{k_x}{k_y} \right]^{\frac{1-n}{2}} \frac{\partial}{\partial y_D} \left(\frac{\mu^* \partial P_D}{\mu_a \partial x_D} \right) + \left[\frac{k_x}{k_z} \right]^{\frac{1-n}{2}} \frac{\partial}{\partial z_D} \left(\frac{\mu^* \partial P_D}{\mu_a \partial x_D} \right) \right] = \frac{\partial P_D}{\partial t_D} - \frac{1}{n} * \frac{2\pi \sqrt{\frac{k_y}{k_x}} h l y_f^2}{\Delta x \Delta y \Delta z} \dots\dots\dots 3.48$$

Equation 3.48 was solved using finite difference approach; however the viscosity ratio $\frac{\mu^*}{\mu_a}$ is also dependent on pressure and varies spatially. Equation 3.48 is similar to equation A-15 in Vongvuthipornchai and Raghavan, (1987).

Equations 5 and 24 in the works of Vongvuthipornchai and Raghavan, (1987) indicate that the viscosity ratio $\frac{\mu^*}{\mu_a}$ can be obtained as follow;

$$\vec{u} = -\frac{k}{\mu_a} \left(\vec{i} \frac{\partial P}{\partial x} + \vec{j} \frac{\partial P}{\partial y} \right) \dots\dots\dots 3.49$$

Thus for a 3 Dimensional system

$$\vec{u} = -\frac{k}{\mu_a} \left(\vec{i} \frac{\partial P}{\partial x} + \vec{j} \frac{\partial P}{\partial y} + \vec{k} \frac{\partial P}{\partial z} \right) \dots\dots\dots 3.50$$

Similarly from equation 6 of Vongvuthipornchai and Raghavan, 1987;

$$\mu_a = H |\vec{u}| \dots\dots\dots 3.51$$

Where H is μ_{eff} , the effective viscosity

In equation 24 of the same reference;

$$\mu^* = H \left| \frac{q_v B}{2\pi h l_{yf}} \right|^{n-1} \dots\dots\dots 3.52$$

Taking the magnitude of \vec{u}

$$|\vec{u}| = \frac{k_x}{\mu_a} \left[\left(\frac{\partial P}{\partial x} \right)^2 + \left(\frac{\partial P}{\partial y} \right)^2 + \left(\frac{\partial P}{\partial z} \right)^2 \right]^{\frac{1}{2}} \dots\dots\dots 3.53$$

Substituting equation 3.53 into equation 3.51 gives;

$$\mu_a = \mu_{eff} \left[\frac{k}{\mu_a} \left[\left(\frac{\partial P}{\partial x} \right)^2 + \left(\frac{\partial P}{\partial y} \right)^2 + \left(\frac{\partial P}{\partial z} \right)^2 \right]^{\frac{1}{2}} \right]^{n-1} \dots\dots\dots 3.54$$

Thus dividing equation 3.52 equation 3.54 yields;

$$\frac{\mu^*}{\mu_a} = \frac{\mu_{eff} \left| \frac{q_v B}{2\pi h l_{xf}} \right|^{n-1}}{\mu_{eff} \left[\frac{k_x}{\mu_a} \left[\left(\frac{\partial P}{\partial x} \right)^2 + \left(\frac{\partial P}{\partial y} \right)^2 + \left(\frac{\partial P}{\partial z} \right)^2 \right]^{\frac{1}{2}} \right]^{n-1}} \dots\dots\dots 3.55$$

$$\frac{\mu^*}{\mu_a} = \left| \frac{q_v B}{2\pi h l_{yf}} \right|^{n-1} \left[\frac{\mu_a}{k_x} \right]^{n-1} \left[\left(\frac{\partial P}{\partial x} \right)^2 + \left(\frac{\partial P}{\partial y} \right)^2 + \left(\frac{\partial P}{\partial z} \right)^2 \right]^{\frac{1-n}{2}} \dots\dots\dots 3.56$$

$$\frac{\mu^*}{\mu_a} = \left| \frac{q_v \mu_a B}{2\pi h k_x l_{yf}} \right|^{n-1} \left[\left(\frac{\partial P}{\partial x} \right)^2 + \left(\frac{\partial P}{\partial y} \right)^2 + \left(\frac{\partial P}{\partial z} \right)^2 \right]^{\frac{1-n}{2}} \dots\dots\dots 3.57$$

Using the dimensionless terms as defined in equations above;

$$\frac{\mu^*}{\mu_a} = \left| \frac{q_v \mu_a B}{2\pi h k_x l_{yf}} \right|^{n-1} \left[\left(\frac{\partial \left(\frac{q_v \mu^* B P_D}{2\pi \sqrt{k_x k_y h}} \right)}{\partial (x_D l_{yf})} \right)^2 + \left(\frac{\partial \left(\frac{q_v \mu^* B P_D}{2\pi \sqrt{k_x k_y h}} \right)}{\partial \left(y_D l_{yf} \sqrt{\frac{k_y}{k_x}} \right)} \right)^2 + \left(\frac{\partial \left(\frac{q_v \mu^* B P_D}{2\pi \sqrt{k_x k_y h}} \right)}{\partial \left(z_D l_{yf} \sqrt{\frac{k_z}{k_x}} \right)} \right)^2 \right]^{\frac{1-n}{2}} \dots\dots\dots 3.58$$

$$\frac{\mu^*}{\mu_a} = \left| \frac{q_v \mu_a B}{2\pi h k_x l_{yf}} \right|^{n-1} \left(\frac{q_v \mu^* B P_D}{2\pi l_{yf} \sqrt{k_x k_y h}} \right)^{1-n} \left[\left(\frac{\partial P_D}{\partial x_D} \right)^2 + \frac{k_x}{k_y} \left(\frac{\partial P_D}{\partial y_D} \right)^2 + \frac{k_x}{k_z} \left(\frac{\partial P_D}{\partial y_D} \right)^2 \right]^{\frac{1-n}{2}} \dots\dots\dots 3.59$$

$$\left(\frac{\mu^*}{\mu_a} \right)^n = \left(\sqrt{\frac{k_x}{k_y}} \right)^{1-n} \left[\left(\frac{\partial P_D}{\partial x_D} \right)^2 + \frac{k_x}{k_y} \left(\frac{\partial P_D}{\partial y_D} \right)^2 + \frac{k_x}{k_z} \left(\frac{\partial P_D}{\partial y_D} \right)^2 \right]^{\frac{1-n}{2}} \dots\dots\dots 3.60$$

$$\frac{\mu^*}{\mu_a} = \left(\sqrt{\frac{k_x}{k_y}} \right)^{\frac{1-n}{n}} \left[\left(\frac{\partial P_D}{\partial x_D} \right)^2 + \frac{k_x}{k_y} \left(\frac{\partial P_D}{\partial y_D} \right)^2 + \frac{k_x}{k_z} \left(\frac{\partial P_D}{\partial y_D} \right)^2 \right]^{\frac{1-n}{2n}} \dots\dots\dots 3.61$$

Equations 3.48 and 3.61 forms the bases of this study following the procedures adopted in the works of Ikoku and Ramey, 1978 and Vongvuthipornchai and Raghavan, 1987.

3.2.1 BOUNDARY CONDITION

No-flow boundary condition was assumed in the modeling, i.e. the pressure gradient across the reservoir surface is zero. Equation 3.48 was discretized using finite difference approach implementing a no-flow boundary condition across the surface of the reservoir cuboid model. The no-flow boundary condition as stated below is also discretized to solve equation 3.48 numerically

$$\left. \frac{\partial P_D}{\partial x_D} \right|_{x_D=0, 0 \leq y_D \leq y_{De}, 0 \leq z_D \leq z_{De}} = \left. \frac{\partial P_D}{\partial y_D} \right|_{0 \leq x_D \leq x_{De}, y_D=0, 0 \leq z_D \leq z_{De}} = \left. \frac{\partial P_D}{\partial z_D} \right|_{0 \leq x_D \leq x_{De}, 0 \leq y_D \leq y_{De}, z_D=0} = 0 \dots\dots\dots 3.62$$

3.2.2 FINITE DIFFERENCE APPROXIMATION OF MODELLED DIFFERENTIAL EQUATION

Equations 3.48 and 3.61 were solved numerically using the finite difference approach, implementing the boundary no flow boundary conditions as stated in equation 3.62.

Recalling equation 3.48;

$$\frac{1}{n} \left[\frac{\partial}{\partial x_D} \left(\frac{\mu^*}{\mu_a} \frac{\partial P_D}{\partial x_D} \right) + \left[\frac{k_x}{k_y} \right]^{\frac{1-n}{2}} \frac{\partial}{\partial y_D} \left(\frac{\mu^*}{\mu_a} \frac{\partial P_D}{\partial y_D} \right) + \left[\frac{k_x}{k_z} \right]^{\frac{1-n}{2}} \frac{\partial}{\partial z_D} \left(\frac{\mu^*}{\mu_a} \frac{\partial P_D}{\partial z_D} \right) \right] = \frac{\partial P_D}{\partial t_D} - \frac{1}{n} * \frac{2\pi \sqrt{\frac{k_y}{k_x}} h l y_f^2}{\Delta x \Delta y \Delta z} \dots\dots\dots 3.48$$

The finite difference discretization of equation 3.48 involves using the central difference approximation as used in Vongvuthipornchai and Raghavan, 1987 for the spatial derivative and backward difference approximation for the derivative with respect to time.

p is denoted here as the time step iteration

$$\begin{aligned} & \frac{1}{n} \left[\frac{1}{\Delta x_D} \left[\left(\frac{\mu^*}{\mu_a} \right)^{p+1} \left(\frac{P_{Di+1,j,k} - P_{Di,j,k}}{\Delta x_D} \right) - \left(\frac{\mu^*}{\mu_a} \right)^p \left(\frac{P_{Di,j,k} - P_{Di-1,j,k}}{\Delta x_D} \right) \right] + \frac{1}{\Delta y_D} \left[\left(\frac{\mu^*}{\mu_a} \right)^{p+1} \left(\frac{P_{Di,j+1,k} - P_{Di,j,k}}{\Delta y_D} \right) - \right. \right. \\ & \left. \left(\frac{\mu^*}{\mu_a} \right)^p \left(\frac{P_{Di,j,k} - P_{Di,j-1,k}}{\Delta y_D} \right) \right] + \frac{1}{\Delta z_D} \left[\left(\frac{\mu^*}{\mu_a} \right)^{p+1} \left(\frac{P_{Di,j,k+1} - P_{Di,j,k}}{\Delta z_D} \right) - \left(\frac{\mu^*}{\mu_a} \right)^p \left(\frac{P_{Di,j,k} - P_{Di,j,k-1}}{\Delta z_D} \right) \right] \right] = \\ & \frac{P_{Di,j,k}^{p+1} - P_{Di,j,k}^p}{\Delta t_D} - \frac{1}{n} * \frac{2\pi \sqrt{\frac{k_y}{k_x}} h l y_f^2}{\Delta x \Delta y \Delta z} \dots\dots\dots 3.63 \end{aligned}$$

It should be noted that the right hand side (RHS) of equation 3.63 is in the p+1 time iteration. Thus simplifying equation 3.63 yields the expression below; Equation 3.63 is similar to the finite difference approximation used in Vongvuthipornchai and Raghavan, 1987 (SPE 13058)

$$\begin{aligned} & -P_{Di,j,k} \left[\alpha (\omega_{i+1,j,k} + \omega_{i-1,j,k}) + \beta (\omega_{i,j+1,k} + \omega_{i,j-1,k}) + \gamma (\omega_{i,j,k+1} + \omega_{i,j,k-1}) + \frac{1}{\Delta t_D} \right] + \alpha \\ & \omega_{i+1,j,k} P_{Di+1,j,k} + \alpha \omega_{i-1,j,k} P_{Di-1,j,k} + \beta \omega_{i,j+1,k} P_{Di,j+1,k} + \beta \omega_{i,j-1,k} P_{Di,j-1,k} + \gamma \omega_{i,j,k+1} P_{Di,j,k+1} + \\ & \gamma \omega_{i,j,k-1} P_{Di,j,k-1} = - \frac{P_{Di,j,k}^p}{\Delta t_D} - \frac{1}{n} * \frac{2\pi \sqrt{\frac{k_y}{k_x}} h l y_f^2}{\Delta x \Delta y \Delta z} \dots\dots\dots 3.64 \end{aligned}$$

Re-writing equation 3.64 gives;

$$\begin{aligned}
 &P_{Di,j,k} \left[\alpha (\omega_{i+1,j,k} + \omega_{i-1,j,k}) + \beta (\omega_{i,j+1,k} + \omega_{i,j-1,k}) + \gamma (\omega_{i,j,k+1} + \omega_{i,j,k-1}) + \frac{1}{\Delta t_D} \right] - \alpha \\
 &\omega_{i+1,j,k} P_{Di+1,j,k} - \alpha \omega_{i-1,j,k} P_{Di-1,j,k} - \beta \omega_{i,j+1,k} P_{Di,j+1,k} - \beta \omega_{i,j-1,k} P_{Di,j-1,k} - \gamma \omega_{i,j,k+1} P_{Di,j,k+1} - \\
 &\gamma \omega_{i,j,k-1} P_{Di,j,k-1} = \frac{P_{Di,j,k}^p}{\Delta t_D} + \frac{1}{n} \frac{2\pi \sqrt{\frac{k_y}{k_x}} h l y_f^2}{\Delta x \Delta y \Delta z} \dots\dots\dots 3.65
 \end{aligned}$$

Where;

$$\alpha = \frac{1}{(x_D)^2}; \beta = \sqrt{\frac{k_x}{k_y}} \frac{1}{(x_D)^2}; \gamma = \sqrt{\frac{k_x}{k_y}} \frac{1}{(x_D)^2}; \omega = \frac{\mu^*}{\mu_a}$$

The Boundary condition equation was also discretized using the backward difference approximation as shown below;

$$\frac{P_{Di,j,k} - P_{Di-1,j,k}}{\Delta x_D} = \frac{P_{Di,j,k} - P_{Di,j-1,k}}{\Delta y_D} = \frac{P_{Di,j,k} - P_{Di,j,k-1}}{\Delta z_D} = 0 \dots\dots\dots 3.66$$

the above equation was incorporated into the final development of the linear systems of equation to aid the solution to the Partial differential equation in equation 3.48.

Depending on the number of grid system being considered, say from 1 to *n grid system*, a system of linear equations is obtained from equation 3.65 to obtain an *n X n* Matrix. In this work, the same numbers of grids were used in all the dimensions in the x,y and z axis. The linear system of equations solved was of the form;

$$[A] * [P_D]^{n+1} = [P]^n \dots\dots\dots 3.67$$

Where;

[A] is the symmetric heptadiagonal coefficient matrix generated from n grids the reservoir model was divided into

[P_D]ⁿ⁺¹ is the unknown dimensionless Pressure at the next time step

[P_D]ⁿ is the known dimensionless Pressure at the present time step

3.2.3 MATLAB R2007b IMPLEMENTATION

A MATLAB R2007b program was written to solve the system of equations generated from equation 3.66 putting into consideration the existing no flow boundary conditions. The MATLAB R2007b code as shown in Appendix was used to iteratively solve equation 3.67 with respect to time and space in dimensionless terms. The MATLAB R2007b program was run for a grid size of 15X15X15, which was the limit of the machine used for the simulation process.

Runs were made basically for a horizontal length (l_{yf}) of 600ft, 1000ft and 1200ft, a Reservoir size of 3000ft by 3000ft with a height ranging from 100ft to 300ft as would be shown in the next chapter. Other inputs into the MATLAB code includes the permeabilities k_x, k_y and k_z . The first set of runs were made for Newtonian Reservoir fluids, identifying the major flow regimes as discussed in standard literature, that is the early linear flow, the pseudo-radial flow, the transition flow and the pseudo steady state flow regimes. Results are as shown in the next chapter.

Consequently, a similar MATLAB R2007b code was written for cases whereby the reservoir fluid is Non-Newtonian, this new MATLAB R2007b code required written a convergence algorithm for the viscosity ratio $\left(\frac{\mu^*}{\mu_a}\right)$ which varies with pressure. The approach for the convergence algorithm is as listed below;

- Solving systems of equation from equation 3.56 when the reservoir fluid is Newtonian, that is $n=1$ and the viscosity ratio $\frac{\mu^*}{\mu_a} = 1$ to obtain the dimensionless pressure for the new time step.
- The new dimensionless pressure obtained is substituted into discretized version of equation 3.61 as shown in equation 3.68 below to obtain the viscosity ratio for the present time step.

$$\left(\frac{\mu^*}{\mu_a}\right)_{i,j,k} = \left(\sqrt{\frac{k_x}{k_y}}\right)^{\frac{1-n}{n}} \left[\left(\frac{P_{Di,j,k} - P_{Di-1,j,k}}{\Delta x_D}\right)^2 + \frac{k_x}{k_y} \left(\frac{P_{Di,j,k} - P_{Di,j-1,k}}{\Delta y_D}\right)^2 + \frac{k_x}{k_z} \left(\frac{P_{Di,j,k} - P_{Di,j,k-1}}{\Delta z_D}\right)^2 \right]^{\frac{1-n}{2n}}$$

.....3.68

- A new system of equations is solved to obtain the viscosity ratio $\frac{\mu^*}{\mu_a}$ for each of the grid cells from the substituted dimensionless pressures and permeabilities.

- The viscosity ratio obtained in step 3 is substituted back into equation 3.56 to obtain a new set of dimensionless pressures.
- Step 2 and step 4 are repeated until the dimensionless pressure obtained converges. An error margin of 10^{-30} was used to ensure convergence between the last obtained dimensionless pressure and the new.

The flow chart below shows the summary of the algorithm from which the MATLAB R2007b code was developed.

3.2.4 LOCATION OF HORIZONTAL WELL

The horizontal well was located spatially at the middle of the reservoir. The horizontal well is located such that it cuts across an exact number of grids for convenience. The bottom-hole flowing pressure of the middle grid cell through which the horizontal cuts across was taken as the bottom-hole flowing pressure of the well.

3.3 ORDERING OF GRIDS AND COEFFICIENT MATRIX DEVELOPMENT

In order to obtain a hepta-diagonal symmetrical diagonal matrix the grid blocks were ordered as shown in figure 3.1. The symmetric matrix as shown in figure 3.2 reduces the computational requirements to solve the systems of equation as generated from equation 3.64.

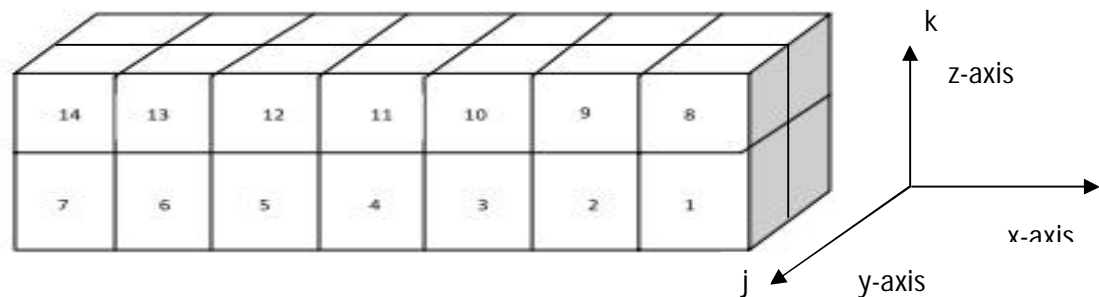


Figure 3.2: ordering of grid blocks to give a diagonal symmetrical Matrix

For example in grid block 1 in figure 3.2. The grid block is described in the x, y, z coordinates as $(1, 1, 1)$. The discretized equation for the grid cell is as written below from equation 3.65

$$P_{D1,1,1} \left[\alpha (\omega_{2,1,1} + \omega_{0,1,1}) + \beta (\omega_{1,2,1} + \omega_{1,0,1}) + \gamma (\omega_{1,1,2} + \omega_{1,1,0}) + \frac{1}{\Delta t_D} \right] - \alpha \omega_{2,1,1} P_{D2,1,1} - \alpha \omega_{0,1,1} P_{D0,1,1} - \beta \omega_{1,2,1} P_{D1,2,1} - \beta \omega_{1,0,1} P_{D1,0,1} - \gamma \omega_{1,1,2} P_{D1,1,2} - \gamma \omega_{1,1,0} P_{D1,1,0} = \frac{P_{D1,1,1}^p}{\Delta t_D} + \frac{1}{n} \frac{2\pi \sqrt{\frac{k_y}{k_x}} h l_y f^2}{\Delta x \Delta y \Delta z} \dots 3.69$$

The boundary conditions apply on this grid cell, thus for this grid cell the boundary can be written as below from equation 3.66;

when $x = 1, y = 1$ and $z = 1$

$$\frac{P_{D1,1,1} - P_{D0,1,1}}{\Delta x_D} = \frac{P_{D1,1,1} - P_{D1,0,1}}{\Delta y_D} = \frac{P_{D1,1,1} - P_{D1,1,0}}{\Delta z_D} = 0 \dots 3.70$$

Thus equation 3.70 becomes;

$$P_{D1,1,1} = P_{D0,1,1} = P_{D1,0,1} = P_{D1,1,0} \dots 3.71$$

Substituting the boundary conditions in equation 3.71 into equation 3.69 yield;

$$P_{D1,1,1} \left[\alpha (\omega_{2,1,1}) + \beta (\omega_{1,2,1}) + \gamma (\omega_{1,1,2}) + \frac{1}{\Delta t_D} \right] - \alpha \omega_{2,1,1} P_{D2,1,1} - \beta \omega_{1,2,1} P_{D1,2,1} - \gamma \omega_{1,1,2} P_{D1,1,2} = \frac{P_{D1,1,1}^p}{\Delta t_D} + \frac{1}{n} \frac{2\pi \sqrt{\frac{k_y}{k_x}} h l_y f^2}{\Delta x \Delta y \Delta z} \dots 3.72$$

In a similar manner, the discretization for the second grid cell 2 when $x = 2, y = 1, z = 1$ can be written as follows;

$$P_{D2,1,1} \left[\alpha (\omega_{3,1,1} + \omega_{1,1,1}) + \beta (\omega_{2,2,1} + \omega_{2,0,1}) + \gamma (\omega_{2,1,2} + \omega_{2,1,0}) + \frac{1}{\Delta t_D} \right] - \alpha \omega_{3,1,1} P_{D3,1,1} - \alpha \omega_{1,1,1} P_{D1,1,1} - \beta \omega_{2,2,1} P_{D2,2,1} - \beta \omega_{2,0,1} P_{D2,0,1} - \gamma \omega_{2,1,2} P_{D2,1,2} - \gamma \omega_{2,1,0} P_{D2,1,0} = \frac{P_{D2,1,1}^p}{\Delta t_D} + \frac{1}{n} \frac{2\pi \sqrt{\frac{k_y}{k_x}} h l_y f^2}{\Delta x \Delta y \Delta z} \dots 3.73$$

Implementing the boundary conditions in a similar way as shown in equation 3.70 gives

when $x = 2, y = 1$ and $z = 1$

$$\frac{P_{D2,1,1} - P_{D2,0,1}}{\Delta y_D} = \frac{P_{D2,1,1} - P_{D2,1,0}}{\Delta z_D} = 0 \dots\dots\dots 3.74$$

Thus;

$$P_{D2,1,1} = P_{D2,0,1} = P_{D2,1,0} \dots\dots\dots 3.75$$

Substituting equation into equation 3.73 gives;

$$P_{D2,1,1} \left[\alpha (\omega_{3,1,1} + \omega_{1,1,1}) + \beta (\omega_{2,2,1}) + \gamma (\omega_{2,1,2}) + \frac{1}{\Delta t_D} \right] - \alpha \omega_{3,1,1} P_{D3,1,1} - \alpha \omega_{1,1,1} P_{D1,1,1} - \beta \omega_{2,2,1} P_{D2,2,1} - \gamma \omega_{2,1,2} P_{D2,1,2} = \frac{P_{D2,1,1}^p}{\Delta t_D} + \frac{1}{n} \frac{2\pi \sqrt{\frac{k_y}{k_x}} h l_y f^2}{\Delta x \Delta y \Delta z} \dots\dots\dots 3.76$$

The seventh grid is located at a position where $x = 7, y = 1, z = 1$ as shown in figure 3.1 can also be discretized similarly as shown below;

when $x = 7, y = 1$ and $z = 1$

$$P_{D7,1,1} \left[\alpha (\omega_{8,1,1} + \omega_{6,1,1}) + \beta (\omega_{7,2,1} + \omega_{7,0,1}) + \gamma (\omega_{7,1,2} + \omega_{7,1,0}) + \frac{1}{\Delta t_D} \right] - \alpha \omega_{8,1,1} P_{D8,1,1} - \alpha \omega_{6,1,1} P_{D6,1,1} - \beta \omega_{7,2,1} P_{D7,2,1} - \beta \omega_{7,0,1} P_{D7,0,1} - \gamma \omega_{7,1,2} P_{D7,1,2} - \gamma \omega_{7,1,0} P_{D7,1,0} = \frac{P_{D7,1,1}^p}{\Delta t_D} + \frac{2\pi \sqrt{\frac{k_y}{k_x}} h l_y f^2}{n \Delta x \Delta y \Delta z} \dots\dots\dots 3.77$$

Boundary conditions can is implemented for the last grid cell as shown below;

$$P_{D7,1,1} = P_{D7,0,1} = P_{D7,1,0} \dots\dots\dots 3.78$$

At the last grid cell a special boundary condition is used to ensure consistency

$$P_{D7,1,1} = P_{D8,1,1} \dots\dots\dots 3.79$$

The process is repeated for all the grid cells in the modeled and the system of equations of equation developed is express as matrix and solved. The hepta-diagonal coefficient matrix developed for the 3-dimensional model has the pattern.

3.4 TYPE CURVE DEVELOPMENT

Type curves were obtained by running the MATLAB 7.5.0 (R2007b) codes developed for horizontal well lengths of 600ft, 1000ft and 1200ft for $n=0.1$ to $n=1$. The effect of permeability heterogeneity was also considered by running the MATLAB program for $k = 100md$, $k = 50$ and $k = 25$ and when $k = 75md$, $k = 75$ and $k = 75$ for the various values of n being considered. The type-curves obtained are as shown in the next chapter. It should be noted that the position of the Horizontal well was not changed in obtaining any of these type-curves

CHAPTER FOUR

4.0 VALIDATION, RESULTS AND DISCUSSION

In this chapter, the validation of the methodology used in this study is made with the case when Newtonian fluid is considered. Furthermore sample plots of type curves for different horizontal well lengths, heights and directional permeabilities are presented. Horizontal well length of 600ft, 1000ft and 1200ft are considered and the types curves i.e. the log-log plots of $t * P_D'$ Vs t_D are as shown. Similarly, type curves were made for situations where the directional permeabilities are different with $k_x = 100md$, $k_y = 50md$ and $k_z = 25md$ as well as when the directional permeabilities are equal i.e. $k_x = k_y = k_z = 75md$.

4.1 VALIDATION OF RESULTS

The results of the numerical approach used in this work were validated by using the correction factors in the works of Vongvuthiopornchai and Raghavan, 1987. Equation 26 and equation 30 of the same reference are combined to determine the highest directional permeability k_x using the appropriate fracture correction factor used in falloff analysis as shown in table 3 of their work.

Table 4.1: Correction factors for falloff analysis for Pressure behaviors at fractured wells. (Adapted from Vongvuthiopornchai and Raghavan, 1987)

TABLE 3—CORRECTION FACTORS FOR FALLOFF ANALYSIS			
n	C_r	C_F	C_{FD}
0.9	0.884	1.17	1.13
0.8	0.804	1.41	1.29
0.7	0.711	1.75	1.50
0.6	0.609	2.28	1.79
0.5	0.503	3.16	2.21
0.4	0.393	4.80	2.84
0.3	0.281	8.47	3.92
0.2	0.163	19.4	6.12
0.1	0.0580		

4.1.1 VALIDATION OF k_x FROM EARLY-LINEAR FLOW REGIME ANALYSIS

Using the case of Newtonian fluid for the data in table 4.2, the following equations are used in the determination of k_x through the analysis of the early linear flow;

$$P_{wD} = \sqrt{\pi t_{Dxf}} \dots\dots\dots 4.1$$

$$t^*_{Dxf} = \frac{C_{f1}k\Delta t}{\phi c_t \mu^* L_{xf}^2} \dots\dots\dots 4.2$$

The above equation is applicable to the early-time linear flow where there exists a straight line of slope 0.5 on the log-log coordinates. Combining equation 4.1 with equation 4.2 gives;

$$k_x = k = \frac{(P_{wD})^2 \phi c_t \mu^* L_{xf}^2}{\Delta t * \pi} \dots\dots\dots 4.3$$

The pressure data for the reservoir properties given in table 4.2 is presented in Table 1 of appendix A;

$$L_{xf} = \frac{L_h}{2}$$

Where L_h is the length of the horizontal well.

At the point taken on the early linear flow regime; $P_{wD} = 0.220561213$; $t_D = 0.004$ the equivalent Δt value was read off in the tabulated pressure data in Table 2 appendix A as $t = 327.8714329s$.

Substituting these values into equation 4.7 yields; the plot on log-log of P_{wD} Vs t_D showing the linear flow regime with slope 0.5 is as shown in figure 4.2

$$k_x = k = \frac{(0.220561213)^2 * 0.25 * 9.68 * E-10 * 0.001 * 182.88^2}{3.142 * 327.9}$$

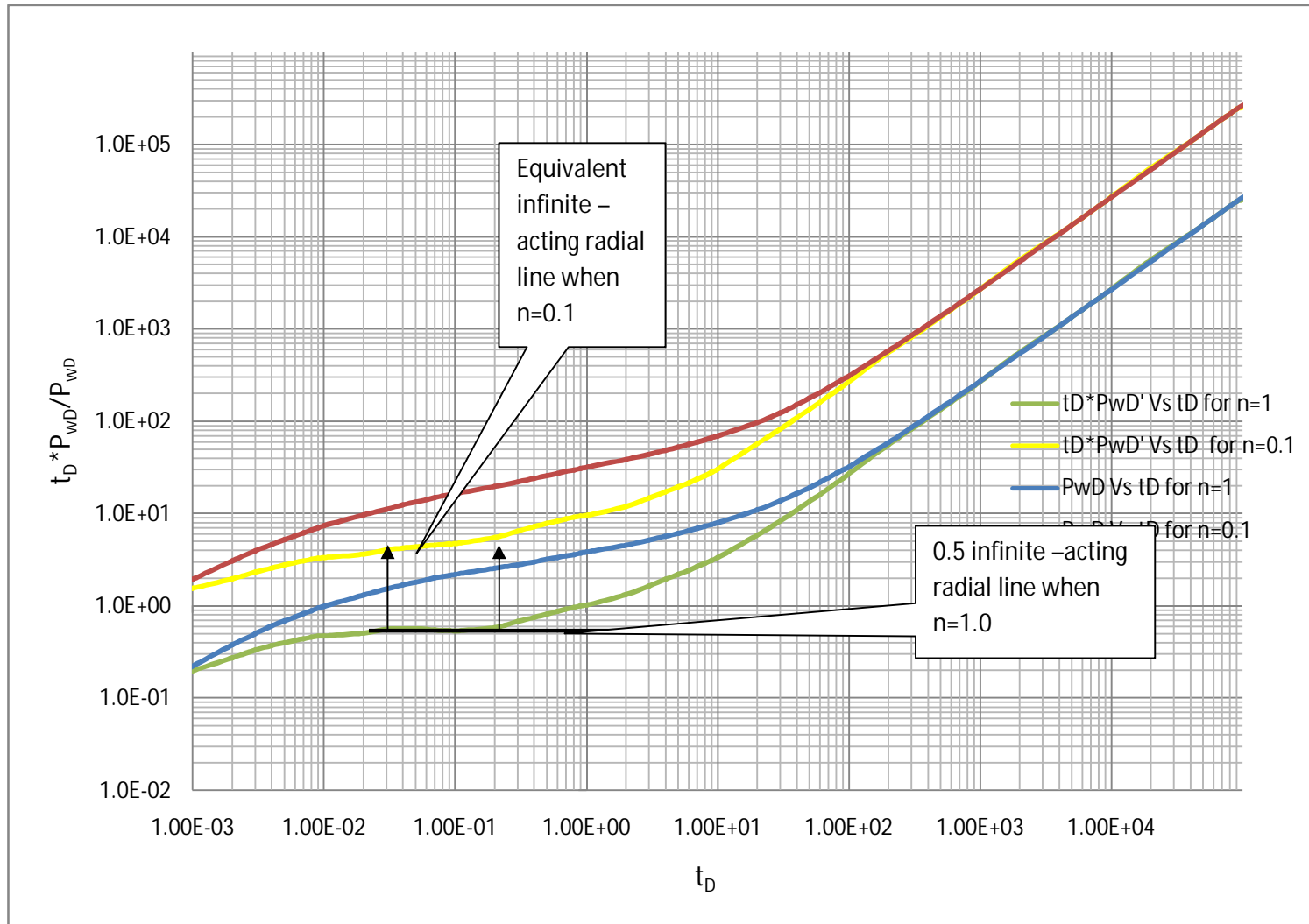


Figure 4.1: Log-Log Plot of $t_D * P_{wD}'$ Vs t_D for determining radial flow region when $n=0.1$

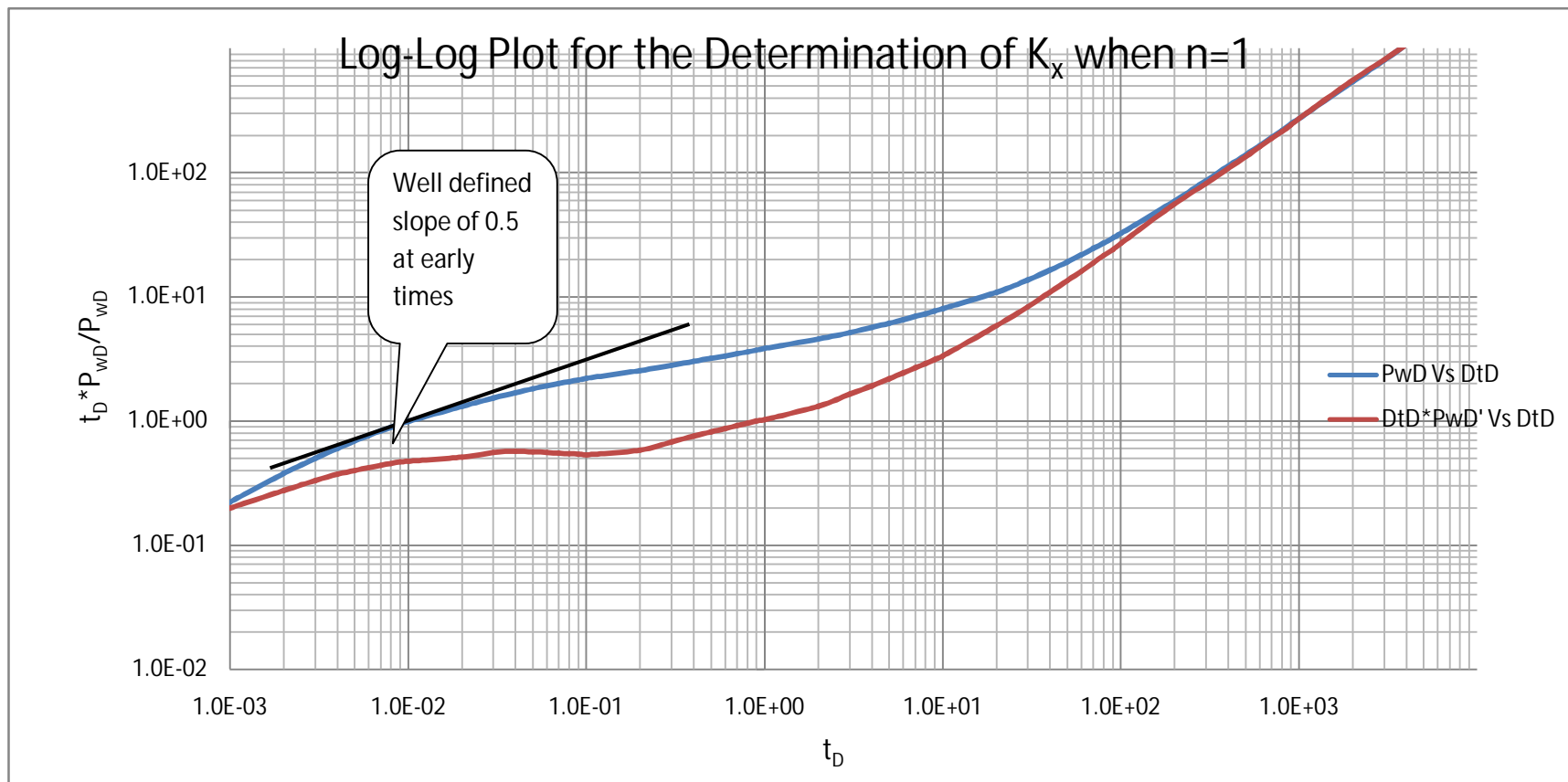


Figure 4.2: Log-Log Plot of P_{wD} Vs t_D for the validation of early linear flow analysis

$$k_x = 9.55 E - 14 m^2$$

In md

$$k_x = \frac{9.55 E - 14}{9.87 E - 16 \frac{m^2}{md}} m^2 = 96.8 md$$

The value of k_x calculated is close to the $100md$ actual permeability of the reservoir in the x -direction.

Table 4.2: Reservoir Properties for generating pressure data to validate k_x

Pi	5000	Psi	34473785	Pa
q	200	bbl/day	0.000368	m ³ /s
ky	50	md	4.93E-14	m ²
kx	100	md	9.87E-14	m ²
kz	25	md	2.47E-14	m ²
h	100	ft	30.48	m
miu	1	cp	0.001	Pa.s
poro	0.25		0.25	
lyf	600	ft	182.88	m
B	1			
Ct	6.67E-06	Psi ⁻¹	9.68E-10	Pa ⁻¹

4.1.2 VALIDATION OF AVERAGE RESERVOIR PERMEABILITY FROM RADIAL FLOW REGIME ANALYSIS

The radial flow regime is used to calculate the average reservoir permeability; the average permeability of the reservoir can be validated by using the Tiab Direct Synthesis Technique. From the expression in equation 15.a of Irina Katime and Tiab, 2001 for the determination of average reservoir permeability as shown in *equation 4.4*, the average reservoir permeability calculated from *equation 4.4* is expected to be close to the average reservoir permeability $\sqrt{k_y k_x}$.

$$\frac{k}{\mu_{eff}} = 0.5 \frac{q}{(t * \Delta P')_r} * \frac{1}{(2\pi h)} \dots\dots\dots 4.4$$

Where $(t * \Delta P')_r$ is the value of $t * \Delta P$ for the infinite acting radial flow at t

The reservoir properties are as shown in table 4.2 above

The value of $\Delta t * \Delta P'$ at the infinite acting radial flow is read from the plot in figure 4.3 or read from the table 2 in Appendix A as 13634.02 substituting this and other reservoir parameters into equation 4 yields;

$$\frac{k}{\mu_{eff}} = 0.5 \frac{0.000368 \text{ m}^3/\text{s}}{13634.02 \text{ Pa}} * \frac{1}{(2\pi * 30.48 \text{ m})}$$

Using $\mu_{eff} = 0.001 \text{ Pa. s}$

Thus;

$$k = 7.0469E - 14 \text{ m}^2$$

Converting k to md gives;

$$k = \frac{7.0469E - 14 \text{ m}^2}{9.869233E - 16 (\text{m}^2/\text{md})} = 71.4 \text{ md}$$

The actual average reservoir permeability can be computed from the k_x and k_y values given in table 4.2 above.

$$k = \sqrt{k_y k_x} = \sqrt{100 * 50} \text{ md} = 70.71068 \text{ md}$$

The Value of the average permeability calculated using the Tiab's direct synthesis Technique is close to the actual reservoir permeability.

4.1.3 VALIDATION OF DRAINAGE AREA FROM PSEUDO STEADY STATE FLOW REGIME ANALYSIS.

The Drainage area can be obtained from the Pseudo steady state flow regime. The expression for calculating drainage area for a horizontal well is as presented below;

$$A = \frac{2\pi k}{\phi\mu_{eff}c_t} \left(\frac{t}{t_D \frac{\partial P_{wD}}{\partial t_D}} \right)_{P_{SS}} \dots\dots\dots 4.5$$

A value of $\Delta t_D * \Delta P_{wD}'$ is read off from the Pseudo steady state flow regime from figure 4.4 and the corresponding t value is read off from figure 4 or obtained from table 2 in the appendix A. A value of $\Delta t_D * \Delta P_{wD}' = 21384.34$ at $t = 6557428658$ is read off. Thus;

$$A = \frac{2 * 96.8 * 9.87 * E-16 * 3.142}{0.25 * 0.001 * 9.68 * E-10} \left(\frac{6557428658}{21384.34} \right) m^2$$

$$A = 760,765.9m^2$$

The value of the drainage area calculated is fairly close to the actual area of the reservoir.

The actual area of the reservoir is;

$$(3000 * 0.3048)m \times (3000 * 0.3048)m = 836,127.36m^2$$

4.2 APPLICATIONS TO NON-NEWTONIAN RESERVOIR FLUIDS

The pressure data as obtained from the simulation study in this work can be applied to established methods in the works of Igbokoyi and Tiab, 2007; Irina Katime and Tiab, 2001 and Vongvuthipornchai and Raghavan, 1987.

4.2.1 ANALYSIS OF EARLY LINEAR FLOW REGIME FOR THE DETERMINATION OF k_x

From equation 26 of Vongvuthiopornchai and Raghavan, 1987;

$$P_{wD} = \left(\frac{\pi}{2} \right)^{\frac{n-1}{2}} \sqrt{\pi t_{Dxf}} \dots\dots\dots 4.6$$

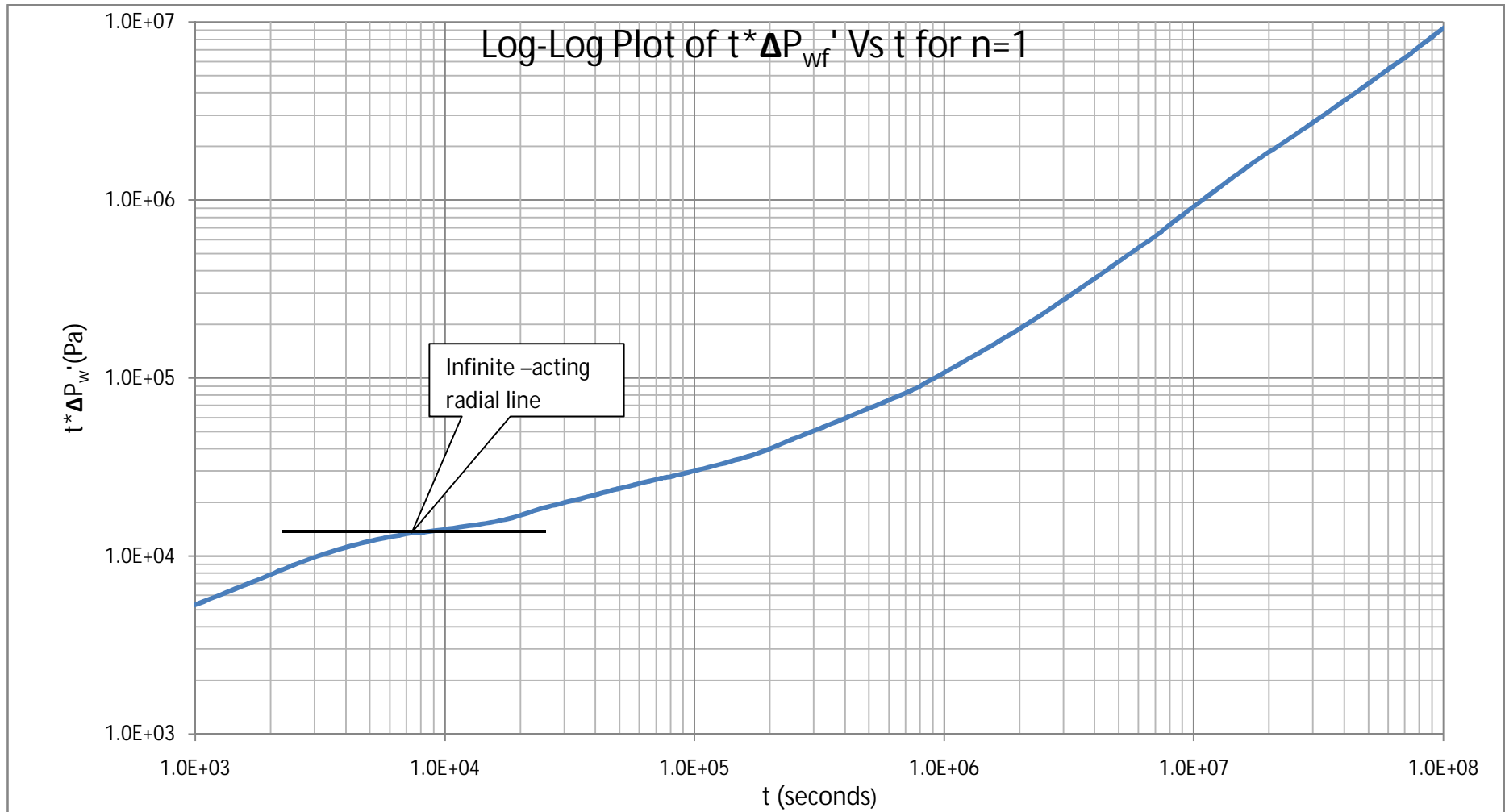


Figure 4.3: Log-Log Plot of $t^* \Delta P_{wf}'$ Vs t for $n=1$ for the validation of average reservoir permeability

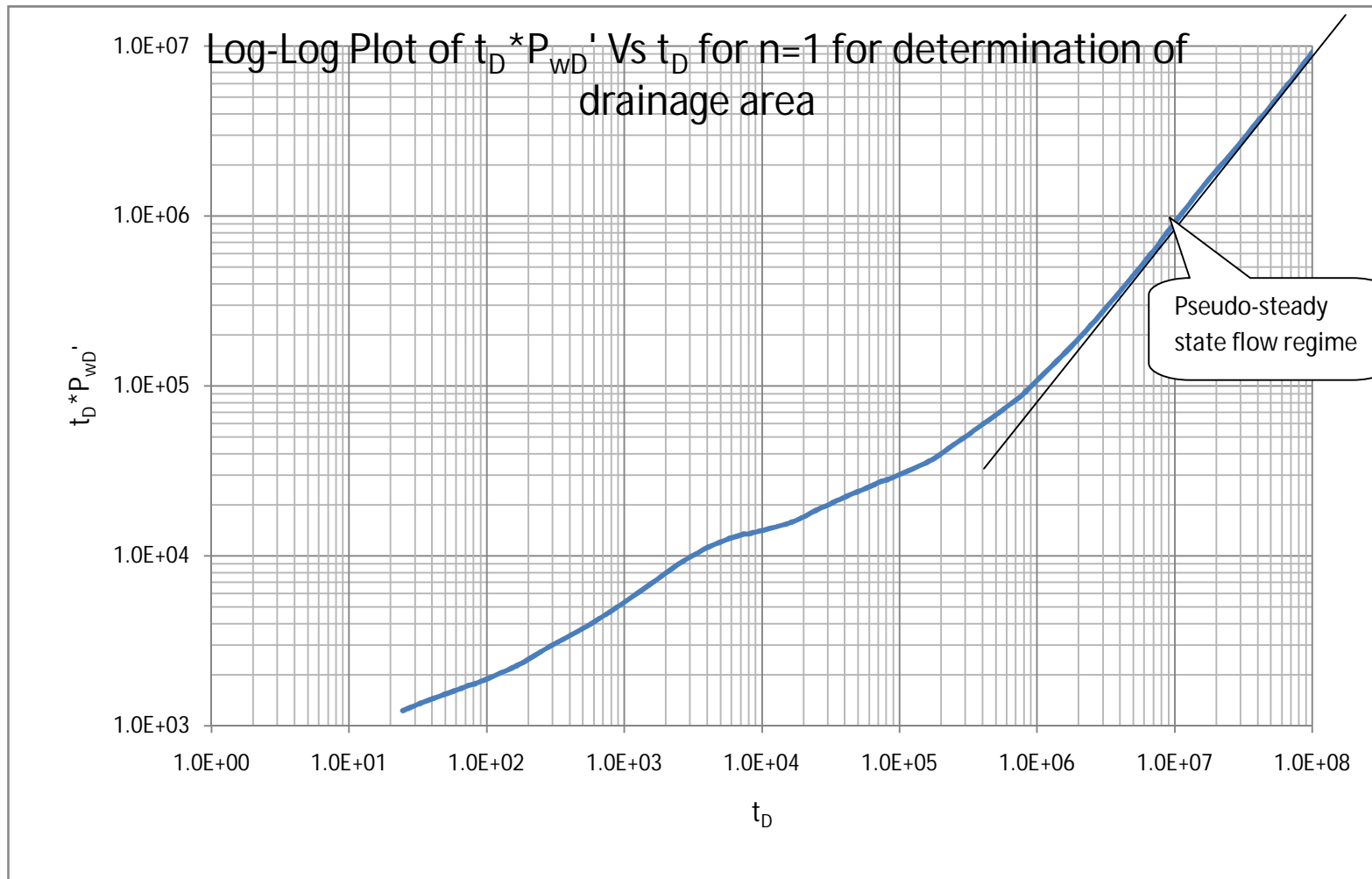


Figure 4.4: Log-Log Plot of $t_D * P'_{WD}$ Vs t_D for $n=1$ for determination of drainage area

P_{wD} is any dimensionless pressure value in the early linear flow interval .The above equation as discussed earlier is applicable to the early-time linear flow where there exists a straight line of slope 0.5 on the log-log coordinates. Combining equation 4.6 with equation 4.2 yields equation 4.7

$$k_x = k = \frac{\phi c_t \mu^* L_{xf}^2 * \left(\frac{\pi}{2}\right)^{1-n} * (P_{wD})^2}{C_{fl} * \Delta t * \pi} \dots\dots\dots 4.7$$

The correlation factor C_{fl} in equation 4.6 is as obtained from the works of Vongvuthiopornchai and Raghavan, 1987 in table 4.1. Equation 6 is used to determine the permeability k_x for flow index values $n = 0.1$ to 1 as a means of Validation. It should also be noted that a correlation value C_{fl} of 79.8 was obtained in this work when $n=0.1$. Table 4.1 shows the reservoir and fluid properties that was used to obtain pressure data when equation 4.7 was used to compute k_x for $n=0.2$ and other values of n as shown in table 4.2. The value of ΔP_{wD} was taken from the early linear flow region where the slope of the log-log plot is 0.5 as seen in figure 4.5. The Pressure data obtained from the simulation model when $n=0.2$ is as shown in table 3 in Appendix A. Taking points where $\Delta tD=0.004$, $\Delta tD=327.9$ and $\Delta P_{wD}= 0.844257668$ K_x can be obtain from equation 4.7 above using the properties in table 4.1 and the appropriate correlation factor for $n=0.2$ as shown in table 4.2

$$k_x = k = \frac{0.25 * 9.68 * E - 10 * 0.001 * 182.88 * (0.844257668)^2 * \left(\frac{3.142}{2}\right)^{\frac{1-0.2}{2}}}{19.4 * 3.142 * 327.9}$$

$$k_x = 1.04 * E - 13 m^2$$

Converting k_x to md

$$k_x = \frac{1.04 * E - 13 m^2}{9.869233E - 16 (m^2/md)} = 105md$$

The calculated value of k_x when $n=0.2$ shows close proximity to the $100md$ original reservoir permeability.

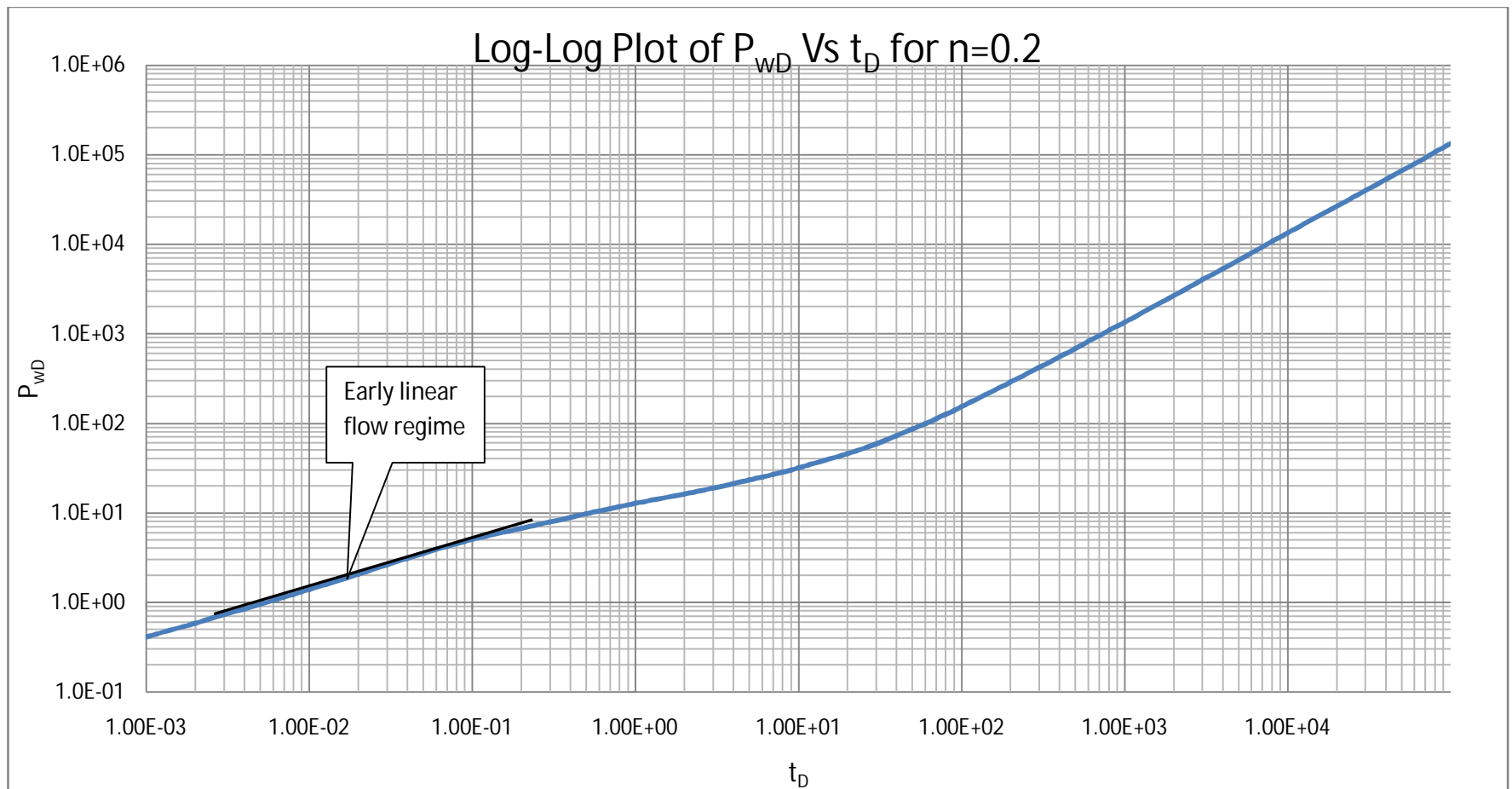


Figure 4.5: Log-Log plot of P_{wD} Vs t_D for the determination of K_x when $n=0.2$

Similar calculations are made for the different values of n with the values of k_x obtained as shown in table 4.2

4.2.2 DETERMINATION OF AVERAGE RESERVOIR MOBILITY OR PERMEABILITY USING TIAB DIRECT SYNTHESIS TECHNIQUE.

Using equation 46 derived in the works of Igbokoyi and Tiab, 2001 to obtain the mobility ratio, the equation is as expressed in equation 4.7 below;

$$\frac{k}{\mu_{eff}} = \left[\frac{0.5 * \left(\frac{q}{2\pi h} \right)^{\frac{1+n}{3-n}}}{(t * \Delta P_w')_{r1sec} (n \phi C_t)^{\frac{1-n}{3-n}}} \right]^{\frac{3-n}{2}} \dots\dots\dots 4.8$$

Considering the situation whereby a non-Newtonian fluid of n=0.1 is considered, the plot of $\Delta t * \Delta P_w'$ Vs Δt is as shown in figure 4.1. The straight line of the radial flow was extrapolated to when $\Delta t=1$ seconds, thus;

$$(t * \Delta P_w')_{r1sec} = 10,000$$

Using the reservoir properties presented in table 4.2 and the power law flow index obtained in section 4.1.1; It should be noted that the original equation was modified by including a correction factor, C_{fl} of 79.8 for a non-Newtonian fluid where n=0.1

C_{fl} at n=0.1 was obtained by finding the ratio of equation 4.7 to the input k_x value thus

$$C_{fl} = \frac{0.25 * 9.68 * E-10 * 0.001 * \frac{182.88}{4} * (1.63466)^2 * \left(\frac{3.142}{2} \right)^{\frac{1-0.1}{2}}}{\frac{3.142 * 327.9}{100}} = 79.8$$

$$\frac{k}{\mu_{eff}} = \left[\frac{0.5 * \left(\frac{0.000368}{2 * 3.142 * 30.48} \right)^{\frac{1.1}{2.9}}}{79.8 * 10,000 * (0.1 * 0.25 * 9.68 * E-10)^{\frac{0.9}{2.9}}} \right]^{\frac{2.9}{2}}$$

Table 4.3: Calculated values of k_x from equation 3 for $n = 0.1$ to 1

n	Calculated Kx (md)
0.1	100
0.2	105
0.3	109
0.4	110
0.5	110
0.6	108
0.7	106
0.8	103
0.9	100
1	97

$$\frac{k}{\mu_{eff}} = 4.3 * E - 09 m^{1.1} / Pa.s$$

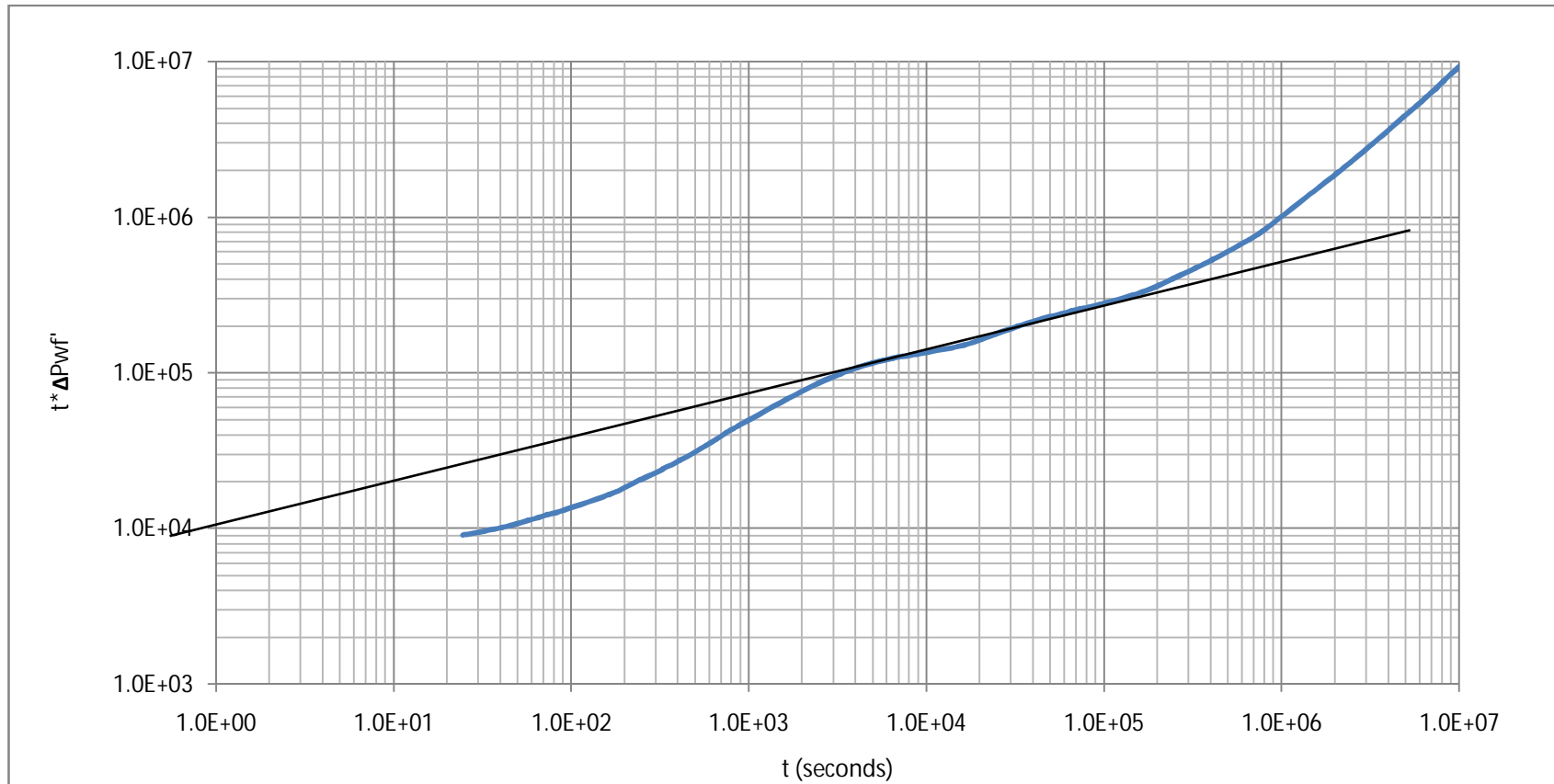


Figure 4.1: Log-Log Plot of $t^* \Delta P_{wf}'$ Vs t for the determination of mobility ratio for non-Newtonian fluid $n=0.1$.

Thus the average reservoir mobility is;

$$k = \mu_{eff} \rho a.s * 4.3 * E - 09 m^{1.1} / \rho a.s$$

4.3 DEVELOPMENT OF TYPE CURVES

Type curves including log-log plots of ΔP_{wD} Vs Δt_D and $\Delta t_D * \Delta P'_{wD}$ Vs Δt_D were made for different horizontal well lengths, reservoir thickness, directional permeabilities and flow index n. regimes. As the flow index increase from $n = 0.1$ to 1.0 as would be shown in the next sections.

4.3.1 Horizontal Well length of 600ft $k_x = 100md$, $k_y = 50md$ $k_y = 25md$ $h = 300ft$

Type curves were made for cases where the flow index vary from $n = 0.1$ to 1.0 as shown in the log-log plots of dimensionless pressure plots against dimensionless time in figure 4.6 as well as the plots of log-log dimensionless pressure derivative plots as shown in figure 4.7. From the plots it can be seen that as the flow index n decreases from 1.0 to 0.1 the pressure drop increases. Although the flow regimes are obvious for the Newtonian plots, they are not obvious for the non-Newtonian case. The type curves when $n=0.9$ to 0.7 are similar to when $n=1.0$ the pseudo Steady state flow regime exist for all values of n .

4.3.2 Horizontal Well length of 1000ft $k_x = 100md$, $k_y = 50md$ $k_y = 25md$ $h = 300ft$

The type-curve for the case whereby the horizontal well length is 1000ft is as presented in figure 4.8-4.9 For flow index $n=0.1$ to 1.0 . In the derivative log-log plots the early radial flow is absent, but the, Pseudo radial flow, early linear, a transition zone and pseudo steady state flow regimes can be seen in the plots. Similarly as for the case when the horizontal well was 600ft, the pressure drop increased as the non-Newtonian flow index n decreased. Also as the value of n tends to 1 the type curve and log-log pressure drop plots are similar. The value of $\Delta t_D * \Delta P_{wD}'$ increases from the 0.5 the Newtonian value as the value of n increases from 0.1 to 0.9

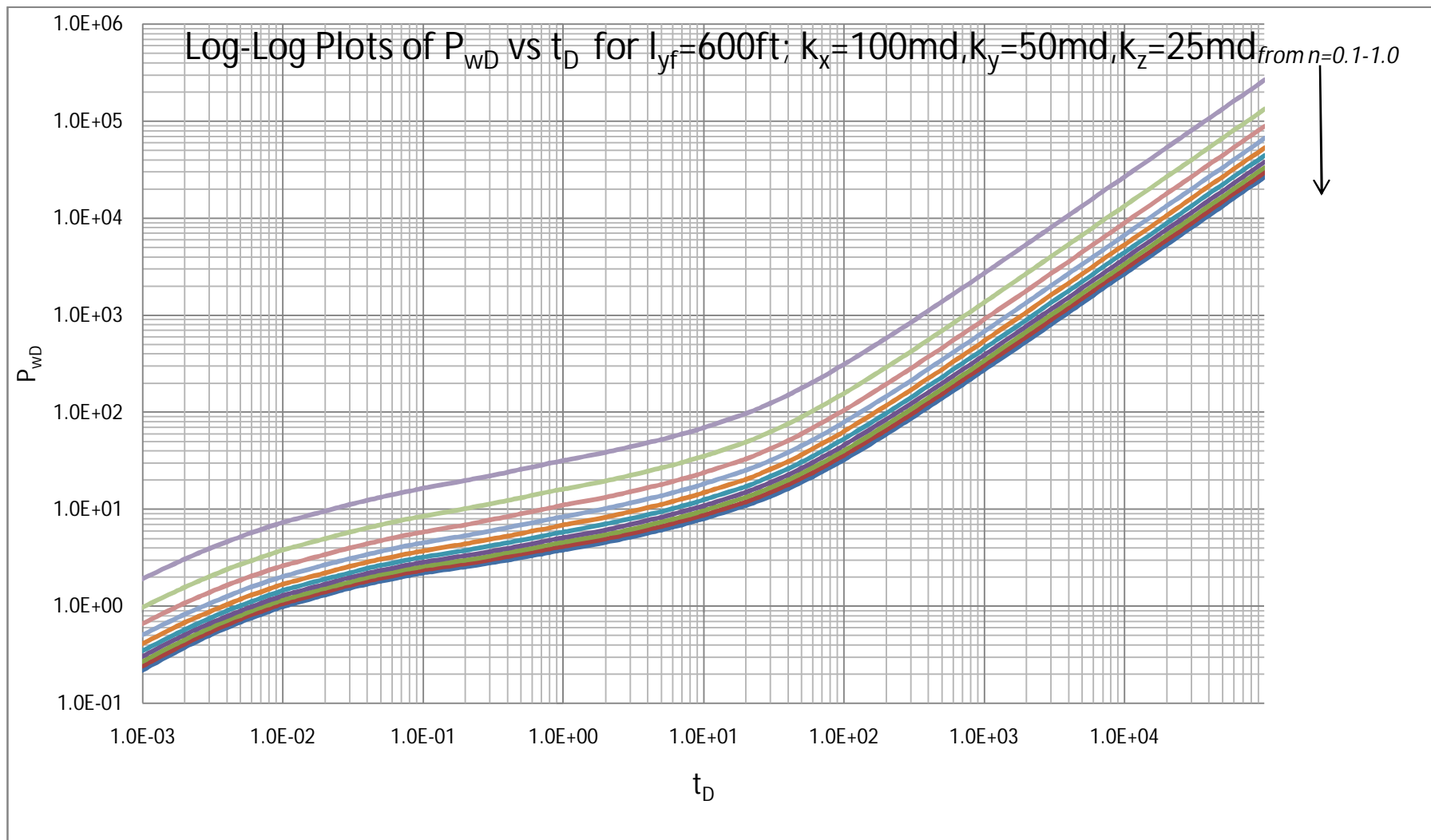


Figure 4.6: Log-Log Plots of P_{wD} vs t_D for $l_{yf}=600\text{ft}$; $k_x=100\text{md}$, $k_y=50\text{md}$, $k_z=25\text{md}$

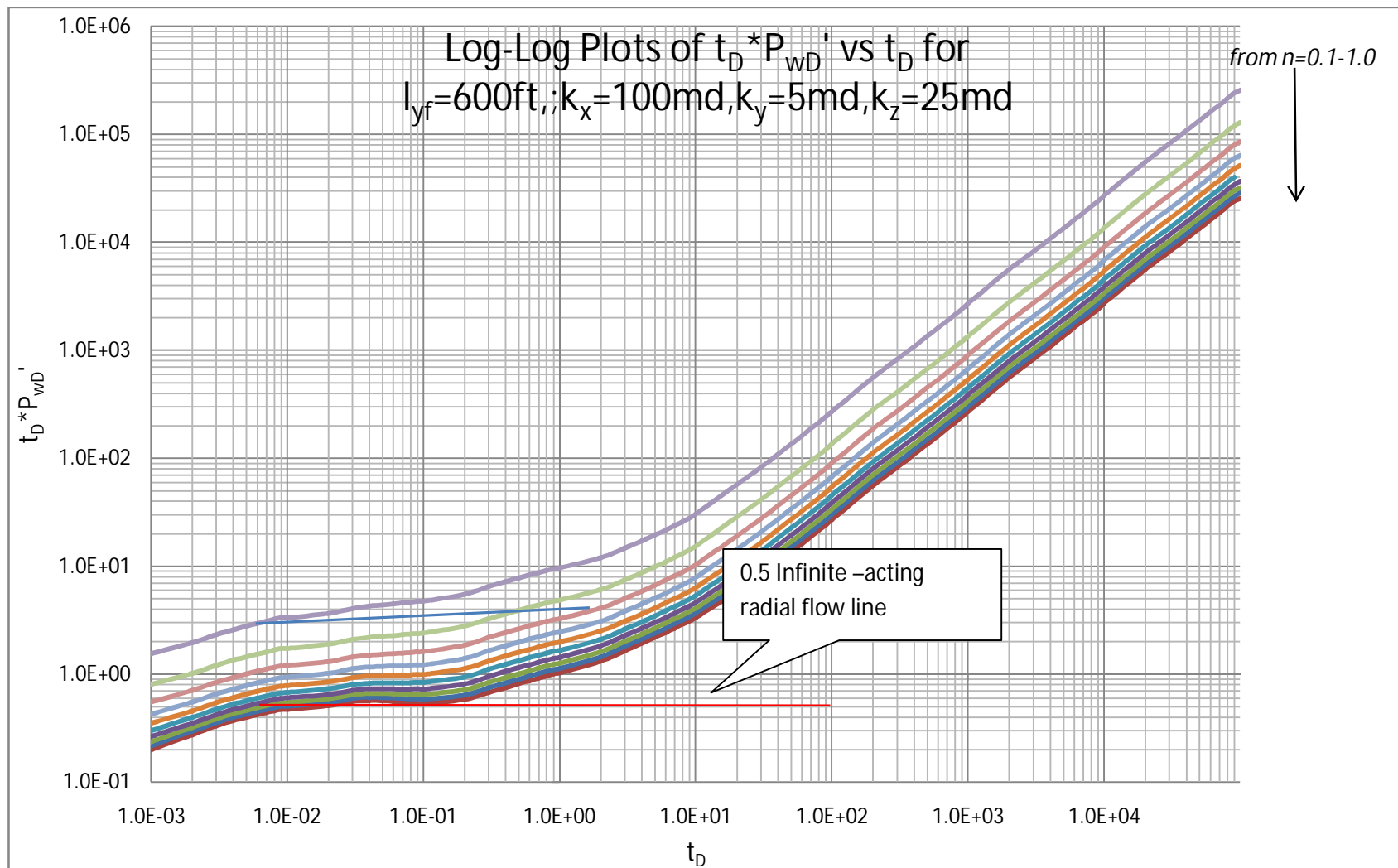


Figure 4.7: Log-Log Plots of $t_D * P_{wD}'$ Vs t_D for $I_{yf}=600\text{ft}; k_x=100\text{md}, k_y=50\text{md}, k_z=25\text{md}$

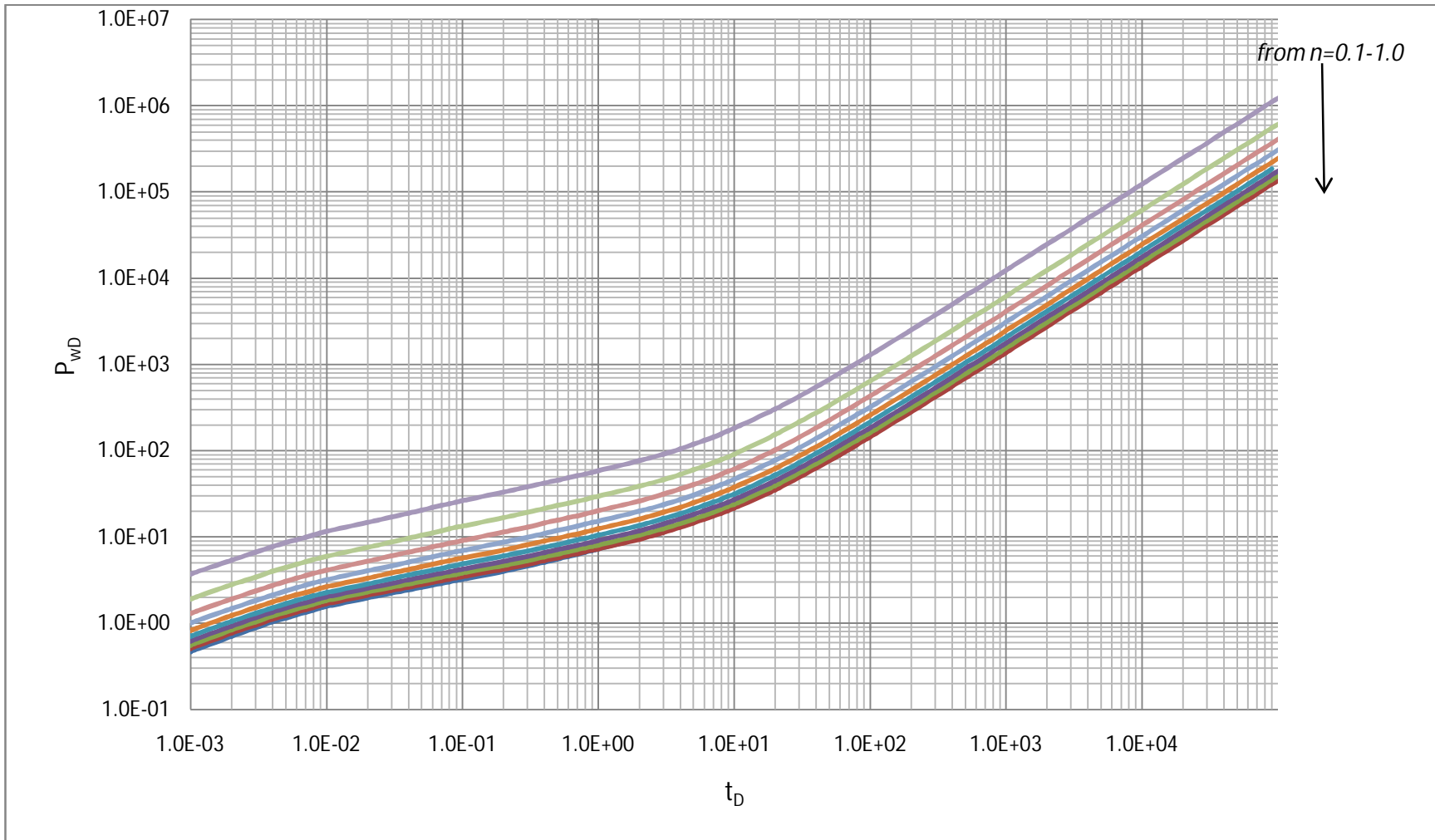


Figure 4.8: Log-Log Plots of P_{wD} Vs t_D for $l_{yf}=1000\text{ft}$; $k_x=100$, $k_y=50$, $k_z=25$

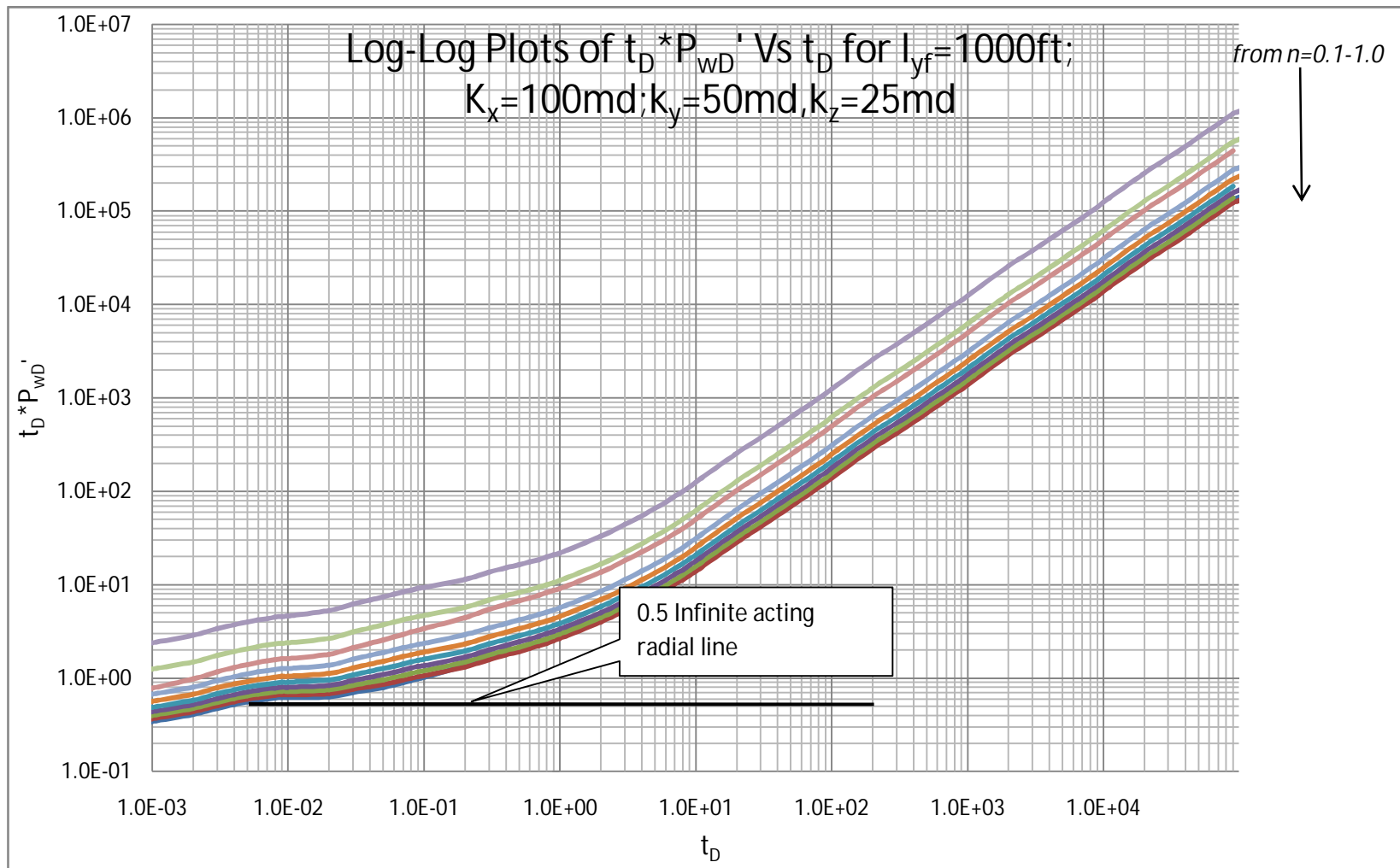


Figure 4.9: Log-Log Plots of $t_D * P_{wD}'$ Vs t_D for $l_{yf}=1000\text{ft}$; $K_x=100\text{md}$; $k_y=50\text{md}$; $k_z=25\text{md}$

4.3.3 Horizontal Well length of 1200ft $k_x = 100md$, $k_y = 50md$ $k_y = 25md$ $h = 300ft$

The type-curve for the case whereby the horizontal well length is 1000ft is as presented in figure 4.10-4.11 For flow index $n=0.1$ to 1.0 . In the derivative log-log plots the early radial flow flow is absent, but the Pseudo radial, early linear and pseudo steady state flow regimes can be seen in the plots. Similarly as for the case when the horizontal well was 600ft, the pressure drop increased as the non-Newtonian flow index n . Also as the value of n tends to 1 the type curve and log-log pressure drop plots are similar.

4.3.4 Horizontal Well length of 600ft $k_x = 75md$, $k_y = 75md$ $k_y = 75md$ $h = 300ft$

The type-curve for the case whereby the horizontal well length is 600ft is as presented in figure 4.12-4.13. For flow index $n=0.1$ to 1.0 . In the derivative log-log plots early radial flow is absent, but a short pseudo radial flow, short early linear, a transition flow regime and a pseudo steady state flow regimes can be seen in the plots. The pressure drop increased as the non-Newtonian flow index n reduced from 1 to 0.1 . Also as the value of n tends to 1 the type curve and log-log pressure drop plots are similar.

4.3.5 Horizontal Well length of 1000ft $k_x = 75md$, $k_y = 75md$ $k_y = 75md$ $h = 300ft$

The type-curve for the case whereby the horizontal well length is 1000ft is as presented in figure 4.14-4.15 For flow index $n=0.1$ to 1.0 . In the derivative log-log plots the Pseudo radial flow is absent, but the early linear and pseudo steady state flow regimes can be seen in the plots. Similarly as for the case when the horizontal well was 600ft, the pressure drop increased as the non-Newtonian flow index n decreases. Also as the value of n tends to 1 the type curve and log-log pressure drop plots are similar.

4.3.6 Horizontal Well length of 1200ft $k_x = 75md$, $k_y = 75md$ $k_y = 75md$ $h = 300ft$

The type-curve for the case whereby the horizontal well length is 1200ft is as presented in figure 4.16-4.17 For flow index $n=0.1$ to 1.0 . In the derivative log-log plots the Pseudo radial flow and early radial flow is absent, but the early linear, a transition flow regime that finally leads to a pseudo steady state flow regimes can be seen in the plots. Pressure drop increased as the non-Newtonian

flow index n decreases. Also as the value of n tends to 1 the type curve and log-log pressure drop plots are similar.

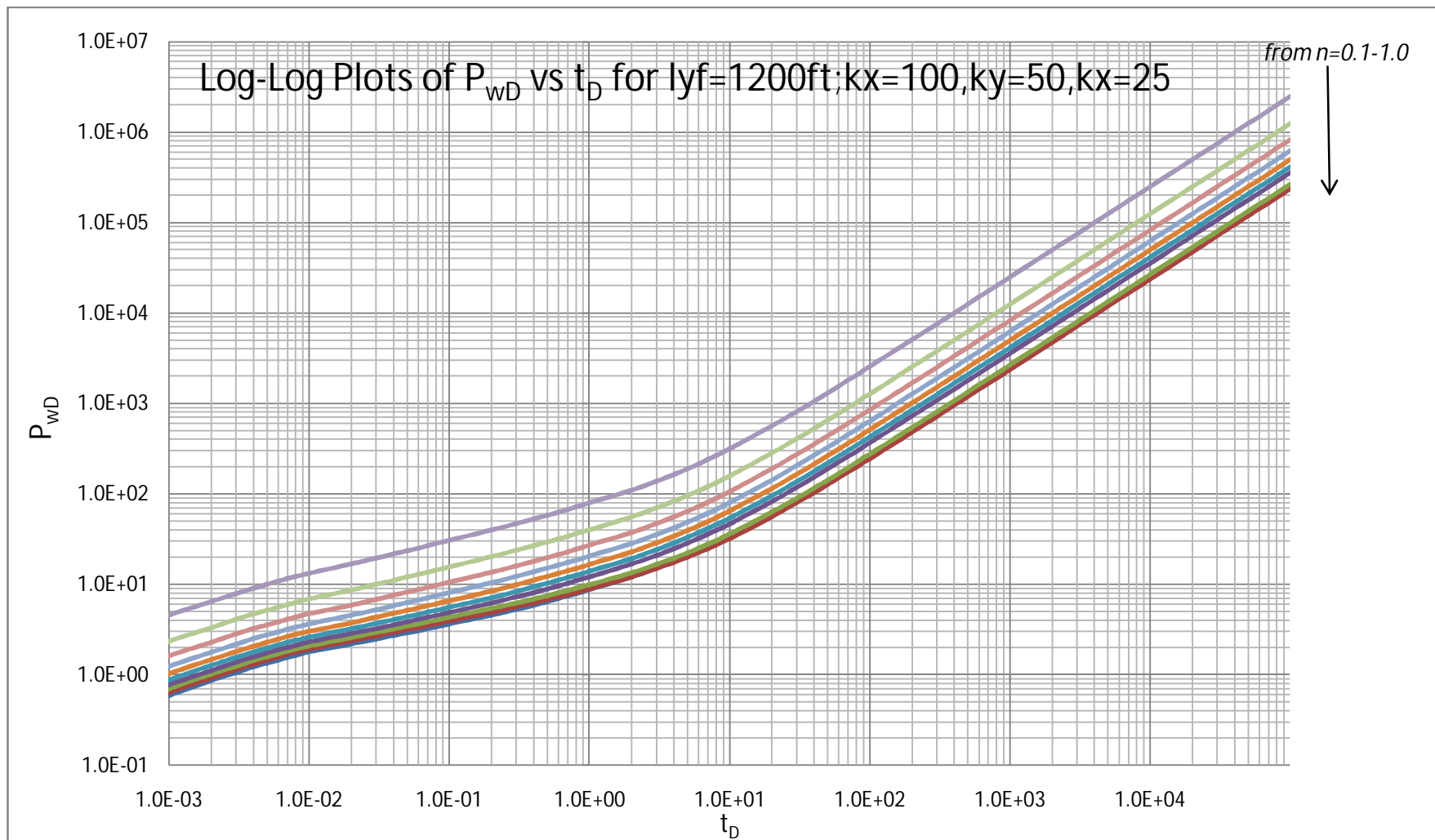


Figure 4.10: Log-Log Plots of P_{wD} Vs t_D for $lyf=1200ft; kx=100, ky=50, kx=25$

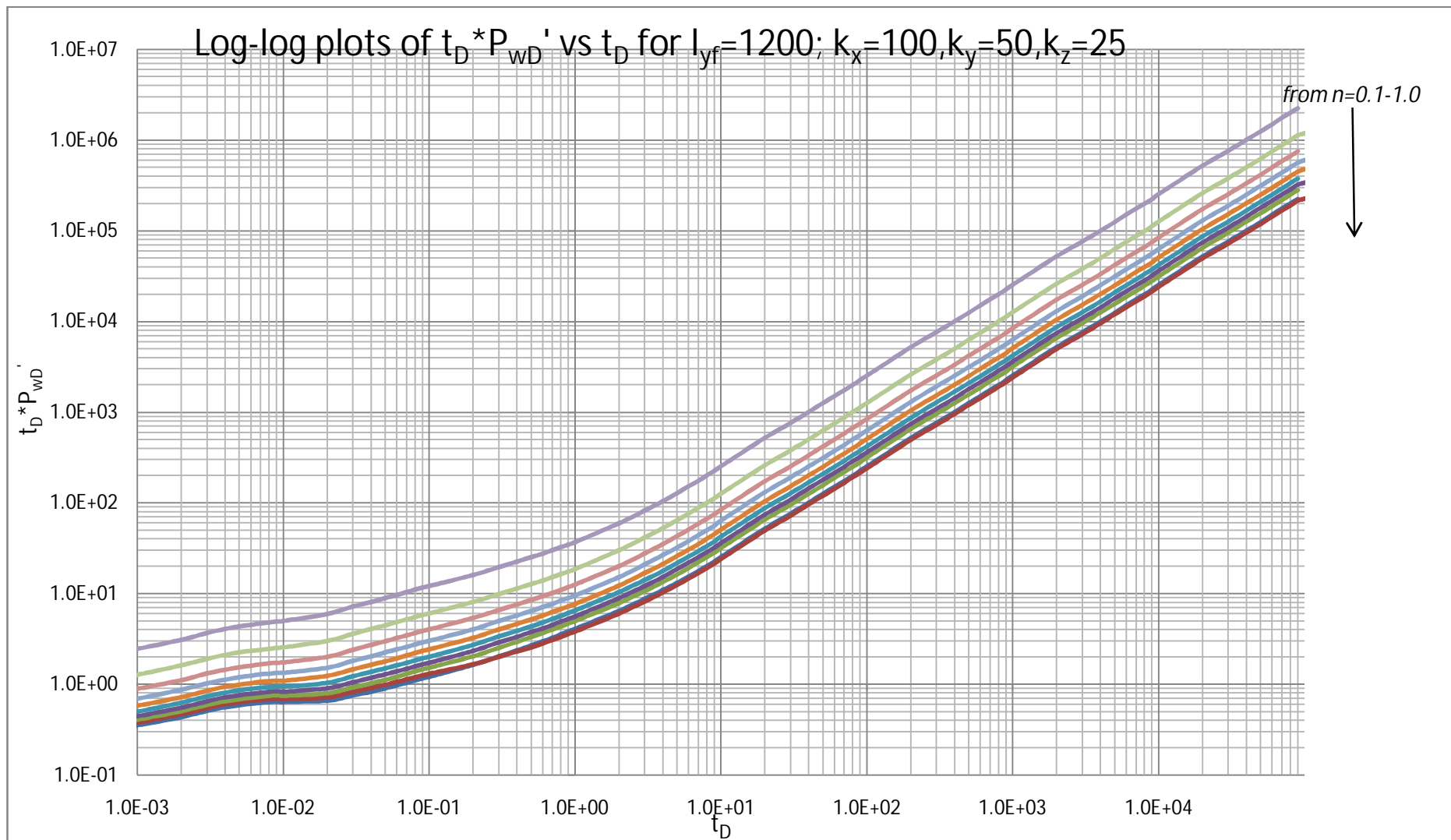


Figure 4.11: Log-log plots of $t_D * P_{wD}'$ Vs t_D for $l_{yf}=1200; k_x=100, k_y=50, k_z=25$

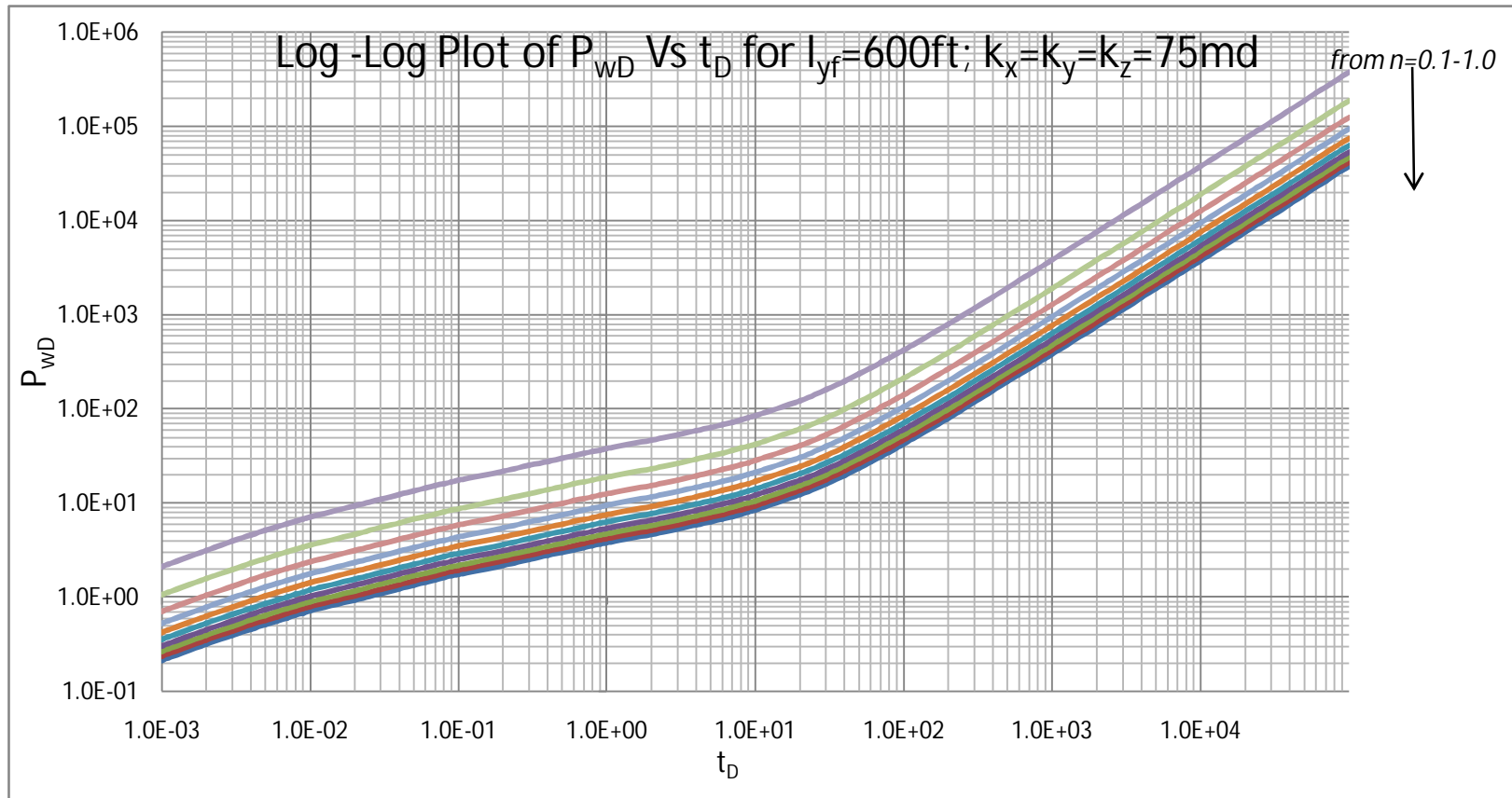


Figure 4.12: Log -Log Plot of P_{wD} Vs t_D for $l_{yf}=600\text{ft}; k_x=k_y=k_z=75\text{md}$

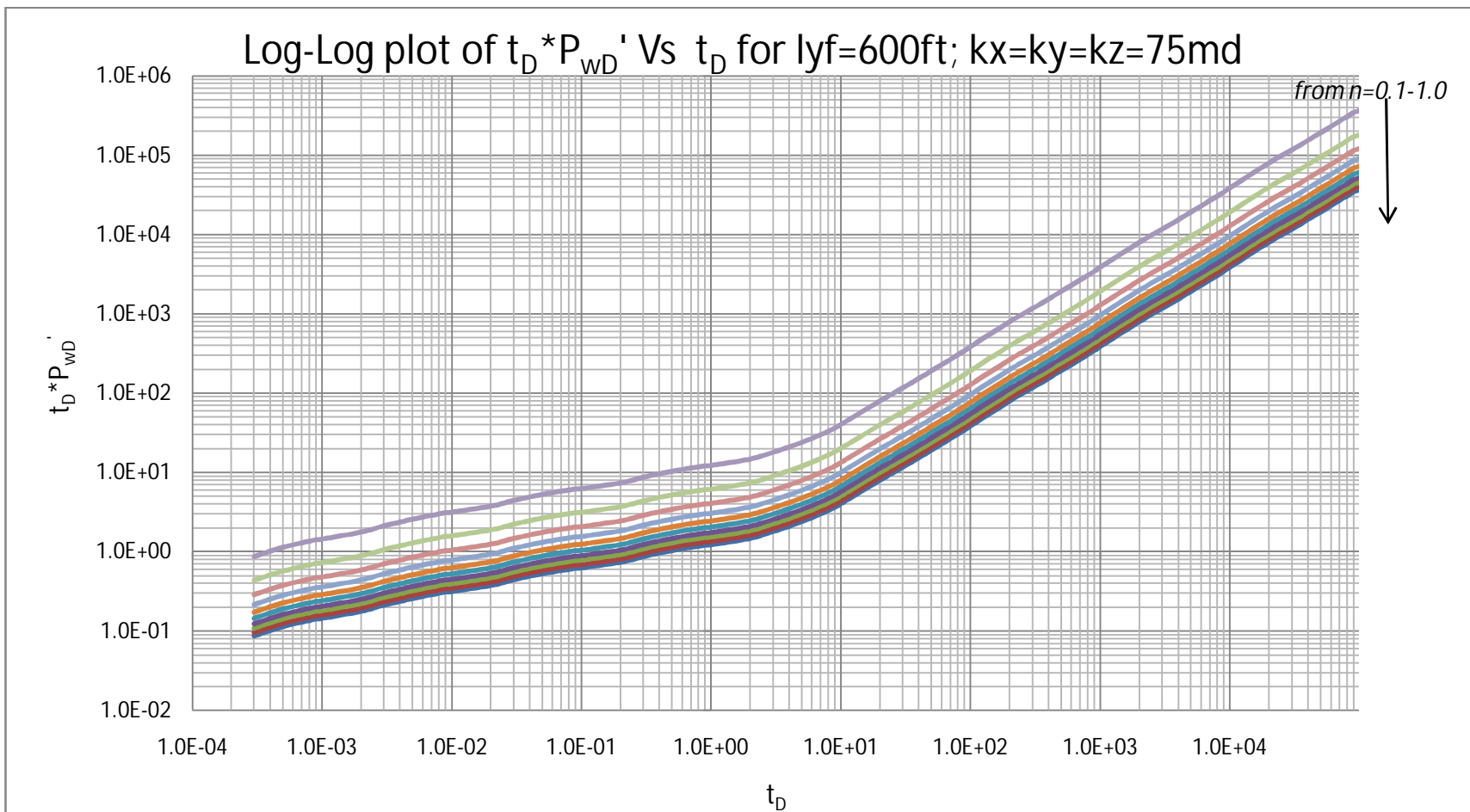


Figure 4.13: Log-Log plot of $t_D * P'_{WD}$ Vs ΔtD for $lyf=600ft$; $kx=ky=kz=75md$

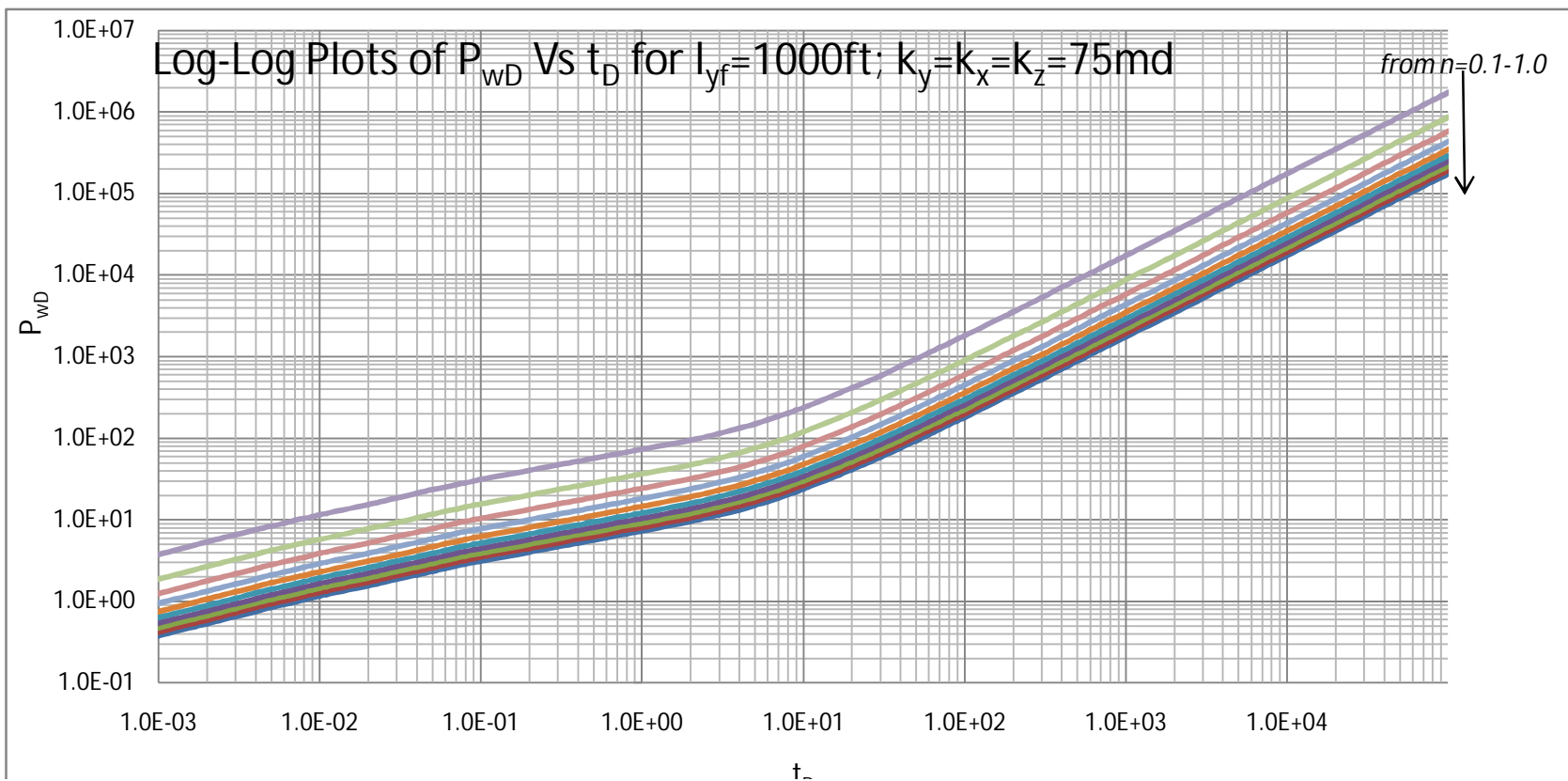


Figure 4.14: Log-Log Plots of P_{wD} Vs t_D for $l_{yf}=1000\text{ft}$; $k_y=k_x=k_z=75\text{md}$

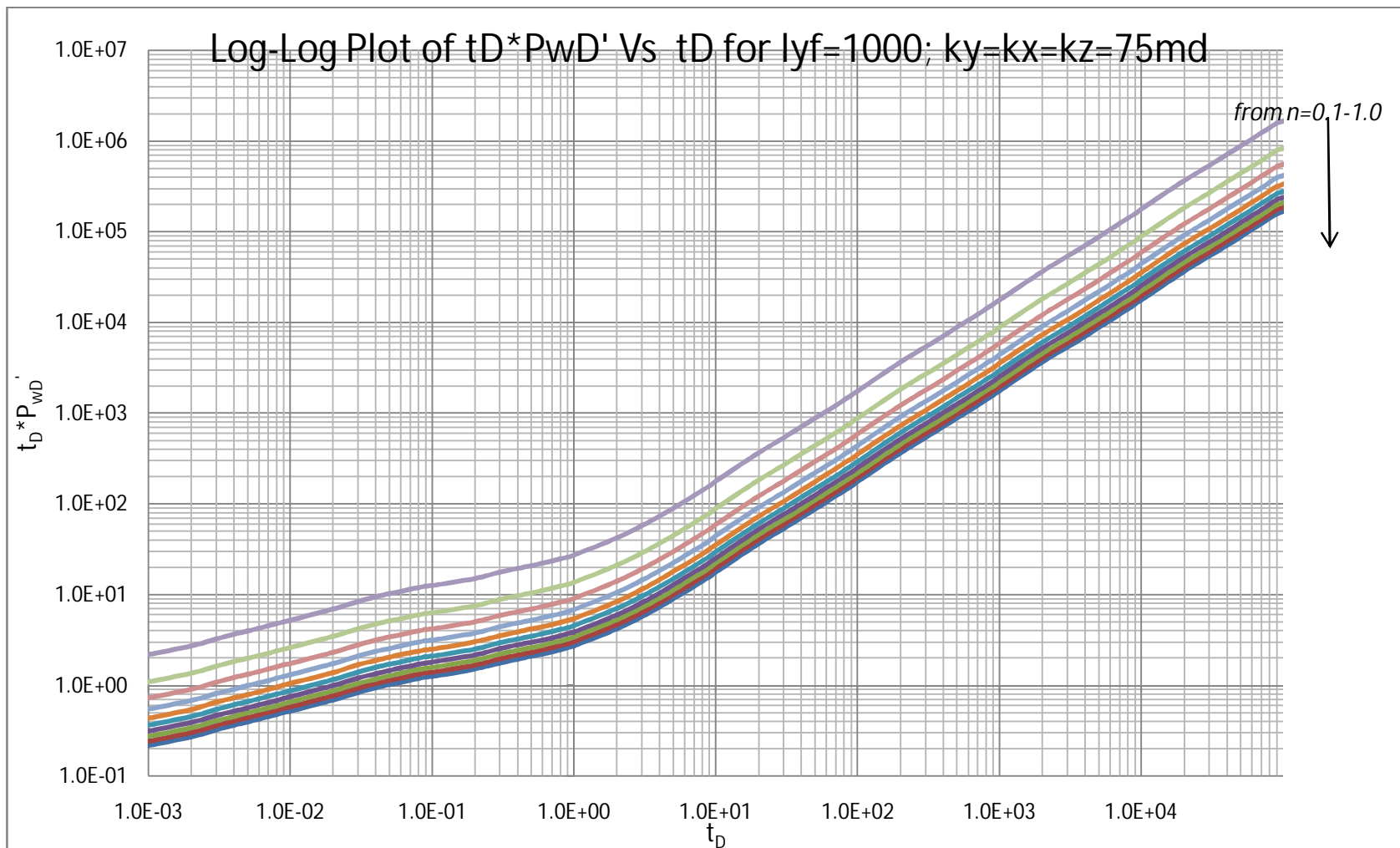


Figure 4.15: Log-Log Plot of $t_D * P_{wD}'$ Vs t_D for $l_{yf}=1000$; $k_y=k_x=k_z=75\text{md}$

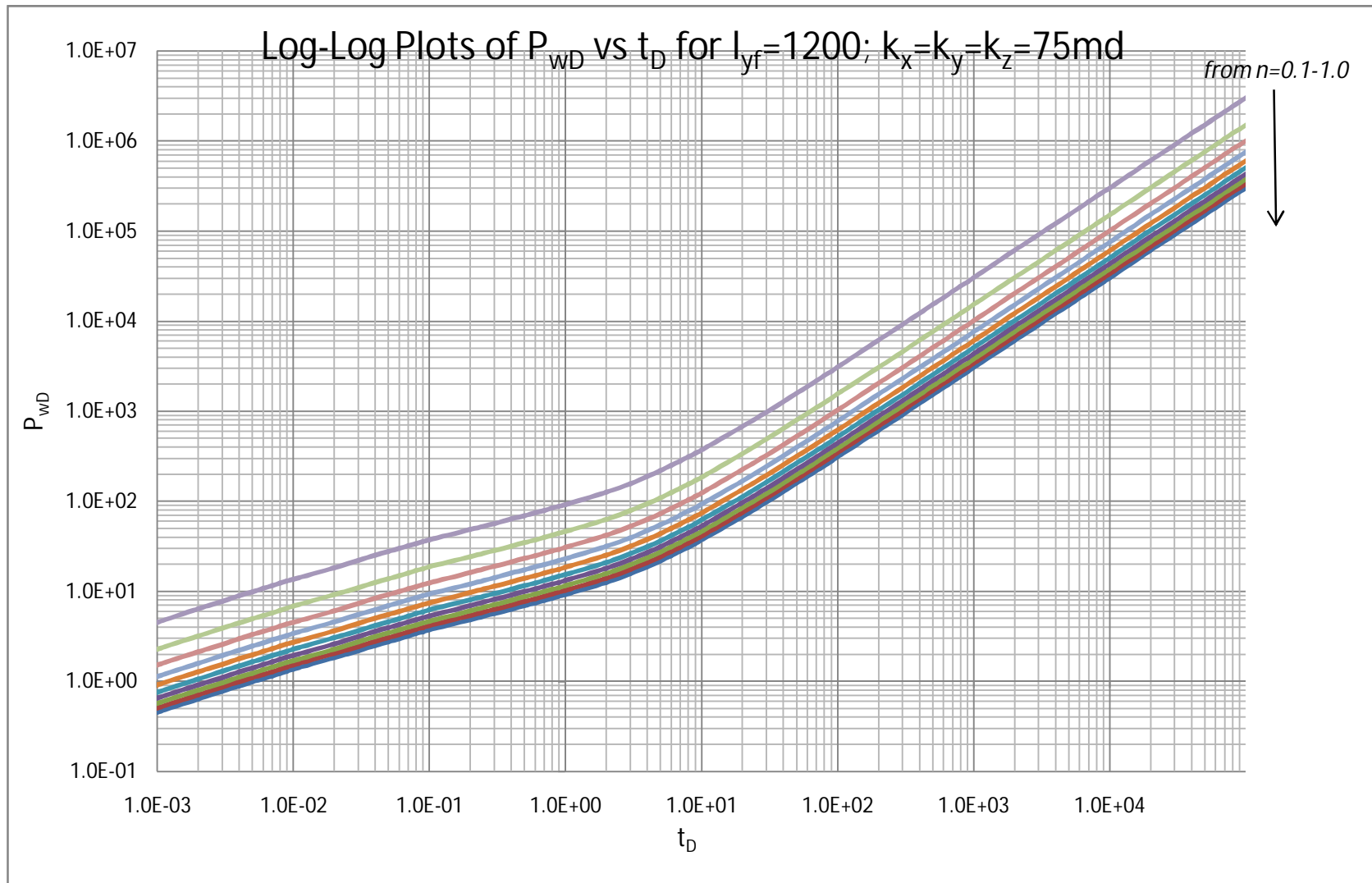


Figure 4.16: Log-Log Plots of P_{wD} Vs t_D for $l_{yf}=1200; k_x=k_y=k_z=75md$

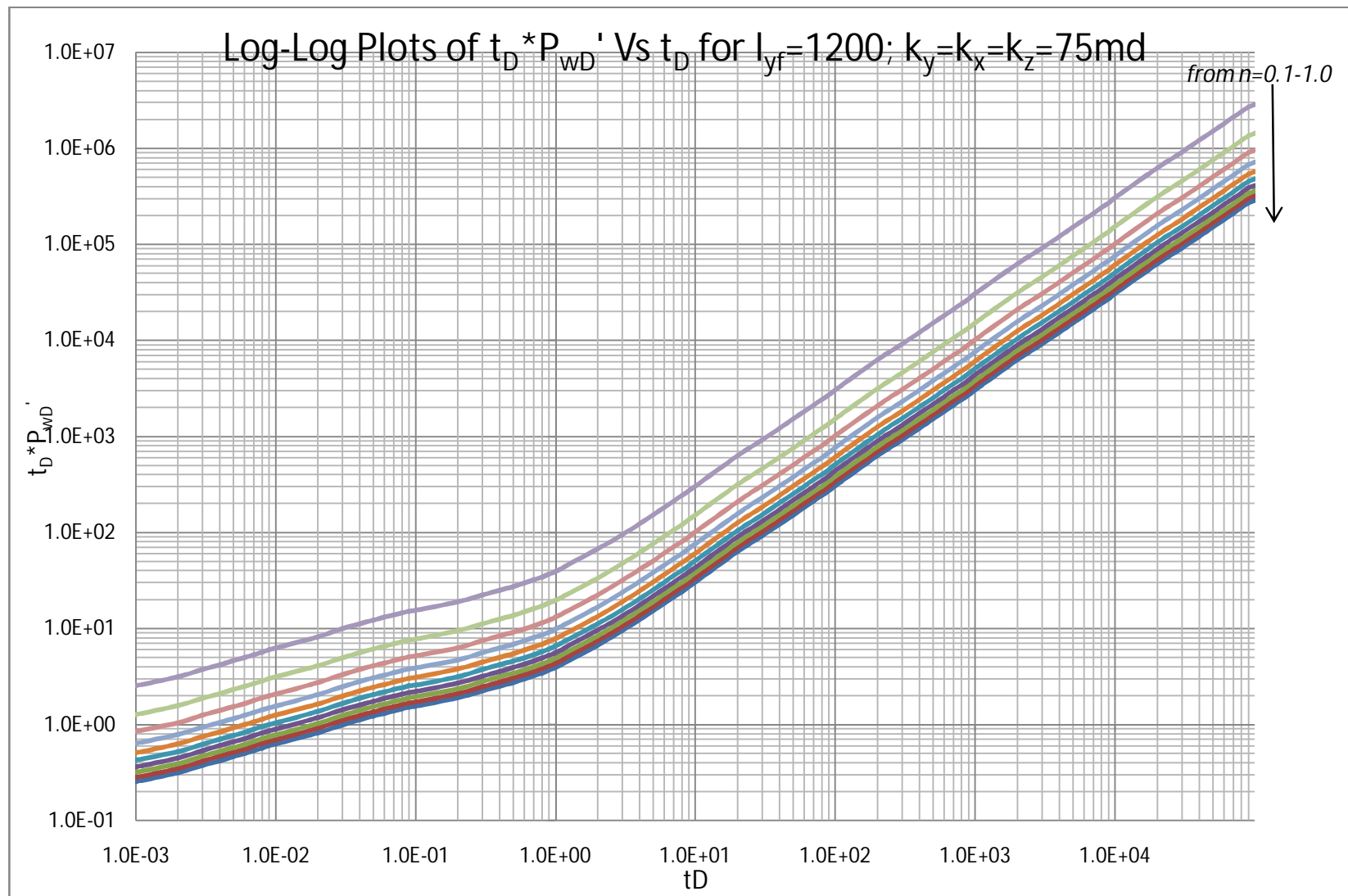


Figure 4.17: Log-Log Plots of $t_D * P_{wD}'$ Vs t_D for $l_{yf}=1200; k_y=k_x=k_z=75md$

CHAPTER FIVE

5.0 CONCLUSIONS AND RECOMMENDATIONS

5.1 CONCLUSIONS

As the application of horizontal wells in enhanced oil recovery operations increases globally with increased exploration and exploitation of heavy crude in places like Venezuela, Canada etc, the following conclusions were made from this study;

- The finite-difference Numerical solution of the partial differential equation as developed in this study describing the flow of non-Newtonian fluid in a reservoir with permeability heterogeneity is valid to a large degree of accuracy. This is because close value of reservoir properties were obtained in the validation when a Newtonian reservoir fluid is considered.
- The pressure drop in the draw-down of a non-Newtonian fluid reservoir is higher compared to the pressure drop in a Newtonian fluid reservoir.
- In cases when the horizontal well length is 600ft in an heterogeneous reservoir, early linear, Pseudo radial , a transition flow regime and Pseudo steady state flow were observed which aided the determination of reservoir properties such as; k_x the average reservoir permeability k , mobility and the Drainage area
- As the horizontal well length increases the type curve indicates the absence of the psedoradial radial flow. A very short linear alongside Pseudo steady state flow regime is observed.
- In the analysis of the pressure transient, the correlation factor obtained in the study of Vongvuthiopornchai and Raghavan, 1987 were found to be applicable and valid for the different values of n
- For cases where the reservoir is homogeneous with respect to permeability and porosity, the early flow regime is not seen irrespective of the horizontal well length.

- The novel approach for the analysis of pressure transient data of horizontal well in non-Newtonian reservoir fluids as presented in this work is found to be consistent with the result obtained in the works of Igbokoyi and Tiab,2007;
- The pressure derivative method can only be used to obtain average permeability when the radial flow exists.

5.2 RECOMMENDATIONS

In order to perfect the study made in this work, the following recommendations are made;

- Further works should consider the effect of skin and wellbore storage in the analysis of pressure transient data of horizontal well in non-Newtonian fluid reservoirs
- Much finer grids size should be used in any further study; this will require a high performance computer which was not used in this study.
- Other numerical method such as finite element method should be used to solve the partial differential equation describing the flow of non-Newtonian fluid in porous media. This will enable the modeling of reservoirs of different geometry or shape and reduce errors due to approximation as encountered when finite difference is used.
- Considering the fact that multiphase conditions exist in the reservoir, a study on the multiphase flow of non-Newtonian fluid in the reservoir should be a right step
- Further works should look into the analysis of horizontal well in non-Newtonian fluids considering a 3 dimensional radial flow.
- Further works on this subject matter should consider local grid refinement throughout the length of the horizontal well to improve on the results obtained.
- The application of this work to the characterization of heavy oil reservoirs should also be looked into by subsequent studies.

REFERENCES

- Adam T. Bourgoyne Jr., Keith K. Millheim, Martin E. Chenevert, F.S. Young Jr: 'Applied Drilling Engineering' first printing Society of Petroleum Engineers Richardson TX, 1986
- A. S. Odeh and H. T. Yang: 'Flow of Non-Newtonian Power-Law Fluids through Porous Media' April, 1979 (SPE 7150)
- Alpheus O. Igbokoyi and Djebbar Tiab, SPE, U. of Oklahoma: 'New Type Curves for the Analysis of Pressure Transient Data Dominated by Skin and Wellbore Storage-Non-Newtonian Fluid' April, 2007. (SPE 106997)
- Aziz S. Odeh and D.K Babu: Transient Flow behavior of Horizontal Wells: Pressure Drawdown and Buildup Analysis. SPE Formation Evaluation, March 1990.
- Aziz, K and Settari, A.: Petroleum Reservoir Simulation, Applied Science Publishers Ltd., London (1979) 69-92.
- Bird, B. R., Stewart, W. E and Lightfoot, E.N.: Transport Phenomena, John Wiley and Sons Inc. New York City (1960) 206
- Chi U. Ikoku, University of Tulsa; 'Practical Application of Non-Newtonian Transient Flow Analysis' SPE Las Vegas, 1979 (SPE 8351)
- Christopher, R. H. and Middleman, S.: 'Power-Law Flow Through a Packed Tube,' Ind & Eng. Chem. Fund. (Nov. 1965) 4, No. 4 422-426
- Chi U. Ikoku and Henry J. Ramey; 'Wellbore Storage and Skin Effects during the Transient Flow of Non-Newtonian Power-Law fluids in Porous Media' February, 1980 (SPE 7449)
- D. K. Babu, G.B. Asher, A.S. Odeh: 'A Reliable Method for Analyzing Constant-Rate Drawdown Data From a Horizontal well'. SPE, 1992 (SPE 02450)
- Engler, T. and Tiab, D.: 'Analysis of Pressure and pressure derivative without tpe curve matching, for Naturally fractured reservoirs' Journal of Petroleum Science and Engineering, Nov, 1995.
- F. Medeiros Jr., E. Ozkan and H. Kazemi: 'A Semianalytical Approach to Model Pressure Transient in Heterogeneous Reservoirs' April, 2010 SPE Reservoir Evaluation and Engineering. (SPE 102834)
- Gencer, S and Ikoku, C. U.: 'Well Test Analysis for Two -Phase Flow of Non-Newtonian Power-law and Newtonian Fluids,' J. Energy Resources Tech. (June 1984) 106,295-305.

- Ikoku, C.U and Ramey, H. J. Jr; 'Transient Flow of Non-Newtonian Power-Law Fluids in Porous Media' January, 1979 (SPE 7139)
- Irina Katime-Meindl and Djebbar Tiab; 'Analysis of Pressure Transient Test of Non-Newtonian Fluids in Infinite Reservoir and in the Presence of a single linear Boundary by the Direct Synthesis Technique' September, 2001 (SPE 71587)
- Joseph S. Olarewaju: 'A Reservoir Model of Non-Newtonian Fluid Flow. SPE, Tulsa Oklahoma, June 1992' (SPE 25301)
- M. B. Issaka and A.K Ambastha.: 'Drawdown and Buildup Pressure Derivative Analyses for Horizontal wells' paper SPE 24323 presented at the SPE Rocky Mountain Regional Meeting, Wyoming, May, 1992.
- M.D. Clonts and H.J Ramey.: 'Pressure Transient Analysis for wells with Horizontal Drainholes' paper SPE 15116 presented at the 56th California Regional meeting of SPE CA. April, 1966.
- McDonald, A.E.: Approximate Solutions for Flow of Non-Newtonian Power-Law Fluids Through Porous Media,' Paper SPE 7690 Presented at the 1979 SPE Reservoir simulation symposium, Denver, Feb
- Micheal J. Economides, Franz X. Delmbacher, Clemens W. Brand and Zoltan E. Heinemann: 'Comprehensive Simulation of Horizontal-well Performance', SPE Formation Evaluation, December 1991 (SPE 20717)
- M.Y. Soliman, J.Ansah, J.Burris, S. Stephenson, M. Proett: 'Well Test Analysis in the New Economy', July, 2003, Volume 42, No.7 Journal of Canadian Petroleum Technology.
- Murtha, J. A. and Ertekin, T.: 'Numerical Simulation of Power-law Fluid Flow in Vertically Fractured Reservoir,' paper SPE 12011 presented at the 1983 SPE Annual Technical Conference and ExhibitioB, San Francisco.
- N. Al-Mohannadi, E. Ozkan and H. Kazemi; 'Grid-System requirements in Numerical Modeling of Pressure-Transient Tests in Horizontal Wells' February, 2007 (SPE 92041)
- O. Lund and Chi U. Ikoku; 'Pressure Transient Behavior of Non-Newtonian/ Newtonian Fluid Composite Reservoirs' April, 1981 (SPE 9401)
- P.A. Goode and R.K.M. Thambynayagam: 'Pressure Drawdown and Buildup Analysis of Horizontal Wells in Anisotropic Media' SPE Formation Evaluation, December 1987. (SPE 14250)
- Puthigai, S.K and Tiab, D.: 'Application of P_D ' Function of vertically Fractured Wells-Field Cases' paper SPE 11028 presented at the 1982 SPE Annual Technical Conference and Exhibition, New Orleans, Sept. 26-29
- S. Al Rbeawi and D. Tiab.: 'Pressure Transient Analysis of Horizontal wells in a Multi-Boundary System' paper SPE 142316, Present at the SPE Production and Operations Symposium held in Oklahoma March,2011
- Savins, J.G.: 'Non-Newtonian Flow through Porous Media' Ind. & Eng. Chem. (oct. 1969) 61. NO. 10, 18-47.

- S. Vongvuthipornchai and R. Raghavan: 'Pressure Falloff Behavior in Vertically Fractured Wells: Non-Newtonian Power-Law Fluids' SPE Formation Evaluation, December 1987. (SPE 13058)
- S. Vongvuthipornchai and Rajagopal Raghavan; 'well test Analysis of Data Dominated by Storage and Skin: Non-Newtonian Power-Law Fluids' December, 1987 (SPE 14454)
- Tiab, D.: 'Analysis of Pressure and Pressure derivative without type curve matching- Skin and wellbore storage' Journal of Petroleum Science and Engineering. Nov, 1994.
- Turgay Ertekin, Jamal H. Abou-Kassem and Gregory R. King: 'Basic Applied Reservoir Simulation', SPE, 2001
- T. Ertekin, O. Cicek and M.A. Adequmi,' Pennsylvania State U. and M.E. Daud, Petronas: Pressure Transient Behavior of Non-Newtonian/Newtonian Fluid Composite Systems in porous Media with a Finite Conductivity Vertical Fracture' SPE pittsburgh, Pennsylvania, 1987 (SPE 17053)
- Van Poolen, H.K and Jargon, J. R: 'Steady-State and Unsteady-State Flow of Non-Newtonian Fluids through Porous Media' Society of Petroleum Engineering Journal, 1969, 80-88 (SPE 1567)
- V.R Penmatcha and Khalid Aziz: 'Comprehensive Reservoir/Wellbore Model for Horizontal Wells', SPE Journal September, 1999 (SPE 571942)
- Wong, D. W., Harrington, A.G., and Cinco-L., H.; 'Application of the Pressure Derivative Function in the Pressure Transient Testing of Fractured Wells,' paper SPE 13056 presented at the 1984 SPE Annual Technical Conference and Exhibition, Houston, Sept. 16-19.

NOMENCLATURE

τ = shear stress in $\frac{\text{lb}_f}{\text{ft}^2}$ or N/m^2

L_{xf} = fracture half length or horizontal well length m or ft

γ = shear rate in sec^{-1}

μ = viscosity in $\text{lb}_f \cdot \frac{\text{s}}{\text{ft}^2}$ or $\text{Pa} \cdot \text{s}$

K = consistency index $\text{lb}_f \cdot \frac{\text{s}^n}{\text{ft}^2}$ or $\text{Pa} \cdot \text{s}^n$

n = power law exponent or the flow – behavior index

μ_p = Plastic viscosity $\text{lb}_f \cdot \frac{\text{s}}{\text{ft}^2}$ or $\text{Pa} \cdot \text{s}$

q = flow rate ft^3/s or m^3/s

k = permeability md or m^2

P = pressure Psia or N/m^2

D_p = Diameter of bead particles inches

u = velocity ft/s

r_D = dimensionless radius

ΔP_{wf} = Bottom hole well bore flowing pressure

c_t = total compressibility Psia^{-1}

B = formation volume factor rb/stb

P_i = initial reservoir Pressure, psia or N/m^2

μ_{eff} = effective viscosity $\text{lb}_f \cdot \frac{\text{s}}{\text{ft}^2} \text{ft}^{1-n}$ or $\text{Pa} \cdot \text{s} \text{m}^{1-n}$

r_w = wellbore radius, ft or m

s = skin factor

C = wellbore storage coefficient $\frac{\text{bbl}}{\text{psi}}$ or $\frac{\text{m}^3}{\text{Pa}}$

L = length m or ft

H = bed factor of the formation Pa. s m^{1-n}

μ^* = characteristic viscosity Pa. s

t = time seconds or hour

x = distance in the x – direction m or ft

y = distance in the y – direction m or ft

z = distance in the z – direction m or ft

μ_a = apparent viscosity Pa. s

β_c = constant = 1.127 (field units) or 86.4×10^{-6} (metric units)

V_b = bulk volume of a reservoir ft^3 or m^3

A = Crosssectional Area ft^2 or m^2

ρ = density $\left(\frac{\text{lb}}{\text{ft}^3}\right)$

m = mass flow rate $\left(\frac{\text{lb}}{\text{s}}\right)$

ϕ = porosity (%)

Δ = change

\vec{i} = unit vector in the x – direction

\vec{j} = unit vector in the y – direction

\vec{k} = unit vector in the z – direction

C_{fi} = correction factor for infinite – conductivity idealization

C_{fu} = correction factor for uniform – flux idealization

C_r = correction factor for plane radial flow

Subscript

D = dimensionless

e = external boundary

i, j, k = spatial grid index

r = radial

lr = late radial

il = intermediate linear

er = early radial

l = liquid phase

sc = standard conditions

a = apparent

s = skin region

APPENDIX A

A.1 Pressure data used for the validation of flow index $n = 0.1$

Δt	ΔP	$t^* \Delta P w_f^i$
8.196785823	769.6171462	
16.39357165	5695.404892	
24.59035747	9181.381924	9031.183504
32.78714329	11868.0169	9654.433169
40.98392912	14076.95449	10190.02902
49.18071494	15978.1439	10712.89047
57.37750076	17666.71649	11234.42752
65.57428658	19199.2978	11750.61189
73.77107241	20611.71432	12256.1589
81.96785823	21927.95617	12619.13934
163.9357165	31251.25524	16507.56434
245.9035747	38669.53482	20493.06093
327.8714329	45013.52664	23988.46
409.8392912	50701.55014	27346.8401
491.8071494	55964.01453	30694.16605
573.7750076	60934.11777	34054.1322
655.7428658	65691.04032	37409.78313
737.7107241	70282.80655	40732.59067
819.6785823	74739.12491	43704.06543
1639.357165	111453.8077	67771.16037
2459.035747	142443.6685	85758.04087
3278.714329	169018.6183	98671.60753
4098.392912	192126.199	107998.1781
4918.071494	212478.5176	114904.3463
5737.750076	230618.0239	120204.1533
6557.428658	246961.7307	124448.6815
7377.107241	261832.9325	128006.1228
8196.785823	275484.36	129418.6002
16393.57165	364505.9275	151075.1863
24590.35747	431132.4412	178139.4463

32787.14329	485200.4591	198215.02
40983.92912	531208.6686	214412.6024
49180.71494	571526.7836	227971.6135
57377.50076	607559.4832	239560.3296
65574.28658	640220.4057	249636.6602
73771.07241	670147.3042	258552.4246
81967.85823	697809.571	263602.3654
163935.7165	885329.5965	327917.4802
245903.5747	1031898.965	403620.5264
327871.4329	1156613.885	470451.0021
409839.2912	1267984.752	533347.8872
491807.1494	1370327.446	593961.5912
573775.0076	1466139.891	653269.067
655742.8658	1557040.702	712078.9074
737710.7241	1644166.873	771051.3089
819678.5823	1728358.392	838945.9942
1639357.165	2491662.13	1561108.886
2459035.747	3233715.926	2256729.373
3278714.329	3970011.308	2972348.451
4098392.912	4704745.161	3697098.566
4918071.494	5439055.484	4425980.116
5737750.076	6173250.925	5156801.986
6557428.658	6907415.206	5888623.392
7377107.241	7641571.034	6621023.037
8196785.823	8375724.569	7446132.373
16393571.65	15717251.69	15332926.14
24590357.47	23058778.52	22442848.37
32787143.29	30400305.34	29676281.18
40983929.12	37741832.16	36954515.99
49180714.94	45083358.98	44254336.9
57377500.76	52424885.8	51566266.88
65574286.58	59766412.62	58885684.89
73771072.41	67107939.43	66210061.48
81967858.23	74449466.25	74461252.82
163935716.5	147864734.4	153329259.5
245903574.7	221280002.5	224428483.4
327871432.9	294695270.7	296762811.5
409839291.2	368110538.8	369545159.4
491807149.4	441525806.8	442543368.3
573775007.6	514941074.9	515662667.9
655742865.8	588356343	588856847.8
737710724.1	661771611	662100613.4

819678582.3	735186879	744612526.3
1639357165	1469339558	1533292587
2459035747	2203492235	2244284819
3278714329	2937644910	2967628088
4098392912	3671797584	3695451554
4918071494	4405950257	4425433627
5737750076	5140102927	5156626604
6557428658	5874255597	5888568381
7377107241	6608408264	6621006012
8196785823	7342560930	7000912533

A.2 Pressure data for the validation of kx , k and Drainage area

t_D	$P_{WD} @n=1$	$t_D * P_{WD}'$	$\Delta P(Psia)$	t (seconds)	$t * \Delta P'$
0.0001	0.002884151		79.42039	8.196785823	
0.0002	0.024407363		672.1014	16.39357165	
0.0003	0.041174515	0.044807	1133.816	24.59035747	1233.857
0.0004	0.054769963	0.049463	1508.191	32.78714329	1362.055
0.0005	0.066188867	0.05283	1822.632	40.98392912	1454.761
0.0006	0.076067644	0.055595	2094.662	49.18071494	1530.909
0.0007	0.084821631	0.058086	2335.719	57.37750076	1599.505
0.0008	0.092728025	0.060448	2553.436	65.57428658	1664.542
0.0009	0.099976355	0.062739	2753.032	73.77107241	1727.624
0.001	0.106699535	0.064302	2938.167	81.96785823	1770.667
0.002	0.153507157	0.081823	4227.101	163.9357165	2253.148
0.003	0.190073815	0.099422	5234.031	245.9035747	2737.765
0.004	0.220561213	0.11313	6073.557	327.8714329	3115.24
0.005	0.24704366	0.124807	6802.8	409.8392912	3436.794
0.006	0.270711604	0.135415	7454.54	491.8071494	3728.905
0.007	0.292315922	0.145486	8049.454	573.7750076	4006.219
0.008	0.31235997	0.155315	8601.404	655.7428658	4276.876
0.009	0.331194417	0.165054	9120.045	737.7107241	4545.067
0.01	0.349069619	0.17388	9612.271	819.6785823	4788.103

0.02	0.488848841	0.256231	13461.35	1639.357165	7055.778
0.03	0.605684836	0.323658	16678.64	2459.035747	8912.524
0.04	0.706042635	0.373459	19442.18	3278.714329	10283.87
0.05	0.793636898	0.410205	21854.25	4098.392912	11295.74
0.06	0.871056523	0.437746	23986.14	4918.071494	12054.15
0.07	0.940244588	0.458954	25891.36	5737.750076	12638.15
0.08	1.00270006	0.475863	27611.18	6557.428658	13103.77
0.09	1.059594562	0.489877	29177.88	7377.107241	13489.67
0.1	1.111852221	0.495119	30616.89	8196.785823	13634.02
0.2	1.451077257	0.573739	39958.07	16393.57165	15798.94
0.3	1.703712281	0.674551	46914.84	24590.35747	18574.99
0.4	1.90827537	0.750208	52547.86	32787.14329	20658.36
0.5	2.082453098	0.812948	57344.16	40983.92912	22386
0.6	2.235495119	0.867223	61558.45	49180.71494	23880.57
0.7	2.372803381	0.915153	65339.49	57377.50076	25200.41
0.8	2.497828839	0.958088	68782.29	65574.28658	26382.7
0.9	2.612938899	0.997057	71952.06	73771.07241	27455.79
1	2.719850846	1.022367	74896.07	81967.85823	28152.74
2	3.463348735	1.316078	95369.65	163935.7165	36240.62
3	4.054711448	1.638956	111653.9	245903.5747	45131.66
4	4.563047428	1.923019	125651.9	327871.4329	52953.86
5	5.019160105	2.185242	138211.8	409839.2912	60174.64
6	5.438612493	2.431178	149762.2	491807.1494	66946.93
7	5.830396296	2.664368	160550.6	573775.0076	73368.26
8	6.200377887	2.888167	170738.8	655742.8658	79530.96
9	6.552753977	3.105715	180442.1	737710.7241	85521.54
10	6.890715675	3.33747	189748.5	819678.5823	91903.33
20	9.795973118	5.820734	269750.1	1639357.165	160284.6
30	12.5425258	8.287623	345381.4	2459035.747	228214.9
40	15.23571188	10.84117	419543.2	3278714.329	298531.4
50	17.91092377	13.44774	493210.1	4098392.912	370308.1
60	20.58007863	16.08235	566710.1	4918071.494	442856.9

70	23.24719202	18.73082	640154	5737750.076	515787.4
80	25.9136173	21.3861	713578.9	6557428.658	588905.3
90	28.57981063	24.04486	786997.4	7377107.241	662119.1
100	31.24592579	27.04093	860413.8	8196785.823	744621.6
200	57.90669911	55.68153	1594567	16393571.65	1533293
300	84.56745411	81.5012	2328720	24590357.47	2244285
400	111.2282082	107.7694	3062872	32787143.29	2967628
500	137.8889623	134.2003	3797025	40983929.12	3695452
600	164.5497164	160.7096	4531178	49180714.94	4425434
700	191.2104705	187.2629	5265330	57377500.76	5156627
800	217.8712245	213.8434	5999483	65574286.58	5888568
900	244.5319786	240.4418	6733636	73771072.41	6621006
1000	271.1927327	270.406	7467788	81967858.23	7446125
2000	537.8002733	556.8152	14809315	163935716.5	15332926
3000	804.4078139	815.012	22150842	245903574.7	22442848
4000	1071.015354	1077.694	29492369	327871432.9	29676281
5000	1337.622895	1342.003	36833896	409839291.2	36954516
6000	1604.230435	1607.096	44175423	491807149.4	44254337
7000	1870.837976	1872.629	51516949	573775007.6	51566267
8000	2137.445516	2138.434	58858476	655742865.8	58885685
9000	2404.053056	2404.418	66200003	737710724.1	66210061
10000	2670.660596	2704.06	73541530	819678582.3	74461253
20000	5336.735992	5568.152	1.47E+08	1639357165	1.53E+08
30000	8002.811382	8150.12	2.2E+08	2459035747	2.24E+08
40000	10668.88677	10776.94	2.94E+08	3278714329	2.97E+08
50000	13334.96214	13420.03	3.67E+08	4098392912	3.7E+08
60000	16001.03752	16070.96	4.41E+08	4918071494	4.43E+08
70000	18667.11288	18726.29	5.14E+08	5737750076	5.16E+08
80000	21333.18824	21384.34	5.87E+08	6557428658	5.89E+08
90000	23999.2636	24044.18	6.61E+08	7377107241	6.62E+08
100000	26665.33894	25545.93	7.34E+08	8196785823	7E+08

A.3 Pressure data for the determination of kx for non-Newtonian fluid where $n=0.2$

t_D	$P_{wD} @n=1$	$P_{wD} @n=0.2$	t
0.0001	0.002884151	0.014036184	8.196785823
0.0002	0.024407363	0.105588268	16.39357165
0.0003	0.041174515	0.171067132	24.59035747
0.0004	0.054769963	0.221759603	32.78714329
0.0005	0.066188867	0.263486663	40.98392912
0.0006	0.076067644	0.299390291	49.18071494
0.0007	0.084821631	0.331256698	57.37750076
0.0008	0.092728025	0.360159532	65.57428658
0.0009	0.099976355	0.386781438	73.77107241
0.001	0.106699535	0.411580197	81.96785823
0.002	0.153507157	0.586876942	163.9357165
0.003	0.190073815	0.725902636	245.9035747
0.004	0.220561213	0.844257668	327.8714329
0.005	0.24704366	0.949839615	409.8392912
0.006	0.270711604	1.047054418	491.8071494
0.007	0.292315922	1.138494716	573.7750076
0.008	0.31235997	1.225733019	655.7428658
0.009	0.331194417	1.30974257	737.7107241
0.01	0.349069619	1.391136555	819.6785823
0.02	0.488848841	2.060254744	1639.357165
0.03	0.605684836	2.625175556	2459.035747
0.04	0.706042635	3.109895577	3278.714329
0.05	0.793636898	3.531584072	4098.392912
0.06	0.871056523	3.903130315	4918.071494
0.07	0.940244588	4.234362732	5737.750076
0.08	1.00270006	4.532847101	6557.428658
0.09	1.059594562	4.804456499	7377.107241

0.1	1.111852221	5.053787612	8196.785823
0.2	1.451077257	6.678580009	16393.57165
0.3	1.703712281	7.894007842	24590.35747
0.4	1.90827537	8.880244136	32787.14329
0.5	2.082453098	9.719667768	40983.92912
0.6	2.235495119	10.45560773	49180.71494
0.7	2.372803381	11.11369293	57377.50076
0.8	2.497828839	11.71055635	65574.28658
0.9	2.612938899	12.25778664	73771.07241
1	2.719850846	12.76390147	81967.85823
2	3.463348735	16.20444534	163935.7165
3	4.054711448	18.89846623	245903.5747
4	4.563047428	21.19291741	327871.4329
5	5.019160105	23.24244465	409839.2912
6	5.438612493	25.12545337	491807.1494
7	5.830396296	26.88733522	573775.0076
8	6.200377887	28.55755171	655742.8658
9	6.552753977	30.15686458	737710.7241
10	6.890715675	31.70068145	819678.5823
20	9.795973118	45.6156455	1639357.165
30	12.5425258	59.10849205	2459035.747
40	15.23571188	72.48404969	3278714.329
50	17.91092377	85.82699305	4098392.912
60	20.58007863	99.16086541	4918071.494
70	23.24719202	112.4922147	5737750.076
80	25.9136173	125.8228622	6557428.658
90	28.57981063	139.1533144	7377107.241
100	31.24592579	152.4837124	8196785.823
200	57.90669911	285.7874905	16393571.65
300	84.56745411	419.0912612	24590357.47
400	111.2282082	552.3950316	32787143.29
500	137.8889623	685.6988019	40983929.12

600	164.5497164	819.0025723	49180714.94
700	191.2104705	952.3063426	57377500.76
800	217.8712245	1085.610113	65574286.58
900	244.5319786	1218.913883	73771072.41
1000	271.1927327	1352.217654	81967858.23
2000	537.8002733	2685.255356	163935716.5
3000	804.4078139	4018.293059	245903574.7
4000	1071.015354	5351.330761	327871432.9
5000	1337.622895	6684.368462	409839291.2
6000	1604.230435	8017.406162	491807149.4
7000	1870.837976	9350.443863	573775007.6
8000	2137.445516	10683.48156	655742865.8
9000	2404.053056	12016.51926	737710724.1
10000	2670.660596	13349.55696	819678582.3
20000	5336.735992	26679.93391	1639357165
30000	8002.811382	40010.31081	2459035747
40000	10668.88677	53340.68766	3278714329
50000	13334.96214	66671.06447	4098392912
60000	16001.03752	80001.44123	4918071494
70000	18667.11288	93331.81795	5737750076
80000	21333.18824	106662.1946	6557428658
90000	23999.2636	119992.5712	7377107241
100000	26665.33894	133322.9478	8196785823

APPENDIX B

DERIVATION OF DARCY EQUATION FOR NON-NEWTONIAN POWER-LAW FLUIDS

From Darcy and the Blake-Kozeny's equation

$$u_0 = \frac{k \, dP}{\mu L} = \frac{D_p^2 \Phi^3 \Delta P}{150 \mu (1-\Phi)^2 L} \dots\dots\dots 1$$

From permeability of packed bed

$$k = \frac{D_p^2 \Phi^3}{150 (1-\Phi)^2} \dots\dots\dots 2$$

The modified Blake- Kozeny equation for one dimensional flow in power law fluid is as given thus

$$u_0 = \frac{n\Phi}{3n+1} \left(\frac{D_p \Phi}{3(1-\Phi)} \right)^{\frac{n+1}{n}} \left(\frac{6\Delta p}{25HL} \right)^{\frac{1}{n}} \dots\dots\dots 3$$

From equation 2;

$$D_p^2 = \frac{150(1-\Phi)^2 k}{\Phi^3} \dots\dots\dots 4$$

$$D_p = \left(\frac{150k}{\Phi} \right)^{\frac{1}{2}} \frac{(1-\Phi)}{\Phi} \dots\dots\dots 5$$

Substituting equation 5 into equation 3

$$u_0 = \frac{n\Phi}{3n+1} \left[\frac{\left(\frac{150k}{\Phi} \right)^{\frac{1}{2}} \frac{(1-\Phi)}{\Phi}}{3(1-\Phi)} \right]^{\frac{n+1}{n}} \left(\frac{6\Delta P}{25HL} \right)^{\frac{1}{n}}$$

$$u_0 = \frac{n\Phi}{3n+1} \left[\left(\frac{150k}{\Phi} \right)^{\frac{1}{2}} \frac{1}{3} \right]^{\frac{n+1}{n}} \left(\frac{6\Delta P}{25HL} \right)^{\frac{1}{n}}$$

$$u_0 = \frac{n\Phi}{3n+1} \left[\left(\frac{150k}{\Phi} \right)^{\frac{n+1}{2}} \left(\frac{1}{3} \right)^{n+1} \left(\frac{6\Delta p}{25HL} \right) \right]^{\frac{1}{n}}$$

$$u_0 = \frac{n\Phi}{3n+1} * \left(\frac{150k}{\Phi}\right)^{\frac{n+1}{2n}} * \left(\frac{1}{3}\right)^{\frac{n+1}{n}} * \left(\frac{6}{25}\right)^{\frac{1}{n}} * \left(\frac{\Delta P}{L}\right)^{\frac{1}{n}} * \left(\frac{1}{H}\right)^{\frac{1}{n}}$$

$$u_0 = \frac{n\Phi}{3n+1} * \left(\frac{150}{\Phi}\right)^{\frac{n+1}{2n}} * k^{\frac{n+1}{2n}} * \left(\frac{1}{3}\right)^{\frac{1}{n}} * \left(\frac{6^2}{25}\right)^{\frac{1}{n}} * \left(\frac{\Delta P}{L}\right)^{\frac{1}{n}} * \left(\frac{1}{H}\right)^{\frac{1}{n}}$$

$$u_0 = \frac{n\Phi}{3n+1} * \left(\frac{150}{\Phi}\right)^{\frac{n+1}{2n}} * k^{\frac{n+1}{2n}} * \left(\frac{1}{3}\right)^{\frac{1}{n}} * \left(\frac{2}{25}\right)^{\frac{1}{n}} * \left(\frac{\Delta P}{L}\right)^{\frac{1}{n}} * \left(\frac{1}{H}\right)^{\frac{1}{n}}$$

$$u_0 = \frac{n\Phi}{9n+3} * \left(\frac{150}{\Phi}\right)^{\frac{n+1}{2n}} * k^{\frac{n+1}{2n}} * \left(\frac{2}{25}\right)^{\frac{1}{n}} * \left(\frac{\Delta P}{L}\right)^{\frac{1}{n}} * \left(\frac{1}{H}\right)^{\frac{1}{n}}$$

$$u_0 = \frac{n\Phi}{9n+3} * \left(\frac{150}{\Phi}\right)^{\frac{1}{2}} * \left(\frac{150}{\Phi}\right)^{\frac{1}{2n}} * k^{\frac{1}{2}} * k^{\frac{1}{2n}} * \left(\frac{2}{25}\right)^{\frac{1}{n}} * \left(\frac{\Delta P}{L}\right)^{\frac{1}{n}} * \left(\frac{1}{H}\right)^{\frac{1}{n}}$$

$$u_0 = \frac{n\Phi}{9n+3} * \left(\frac{150}{\Phi}\right)^{\frac{1}{2}} * \left(\frac{150}{\Phi}\right)^{\frac{1}{n}} * \left(\frac{150}{\Phi}\right)^{-\frac{1}{2n}} * k^{\frac{1}{2}} * k^{\frac{1}{2n}} * \left(\frac{2}{25}\right)^{\frac{1}{n}} * \left(\frac{\Delta P}{L}\right)^{\frac{1}{n}} * \left(\frac{1}{H}\right)^{\frac{1}{n}}$$

$$u_0 = \frac{n\Phi}{9n+3} * \left(\frac{150}{\Phi}\right)^{\frac{1}{2} - \frac{1}{2n}} * \left(\frac{150^6}{\Phi}\right)^{\frac{1}{25}} * k^{\frac{1}{2}} * k^{\frac{1}{2n}} * \left(\frac{\Delta P}{L}\right)^{\frac{1}{n}} * \left(\frac{1}{H}\right)^{\frac{1}{n}}$$

$$u_0 = \frac{n\Phi}{9n+3} * \left(\frac{150}{\Phi}\right)^{\frac{1}{2} - \frac{1}{2n}} * \left(\frac{12}{\Phi}\right)^{\frac{1}{n}} * k^{\frac{1}{2}} * k^{-\frac{1}{2n}} * k^{\frac{1}{n}} * \left(\frac{\Delta P}{L}\right)^{\frac{1}{n}} * \left(\frac{1}{H}\right)^{\frac{1}{n}}$$

$$u_0 = \frac{n\Phi}{9n+3} * \left(\frac{150}{\Phi}\right)^{\frac{1}{2} \left(\frac{n-1}{n}\right)} * \left(\frac{12}{\Phi}\right)^{\frac{1}{n}} * k^{\frac{1}{2} \left(\frac{n-1}{n}\right)} * \left(\frac{k\Delta P}{L}\right)^{\frac{1}{n}} * \left(\frac{1}{H}\right)^{\frac{1}{n}}$$

$$u_0 = \frac{\Phi}{9 + \frac{3}{n}} * \Phi^{-\frac{1}{n}} * \left(\frac{k150}{\Phi}\right)^{\frac{1}{2} \left(\frac{n-1}{n}\right)} * 12^{\frac{1}{n}} * \left(\frac{k\Delta P}{L}\right)^{\frac{1}{n}} * \left(\frac{1}{H}\right)^{\frac{1}{n}}$$

$$u_0 = \frac{1}{\left(9 + \frac{3}{n}\right)} * \Phi^{\left(\frac{n-1}{n} - \frac{n-1}{2n}\right)} * (150k)^{\frac{1}{2} \left(\frac{n-1}{n}\right)} * 12^{\frac{1}{n}} * \left(\frac{k\Delta P}{L}\right)^{\frac{1}{n}} * \left(\frac{1}{H}\right)^{\frac{1}{n}}$$

$$u_0 = \frac{1}{\left(9 + \frac{3}{n}\right)} * (150k\Phi)^{\frac{1}{2} \left(\frac{n-1}{n}\right)} * 12^{\frac{1}{n}} * \left(\frac{k\Delta P}{L}\right)^{\frac{1}{n}} * \left(\frac{1}{H}\right)^{\frac{1}{n}}$$

$$u_0 = \left[\frac{1}{\left(9 + \frac{3}{n}\right)^n} * (150k\Phi)^{\left(\frac{n-1}{2}\right)} * \frac{12}{H} * \left(\frac{k\Delta P}{L}\right) \right]^{\frac{1}{n}}$$

$$u_0 = \left(\frac{k\Delta P}{L}\right)^{\frac{1}{n}} * \left(\frac{\left(9+\frac{3}{n}\right)^n * H}{(150k\Phi)^{\left(\frac{n-1}{2}\right)*12}}\right)^{-\frac{1}{n}}$$

$$u_0 = \left[\left(9 + \frac{3}{n}\right)^{-n} * (150k\Phi)^{\left(\frac{n-1}{2}\right)} * \frac{12}{H} * \left(\frac{k\Delta P}{L}\right)\right]^{\frac{1}{n}}$$

$$u_0 = \left[\left(9 + \frac{3}{n}\right)^{-n} * (150k\Phi)^{\left(\frac{n-1}{2}\right)} * 12 * \left(\frac{k\Delta P}{HL}\right)\right]^{\frac{1}{n}}$$

$$u_0 = \left[\frac{k}{\frac{H\left(9+\frac{3}{n}\right)^n * (150k\Phi)^{\left(\frac{1-n}{2}\right)}}{12}} \frac{\Delta P}{L} \right] \dots\dots\dots 6$$

Comparing equation 6 with the Darcy's equation,

$$\mu_{eff} = \frac{H\left(9+\frac{3}{n}\right)^n * (150k\Phi)^{\left(\frac{1-n}{2}\right)}}{12}$$

Thus, equation 6 can be re-written as;

$$u_0 = - \left[\frac{k}{\mu_{eff}} \frac{\Delta P}{L} \right]^{\frac{1}{n}} \dots\dots\dots 7$$